

VOLUME XLIII

GEMS & GEMOLOGY

SUMMER 2007



Global Rough Diamond Production
Durability Testing of Filled Emeralds
Chinese Freshwater Pearl Culture

THE QUARTERLY JOURNAL OF THE GEMOLOGICAL INSTITUTE OF AMERICA



pg. 99



pg. 140

95 LETTERS _____

FEATURE ARTICLES _____

98 **Global Rough Diamond Production since 1870**



A. J. A. (Bram) Janse

Reports and analyzes annual production statistics (by carat weight and value) for the world's most significant diamond sources, through 2005.

120 **Durability Testing of Filled Emeralds**

Mary L. Johnson

A long-term, systematic study of the stability and durability of nine common emerald-filling substances.

NOTES AND NEW TECHNIQUES _____

138 **Continuity and Change in Chinese Freshwater Pearl Culture**

Doug Fiske and Jeremy Shepherd

Reviews recent developments in China's freshwater cultured pearl production, including the new "fireball" cultured pearls.

RAPID COMMUNICATIONS _____

146 **Yellowish Green Diopside and Tremolite from Merelani, Tanzania**

Eric A. Fritz, Brendan M. Laurs, Robert T. Downs, and Gelu Costin

149 **Polymer-Impregnated Turquoise**

Kyaw Soe Moe, Thomas M. Moses, and Paul Johnson

REGULAR FEATURES _____

153 **Lab Notes**

Diamond with biminerale inclusions • HPHT-treated type Ia diamond with a green component caused by the H2 defect • Diamond with intense "rainbow graining" • Natural color hydrogen-rich blue-gray diamond • Type Ia diamond with intense green color introduced by Ni-related defects • Diamond with zigzag cleavage • HPHT-grown synthetic diamond crystal with unusual morphology and negative trigons • Idocrase in jadeite • Opal with unusual structure

162 **Gem News International**

Bar code technology applied to diamonds • U.S. Supreme Court ruling may affect viability of some diamond cut patents • First discovery of amazonite in Mexico • Astorite—A rhodonite-rich rock from Colorado • Color-change bastnäsite-(Ce) from Pakistan • Citrine with pyrite inclusions • Unusual danburite pair • Fluorite from Ethiopia • Heliodor and other beryls from Connecticut • Cat's-eye K-feldspar and other chatoyant gems from Tanzania • Green opal • Chinese akoya cultured pearls • Pyrope-almandine from Tanzania • Pink-to-red tourmaline from Myanmar • Glass object with circular bands • Heat-treated Kashan flux-grown synthetic ruby • Synthetic star sapphire with hexagonal features • Pink synthetic spinel colored by iron • A new imitation of Imperial topaz • KPMG report on the global jewelry industry

184 **Thank You, Donors**

185 **Book Reviews**

188 **Gemological Abstracts**



pg. 154



pg. 170

EDITORIAL STAFF

Editor-in-Chief

Alice S. Keller
akeller@gia.edu

Managing Editor

Thomas W. Overton
tom.overton@gia.edu

Technical Editor

Sally Magaña
sally.magana@gia.edu

Consulting Editor

Carol M. Stockton

Contributing Editor

James E. Shigley

Editor

Brendan M. Laurs
The Robert Mouawad Campus
5345 Armada Drive
Carlsbad, CA 92008
(760) 603-4503
blaurs@gia.edu

Associate Editor

Stuart Overlin
soverlin@gia.edu

Circulation Coordinator

Debbie Ortiz
(760) 603-4000, ext. 7142
dortiz@gia.edu

Editors, Lab Notes

Thomas M. Moses
Shane F. McClure

Editor, Gem News International

Brendan M. Laurs

Editors, Book Reviews

Susan B. Johnson
Jana E. Miyahira-Smith
Thomas W. Overton

Editors, Gemological Abstracts

Brendan M. Laurs
Thomas W. Overton

PRODUCTION STAFF

Art Director

Karen Myers

Production Assistant

Allison DeLong

Website:

www.gia.edu

EDITORIAL REVIEW BOARD

Shigeru Akamatsu
Tokyo, Japan

Edward W. Boehm
Solana Beach, California

James E. Butler
Washington, DC

Alan T. Collins
London, United Kingdom

John Emmett
Brush Prairie, Washington

Emmanuel Fritsch
Nantes, France

Henry A. Hänni
Basel, Switzerland

Jaroslav Hyršl
Prague, Czech Republic

A. J. A. (Bram) Janse
Perth, Australia

Alan Jobbins
Caterham, United Kingdom

Mary L. Johnson
San Diego, California

Anthony R. Kampf
Los Angeles, California

Robert E. Kane
Helena, Montana

Lore Kiefert
New York, New York

Thomas M. Moses
New York, New York

Mark Newton
Coventry, United Kingdom

George Rossman
Pasadena, California

Kenneth Scarratt
Bangkok, Thailand

James E. Shigley
Carlsbad, California

Christopher P. Smith
New York, New York

Christopher M. Welbourn
Reading, United Kingdom

SUBSCRIPTIONS

Subscriptions to addresses in the U.S. are priced as follows: **\$74.95** for one year (4 issues), **\$194.95** for three years (12 issues). Subscriptions sent elsewhere are **\$85.00** for one year, **\$225.00** for three years. Canadian subscribers should add GST.

Special rates are available for GIA alumni and current GIA students. One year: **\$64.95** to addresses in the U.S., **\$75.00** elsewhere; three years: **\$179.95** to addresses in the U.S., **\$210.00** elsewhere. Please have your student or Alumni number ready when ordering. Go to www.gia.edu or contact the Circulation Coordinator.

Single copies of this issue may be purchased for **\$19.00** in the U.S., **\$22.00** elsewhere. Discounts are given for bulk orders of 10 or more of any one issue. A limited number of back issues are also available for purchase. Please address all inquiries regarding subscriptions and single copy or back issue purchases to the Circulation Coordinator (see above) or visit www.gia.edu.

To obtain a Japanese translation of *Gems & Gemology*, contact GIA Japan, Okachimachi Cy Bldg., 5-15-14 Ueno, Taitoku, Tokyo 110, Japan. Our Canadian goods and service registration number is 126142892RT.

DATABASE COVERAGE

Gems & Gemology's impact factor is 1.762 (ranking 5th out of the 25 journals in the Mineralogy category), according to Thomson Scientific's 2005 Journal Citation Reports (issued June 2006). *Gems & Gemology* is abstracted by the following: Cambridge Scientific Abstracts, CSA Illumina, Chemical Abstracts Service, GEOBASE, Elsevier Scopus, GeoRef, Ingenta, *Mineralogical Abstracts*, and Thomson Scientific products (*Current Contents: Physical, Chemical & Earth Sciences* and Science Citation Index-Expanded, including the Web of Science). For a complete list, see www.gia.edu/gemsandgemology.

MANUSCRIPT SUBMISSIONS

Gems & Gemology welcomes the submission of articles on all aspects of the field. Please see the Guidelines for Authors on our Website, or contact the Managing Editor. Letters on articles published in *Gems & Gemology* are also welcome.

Abstracting is permitted with credit to the source. Libraries are permitted to photocopy beyond the limits of U.S. copyright law for private use of patrons. Instructors are permitted to photocopy isolated articles for noncommercial classroom use without fee. Copying of the photographs by any means other than traditional photocopying techniques (Xerox, etc.) is prohibited without the express permission of the photographer (where listed) or author of the article in which the photo appears (where no photographer is listed). For other copying, reprint, or republication permission, please contact the Managing Editor.

COPYRIGHT AND REPRINT PERMISSIONS

Gems & Gemology is published quarterly by the Gemological Institute of America, a nonprofit educational organization for the gem and jewelry industry, The Robert Mouawad Campus, 5345 Armada Drive, Carlsbad, CA 92008.

Postmaster: Return undeliverable copies of *Gems & Gemology* to The Robert Mouawad Campus, 5345 Armada Drive, Carlsbad, CA 92008.

Any opinions expressed in signed articles are understood to be the opinions of the authors and not of the publisher.

ABOUT THE COVER

For centuries, emeralds have been oiled to mask their abundant inclusions and improve their apparent clarity. A wide range of emerald-filling substances are used today, with varying effectiveness. In this issue, Dr. Mary Johnson compares the stability and durability of nine common emerald-filling substances.

Shown here is a pair of emerald and diamond earrings; the emeralds range from 4 to 18 ct. Courtesy of H. Stern, New York and Rio de Janeiro. Photo © Harold & Erica Van Pelt.

Color separations for Gems & Gemology are by Pacific Plus, Carlsbad, California.

Printing is by Allen Press, Lawrence, Kansas.

© 2007 Gemological Institute of America All rights reserved. ISSN 0016-626X

Letters

ANNOUNCING *GEMS & GEMOLOGY* "RAPID COMMUNICATIONS"

The current issue marks the beginning of a new feature for *G&G*. "Rapid Communications" are short articles (2–3 pages) that provide brief descriptions of notable gem materials, localities, and identification or treatment techniques—as well as related topics such as museum exhibits and historical jewelry—as quickly as possible and in a readily accessible format. If a manuscript is submitted for Rapid Communications no later than eight weeks before the print date of an issue, and is deemed publishable by the editors and the reviewers, every effort will be made to include it in that issue. We feel that readers and authors alike will benefit from the expedited publication of brief, high-quality research results in *Gems & Gemology*. For more information, visit www.gia.edu/gemsandgemology and click on "Publishing in *G&G*."

Brendan M. Laurs, Editor

CULTURED PEARL TERMINOLOGY

When dealing with gemologists, students, and people in the pearl trade, I find that most—despite their education about pearls—have incorrect and misleading ideas about how a cultured pearl is formed and the meaning of certain terms.

In *Gems & Gemology*, the terms *bead nucleated* and *tissue nucleated* are often used (see, e.g., K. Scarratt et al., "Characteristics of nuclei in Chinese freshwater cultured pearls," Summer 2000, pp. 98–109; S. Akamatsu et al., "The current status of Chinese freshwater cultured pearls," Summer 2001, pp. 96–113). The combination of these two terms creates the idea that a cultured pearl is nucleated with either a bead or a piece of mantle tissue, and the term *nucleation* suggests that there is something in the center of the cultured pearl, either a bead or a tissue graft. However, the former does not lead to a cultured pearl if no tissue is added.

The point is that *all cultured pearls are "tissue nucleated."* And, since all cultured pearls start with a piece of mantle tissue, this expression does not adequately differentiate between the two types. It is thus confusing and of no use.

Further, the term *tissue nucleated* causes people to think that the grafted tissue is *in* the cultured pearl. However, research (by myself and others) has indicated that tissue cells from the transplant become part of the pearl sac and do not remain as a residue in the center of the pearl (Joseph Taylor, Atlas South Sea Pearl Ltd., pers. comm., 2006). They do not form a nucleus.

The X-ray-visible dark structure in the center of these cultured pearls is often a void and preliminary precipitation from the growing surface of what will become the pearl sac. The transplanted mantle-tissue cells that produce the nacre grow into a pearl sac by multiple cell division, making a small pocket. This pocket produces an initial crust of CaCO₃ on its inner surface, but this crust does not completely fill the space, leading to the cavity in the center of a beadless cultured pearl (see, e.g., SSEF Tutorial 1 CD-ROM, 2001; H.A. Hänni, "A short review of the use of 'keshi' as a term to describe pearls," *Journal of Gemmology*, Vol. 30, No. 1/2, 2004, pp. 51–58).

For clarity's sake, I proposed several changes that appear in the new CIBJO Pearl Book:

- Omission of the terms *nucleus*, *nucleation*, *bead nucleated*, *tissue nucleated*
- Use of the term *grafting* for the introduction of mantle-tissue cells (with or without a bead)
- Use of the term *beading* for the introduction of a material that gives the shape to the pearl sac (to grow or already present), regardless of the shape of that bead
- Use of the terms *beaded cultured pearl* and *non-beaded (beadless) cultured pearl* for the resulting products

These proposals were accepted by the commission for the new CIBJO rules, and I would appreciate seeing *Gems & Gemology* adhere to them.

H. A. Hänni
SSEF Swiss Gemmological Institute, Basel

Reply: We appreciate Dr. Hänni's comments and suggestions. In light of the recent revisions to the CIBJO nomenclature rules (see the related announcement on p. 182 of the Gem News International section), and with the agreement of Mr. Scarratt and Mr. Akamatsu, we are encouraging our contributors to use the new terminology and are updating the journal's style guidelines accordingly.
— Editors

PIGMENTS IN NATURAL-COLOR CORALS

We read with interest the article titled "Pink-to-red coral: A guide to determining origin of color," by C. P. Smith et al., in the Spring 2007 *G&G* (pp. 5–14). This approach truly parallels the work we recently published on the origin of color of freshwater cultured pearls (see S. Karampelas et al., "Identification through Raman scattering of pigments in cultured freshwater pearls," Fall 2006 *Gems & Gemology*, pp. 99–100; S. Karampelas et al., "Determination by Raman scattering of the nature of pigments in cultured freshwater pearls," *Journal of Raman Spectroscopy*, Vol. 38, No. 2, 2007, pp. 217–230). In

these articles, we mentioned the possibility of extending the type of study we did from freshwater cultured pearls to corals, among other materials. We also demonstrated that the signal identified by Smith et al. as due to "carotene" in the *Corallium* genus (as well as in *Melithaea ochracea*) is actually due to mixtures of polyenes.

Polyenes (or polyacetylenes) are organic compounds that contain several sequences of alternating double and single carbon-carbon bonds, the polyenic chain. Polyenic molecules can have various substitutions on their terminal ends. The polyenes in freshwater cultured pearls are short polymers containing between five and 14 acetylene monomers. Carotenoid pigments are also polyenic molecules and they, too, have various substitutions on their terminal ends. However, they additionally have four methyl groups attached to their chain.

The main Raman scattering peak of polyenes is at about $1130 (\pm 15) \text{ cm}^{-1}$, whereas carotenoids produce a main peak at about $1155 (\pm 10) \text{ cm}^{-1}$. This is because the latter peak results from the coupling of the single carbon-carbon stretching vibration in the central part of the chain, with the CH_3 in plane-bending modes. Thus, for carotenoids that contain methyl groups in their polyenic chain, the position of this band is shifted by about 20 cm^{-1} compared to polyenic chains without CH_3 .

This, however, does not take away from the general method proposed by the authors, which we confirm from our own experience works very well, even if the use of Raman spectroscopy to conclusively identify the presence or absence of dye in coral is still little known.

Stefanos Karampelas (steka@physics.auth.gr)
Department of Geology
University of Thessaloniki, Greece;
Institut des Matériaux Jean Rouxel (IMN)
Université de Nantes, France
Emmanuel Fritsch, IMN

Reply: We want to thank and acknowledge Dr. Karampelas and Dr. Fritsch for this clarification and the excellent research they have conducted. It is a bit unfortunate that our publications came out in parallel; however, theirs was a very important discovery, and we strongly encourage the readers of *G&G* to review their articles.

Christopher P. Smith and Shane F. McClure

MORE ON DYED CORAL

Reading the article by C.P. Smith et al. in the Spring 2007 *G&G*, I was surprised that no mention was made of bamboo coral (belonging to the genus *Isis*), as, in my experience, that is the coral type that we frequently encounter in modern, lower-end jewelry and carvings. It is available at every fair, market, and in the less exclusive shop.

While it is true that expensive or antique red coral items tend to be *Corallium* corals—dyed or not—there are masses of bamboo coral about that are simulating red *Corallium* coral.

Bamboo coral also has the striations that are typical of *Corallium* corals, but whereas the *Corallium*'s striations are

very fine—0.25 to 0.5 mm apart—those of bamboo coral are ~1 mm apart, so the two corals are easily distinguishable. Further, bamboo coral items often show a hint of the nodes of horny material that separate the internodes of calcium carbonate. These do not occur in *Corallium* corals and so help with identification. As regards color, bamboo coral does not naturally occur in red, so any bamboo coral encountered in red (and quite often orange) is dyed, and therefore does not need to be tested.

I feel that to omit mention of bamboo corals altogether could lead your readers to believe that any coral displaying striations is a *Corallium* coral which needs to be tested. This is not the case.

Maggie Campbell Pedersen
Organic Gems, London, England

Reply: We would like to thank Ms. Pedersen for her insightful comments. Within the content of the article, we did not state that the presence of striations in and of themselves would identify a piece as *Corallium* coral, and, as we indicated, the identification of coral species was outside the scope of the paper. Our intent was to detail those techniques that are most effective and routinely utilized to make a proper identification of natural-color and dyed pink-to-red coral. Although bamboo coral was not specifically discussed in our study, it is possible that some of the "samples of unknown species" may have been bamboo coral. In this regard, all samples tested could be positively identified as being either natural color or dyed based on the techniques described. We feel confident that those same techniques would properly identify an item of dyed pink-to-red bamboo coral or other coral species.

Christopher P. Smith and Shane F. McClure

PROPER TERMINOLOGY FOR DIAMOND GROWTH

I appreciated the detailed description of diamonds with atypical growth patterns in the Spring 2007 Lab Notes section ("Translucent greenish yellow diamonds," pp. 50–52, and "Unusual natural-color black diamond," pp. 52–53). However, I was dismayed by the incorrect terminology used to describe these nearly cubic growth modes. Both notes used the term *cubic* to describe very different materials, namely a fibrous cube and mixed-habit cuboid-octahedral growth. The terms *cuboid* and *fibrous cube* have been agreed upon since the early 1970s (see M. Moore and A. R. Lang, "On the internal structure of natural diamonds of cubic habit," *Philosophical Magazine*, Vol. 26, No. 6, 1972, pp. 1313–1325) and have been used extensively since by authors dealing with diamond morphology (e.g., C. M. Welbourn et al., "A study of diamonds of cube and cube-related shape from the Jwaneng mine," *Journal of Crystal Growth*, Vol. 94, 1989, pp. 229–252). This terminology has been more recently reviewed in an article of mine (B. Rondeau et al., "Diamants cubiques et presque cubiques: Quelques définitions utiles sur la morphologie," *Revue de Gemmologie a.f.g.*, Vol. 153, 2005, pp. 13–16 ["Cubic and nearly cubic diamonds: Some useful definitions on morphology," in French]).

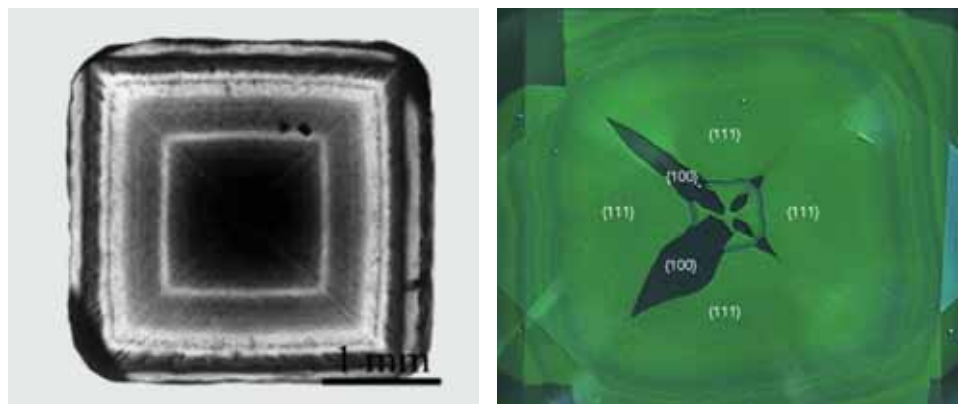


Figure 1. In the left image (adapted with permission from Zedgenizov et al., 2004), nearly straight growth layers can be seen in a cuboid diamond. The DiamondView image of a 2.50 ct greenish gray round brilliant natural diamond at right shows cubic {100} growth sectors, which are dominated by octahedral {111} sectors. Image by Kyaw Soe Moe.

The term *cubic* should be used only for [100] growth sectors leading to smooth faces with sharp edges; these are observed only in synthetic diamond. The term *cuboid* has been ascribed to a slow, undulating growth mode in the {100} cubic direction in the mean (again, see Moore and Lang, 1972). The term *fibrous cube* describes a diamond that grew rapidly in the fibrous mode of octahedral growth (analogous to dendritic growth). Fibrous diamonds commonly incorporate micro-inclusions of water, brines, carbonates, quartz, and the like, in various proportions, as revealed by infrared spectroscopy (see, e.g., E. Tomlinson et al., "Trace element composition of submicroscopic inclusions in coated diamond: A tool for understanding diamond petrogenesis," *Geochimica et Cosmochimica Acta*, Vol. 69, No. 19, 2005, pp. 4719–4732, and references therein).

Clearly, the diamonds described in the first note correspond to a fibrous cube—not cubic growth—that shows growth *layers*, not growth *sectors*. The black diamond described in the second note most probably corresponds to a mixed-habit diamond with octahedral and *cuboid* growth sectors (not cubic growth sectors). Details on how such mixed growth may leave an apparently colorless core are given in B. Rondeau et al. ("Three historical 'asteriated' hydrogen-rich diamonds: Growth history and sector-dependent impurity incorporation," *Diamond and Related Materials*, Vol. 13, 2004, pp. 1658–1673).

This use of the terms *cubic diamond* and *cubic sectors* is hence confusing for readers, who would expect to see them only when dealing with synthetic diamonds (as previously discussed in numerous *Gems & Gemology* articles on the subject). I would greatly appreciate it if you could, in the future, help authors use the correct terminology for describing the many different nearly cubic morphologies of diamonds.

Benjamin Rondeau
Muséum National d'Histoire Naturelle, Paris

Reply: I appreciate Dr. Rondeau's detailed and valuable comments. The term *cuboid* is indeed used widely for natural diamonds. However, the term *cubic* for natural diamonds has also been used extensively. To cite a few examples, M. Moore et al. used *cubic growth* to explain the fourth mode of diamond growth ("Cubic growth of natural diamond," *Acta Crystallographica*, Vol. A62, No. a1, 2006, p. s65). H. Kagi et al. applied the term *cubic growth habit* to a natural cuboid diamond ("Near-infrared spectroscopic determination of salin-

ity and internal pressure of fluid inclusions in minerals," *Applied Spectroscopy*, Vol. 60, 2006, pp. 430–436). I. Sunagawa described cuboid diamonds using *cubic or cuboid morphology* (*Crystals: Growth, Morphology and Perfection*, Cambridge Press, Cambridge, UK, 2005, p. 188). K. J. Westerlund et al. explained the Klipspringer eclogitic diamonds using the phrase *cubic and octahedral growth zones* ("A metasomatic origin for late Archean eclogitic diamonds...," *South African Journal of Geology*, Vol. 107, 2004, pp. 119–130). D. A. Zedgenizov et al. discussed cuboid diamonds and used *cubic habit* ("Carbonatitic melts in cuboid diamonds from Udachnaya kimberlite pipe (Yakutia): Evidence from vibrational spectroscopy," *Mineralogical Magazine*, Vol. 68, No. 1, 2004, pp. 61–73). R. M. Davies et al. used *fibrous cubic growth layers* for natural diamonds ("Diamonds from Wellington, NSW...," *Mineralogical Magazine*, Vol. 63, 1999, pp. 447–471). Y. L. Orlov et al. also used the term *cubic growth sectors* for natural diamonds ("A study of the internal structure of variety III diamonds by X-ray section topography," *Physics and Chemistry of Minerals*, Vol. 8, No. 3, 1982, pp. 105–111).

I do agree that *cuboid* is appropriate for undulating growth in the cubic direction in a natural diamond. However, I believe that *cubic* is the appropriate term for natural diamond growth with straight or nearly straight layers. Moore et al. (2006) proposed that the fourth mode of diamond growth occurred in {100} planes or cube facets; it is rare but *can* be found in nature. A fine example can be seen in figure 1 (left), which shows cubic growth layers in a cuboid diamond. Readers would be confused if we used *cuboid growth* for such a specimen. From time to time in the GIA Laboratory, we have observed cubic {100} growth sectors along with octahedral {111} sectors in natural diamond, as seen in figure 1 (right). Consequently, neither I nor my colleagues agree that the term *cubic* should be limited to synthetic diamonds.

With respect to the Spring 2007 lab note on translucent greenish yellow diamonds, in the DiamondView images accompanying the entry one can see many growth layers originating from three different sources. Therefore, I think it is appropriate to use *growth sectors* (or *cuboid growth sectors*), which are composed of *growth layers*. Please also note (as mentioned in the entry) that these layers are not associated with a fibrous texture, and thus the term *fibrous cube* is not appropriate for these two diamonds.

Kyaw Soe Moe

GLOBAL ROUGH DIAMOND PRODUCTION SINCE 1870

A. J. A. (Bram) Janse

Data for global annual rough diamond production (both carat weight and value) from 1870 to 2005 were compiled and analyzed. Production statistics over this period are given for 27 diamond-producing countries, 24 major diamond mines, and eight advanced projects. Historically, global production has seen numerous rises—as new mines were opened—and falls—as wars, political upheavals, and financial crises interfered with mining or drove down demand. Production from Africa (first South Africa, later joined by South-West Africa [Namibia], then West Africa and the Congo) was dominant until the middle of the 20th century. Not until the 1960s did production from non-African sources (first the Soviet Union, then Australia, and now Canada) become important. Distinctions between carat weight and value affect relative importance to a significant degree. The total global production from antiquity to 2005 is estimated to be 4.5 billion carats valued at US\$300 billion, with an average value per carat of \$67. For the 1870–2005 period, South Africa ranks first in value and fourth in carat weight, mainly due to its long history of production. Botswana ranks second in value and fifth in carat weight, although its history dates only from 1970. Global production for 2001–2005 is approximately 840 million carats with a total value of \$55 billion, for an average value per carat of \$65. For this period, USSR/Russia ranks first in weight and second in value, but Botswana is first in value and third in weight, just behind Australia.

Although diamonds from alluvial deposits have been known since antiquity (figure 1), production from primary deposits (kimberlites and, since 1985, lamproites) began only in the 1870s. Over the last 135 years or so, annual production has risen from ~1 million carats (Mct) in 1872 to 176.7 Mct in 2005, though this increase has been anything but smooth. Production has followed the ups and downs of the world economy, with sudden increases brought about by new discoveries and just as precipitous drops caused by political upheavals and similar events. An awareness of the production figures for the modern history of diamond mining not only helps us understand the impact of both political developments and geologic factors over time, but it also helps the exploration geologist, diamondaire, and jeweler alike plan for future additions and disruptions to the supply chain.

This article represents an expanded version of the data and illustrations previously published in Janse (2006a,b), and is a companion piece to Boyajian (1988)

and Shor (2005). Assembling the data for annual global rough diamond production (gem, near-gem, and industrial) was a difficult task, because the numbers for several countries may vary more than 10% between different publications. To achieve as much consistency as possible, production figures were taken from sources that are believed to be reliable and, for the most part, that were continuously published in the United States. For the period 1870–1934, these included *The Mineral Industry* (from the Scientific Publishing Co.) and *Mineral Resources of the United States* (compiled by the U.S. Bureau of Mines). For the period 1934–2005, data were taken from *Minerals Yearbook* (also by the U.S. Bureau of Mines). Wagner (1914) was consulted for early South African production. For 2004 and 2005,

See end of article for About the Author and Acknowledgments.
GEMS & GEMOLOGY, Vol. 43, No. 2, pp. 98–119.
© 2007 Gemological Institute of America



Figure 1. Diamonds have been valued since antiquity, but only since the late 19th century have they become an important element of the world economy. They were first known in India, and then Indonesia and Brazil, but it was the 1867 discovery in South Africa that would launch the modern diamond market. Though India is no longer an important producer, it remains an essential link in the diamond supply chain through its polishing and trading centers. Shown here is an Indian diamond and emerald necklace from the early 19th century. Courtesy of Christie's Images.

Kimberley Process Certification Scheme production reports were also used. A cut-off date of December 31, 2005, was selected because that is the most recent year for which robust data are available. Although 2006 production figures for some mines have been released as of the date of publication of this article (mid-2007), incorporating them would distort the overall picture, as Kimberley Process data for 2006 have not yet been released. Figures for production data are necessarily best estimates compiled from the most reliable sources, but the trend and amplitude of changes in production and cumulative totals are considered by the author to be as close to reality as possible.

In the first part of this article, data are presented in a series of graphs illustrating: (1) annual production by country (divided into 10 groups: eight major source countries, one region [West Africa, including Guinea, Sierra Leone, Liberia, Ivory Coast, and Ghana], and one group representing other and minor producers [including Lesotho, Swaziland, Rhodesia/

Zimbabwe, Central African Republic, Tanzania, Brazil, Venezuela, Guyana, China, United States, India, and Indonesia]); (2) percentage of total by country; (3) percentage by type of deposit; and (4) percentage by category of diamond. The first three categories are further divided according to carat weight and U.S. dollar value of production.

In the second part of the article, data are given regarding the ownership, location, size, and other aspects of the 24 historically most important diamond mines and eight major advanced diamond projects currently in development. In the third part, data are provided for historic and contemporary production for the 27 most significant diamond-producing countries through 2005.

ANNUAL PRODUCTION BY COUNTRY

By Carat Weight. Historically, production has been as much a function of changes in demand as it has been of the introduction or closure of mining operations.

Figure 2 shows the annual production (by weight) of rough diamonds for the 10 most important diamond-producing regions from 1870 to 2005; more detail is provided below. For the most part, the regions are discussed and plotted chronologically by date of earliest production; South Africa is introduced first as it is historically the most important.

South Africa. After mining of diamonds began in 1869, South African production rose rapidly to 1 Mct in 1872 and thereafter to 5 Mct in 1907, in 1909, and in 1913, with a few peaks and dips during this period. A dip in 1900 was due to the Boer War and the Siege of Kimberley. A peak in 1907 in response to rapidly growing U.S. demand was not reached again until 1966; it was followed by a sharp dip in 1908 due to a financial crisis in the U.S., and then production went back up again the next year. A steep drop in 1914 and 1915 was caused by World War I (WWI), but then production rose quickly and stayed at a moderate level from 1916 to 1920. In 1921–22, production fell again due to a general depression in the economy (the aftereffects of WWI and the 1918–19 flu pandemic) as well as a sudden influx of jewelry on the market due to the combination of Russian émigrés from the Bolshevik revolution having to sell their valuables to survive just as the new Soviet government was selling confiscated jewels (Janse, 1996).

Beginning in 1923, South African production rose again in response to the discovery of the Lichtenburg alluvial field and the Namaqualand beach deposits along the Atlantic coast, but it was extremely low from 1932 to 1944 as a result of the Great Depression of the 1930s and the impact of World War II. The Premier mine closed in 1932, and the Kimberley mines were closed for several years during this period. In 1948, the Premier and Kimberley mines reopened, causing production to rise gradually over the next two decades. There was a jump in 1968 when the Finsch mine came into full operation, after which production continued to rise gradually to 10 Mct in 1986. The global stock market crash in October 1987 precipitated a slight decline in production, but the upward trend resumed and gained momentum in 1992 when the Venetia mine came on stream. Production has climbed steadily since then to 15.56 Mct in 2005.

South-West Africa (SWA)/Namibia. Production began in 1909 and quickly reached 1 Mct annually during 1912–13 under German administration; it then fell to virtually zero in 1914–15 because of

WWI. Production resumed after the war but did not reach the 1 Mct mark again until 1962. It reached 2 Mct in the late 1960s and again in the 1970s, but then dropped to 0.9 Mct in the late 1980s. Production increased to 1.5 million in the 1990s, and in 2005 it amounted to 1.87 Mct.

Congo/Zaire/Democratic Republic of the Congo (DRC). The 1932–80 period was the heyday (in terms of its share of world production) for this region. Congo production began in 1917 and reached 18 Mct annually in 1961. After independence in 1960, it eventually declined to less than half that by 1981; however, it rose to 26 Mct in 1998. The fall of then-President Mobutu Sese Seko and the ensuing unrest led to a brief decline. Conditions stabilized in 2001, as Joseph Kabila took over from his assassinated father, and diamond production rose again to around 30 Mct in 2005.

Angola. Production began in 1921, but not until 1969 did it reach 2 Mct, where it stayed until 1974. From 1975 to 1995, production saw many ups and downs due to the country's protracted internal unrest. After conditions improved in 1995 and the Catoca mine came on stream in 1998, official annual production reached 3 Mct in 1999. Still, estimates by Cilliers and Dietrich (2000) indicate that, during the 1990s, "informal" production was much higher than the official figures, accounting for more than twice the official production in 1996 and 1997. Some sources estimate that the total of official production plus UNITA's smuggled production reached close to \$1 billion in 1996 (Partnership Africa Canada, 2004a). It was also claimed that UNITA *alone* accounted for \$1 billion (Partnership Africa Canada, 2005a). These disparate reports illustrate how difficult it is to estimate illicit or informal production. Where it exists to a significant degree, production figures—both official and unofficial—must be viewed with caution.

After the conflict eased in 2000, the government was able to assert greater control, and official production rose to its maximum level of 7.1 Mct. This was due to an increase in both licensed and unlicensed artisanal alluvial mining, and to expansion of Catoca, which is at present Angola's sole producing kimberlite pipe.

West Africa. West African production became significant in the early 1930s. It stayed around 2.5 Mct until 1954, then rose to its maximum level of 7.5 Mct in 1960. Civil disorder over a large part of the region and

CARAT WEIGHT BY COUNTRY/REGION

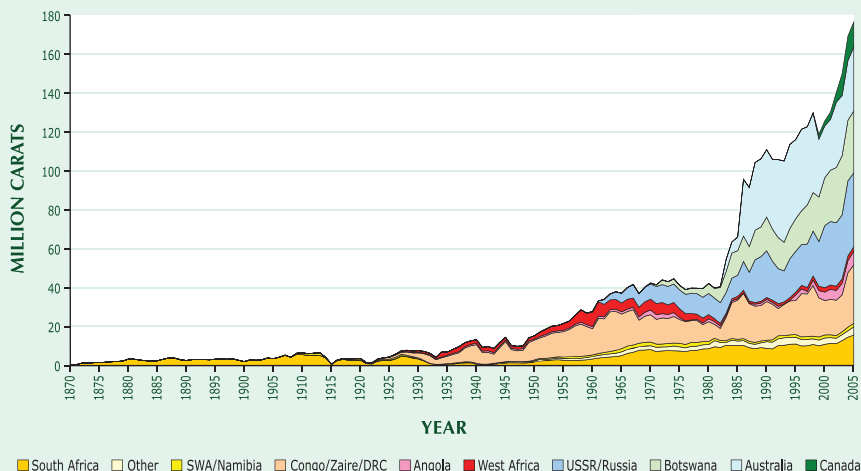


Figure 2. This chart shows global diamond production by carat weight from 1870 to 2005 for eight countries, one region in Africa, and all other producers (“Other”). South Africa’s early dominance gave way to production from the Belgian Congo in the 1930s, which in turn was eclipsed by production from Russia, Botswana, and Australia.

an increase in illicit production brought the official level down during 1960–65. It reached a peak in 1972, after which it declined from 1984 to 1990. It rose again after 1997, amounting to 2.4 Mct in 2005.

Soviet Union/Russia. Soviet production commenced in 1960, and sources used to estimate the caratage mined indicate that it rose quickly to 7 Mct in 1967 and 10.3 Mct in 1977. It stayed around this level until 1985 and then rose to 24 Mct in 1990. Following the dissolution of the Soviet Union in 1991, there was a slight dip in 1993, and from then on a gradual increase to 23 Mct in 2002.

These were the *estimated* figures, however, as the actual numbers were considered state secrets during this period. It appears now that in fact the annual Russian diamond production by weight has been significantly underestimated for years, since production was only reported in *monetary* values. Based on the assumption that the overall value per carat was similar to that of South Africa and Botswana, Russia’s annual production was estimated at around 20–23 Mct for the last 10 years. When Russia became the annual president for the Kimberley Process in 2005, Alrosa (Russia’s major diamond mining company) released data at the end of 2004 that showed the US\$1.68 billion value for 2003 was actually based on \$51/ct (Janse, 2005) and not on the values of about \$80/ct given in world diamond production figures reported by reputable sources (e.g., Government of Northwest Territories, 2001–2004; Even-Zohar, 2002). This raised the production for 2003 from the assumed 19 Mct to a staggering 33 Mct.

The lower value per carat was due to the fact that Russian mines recover diamonds down to 0.2 mm, which increases the grade and the cost, but lowers the value per carat. The production for 2004 was worth about \$2.2 billion, with an average value of \$56.74/ct, which equates to an annual production of 38.7 Mct for 2004 (Kimberley Process Certification Scheme, 2004). The value of production for 2005 was \$2.53 billion, with an average value per carat of \$66.61 (Kimberley Process Certification Scheme, 2005). This translates to an annual production of 38 Mct for 2005. This higher value per carat may be due to the fact that new mines—the Nyurba open pit and the Aikhal and Internationalaya underground operations—have adopted a screen-size cut off of 1.5–2 mm, as is the custom for Western mining companies, which increases the average value per carat (screen size and its effects on grade and value are discussed in more detail in the Major Diamond Mines/Current Value section below).

Botswana. Production began in 1970 and rose to 2.5 Mct in 1972, when the Orapa mine reached full capacity. Orapa’s expansion in 1979 and the opening of the Letlhakane mine brought the level up to 5 Mct in 1980; this doubled to 10 Mct in 1983 as the Jwaneng mine came on board, and doubled again by 1997, after further expansion of Orapa. It has climbed steadily since, to about 32 Mct in 2005.

Australia. Meaningful production commenced after a diamond-bearing lamproite was discovered near Lake Argyle in 1979 (Shigley et al., 2001). The first diamonds (0.5 Mct in 1982) came from alluvial

deposits nearby; alluvial and surface mining produced 7 Mct in 1985. When mining of the AK1 pipe began in 1986, production soared to 29 Mct that first year, then rose gradually to a peak of 43.3 Mct in 1994. Annual production dropped sharply from 40.9 Mct in 1997 to 26.7 Mct in 2000 due to reconstruction of the open pit, which necessitated the removal of much barren ground. Production further declined to 26 Mct in 2001 with the mining of lower-grade ore, after which it rebounded to about 33 Mct in 2005. The open pit will be phased out by 2008, when underground mining will commence. (The Argyle underground mine is discussed further in the Advanced Diamond Projects section below.)

Canada. The latest entry is Canada, which began production in 1998 (Kjarsgaard and Levinson, 2002) and reached 5 Mct in 2002, all derived from the Ekati mine. With the opening of the Diavik mine in 2003, production rose to 11 Mct that year and then to the 2005 level of 12.8 Mct.

Other Producers. Individual production from the remaining producers has generally been less than 0.5% (by weight) of global annual production. The exceptions are the Central African Republic (0.22% by weight, 0.51% by value), which for many years has produced about 400,000 carats valued at about \$60 million annually, and Lesotho (0.03% by weight, 0.55% by value), which started mining in 2004 and in 2005 produced 52,000 carats worth \$64.3 million. Notably, Lesotho has produced some

large diamonds valued at over \$1,240/ct (Kimberley Process Certification Scheme, 2005). Its production will tend to increase as the country's two diamond mines (Letseng and Liphobong) are developed further. Production in Zimbabwe (0.31%) commenced in 2004 and is planned at 250,000 carats (worth \$36 million) annually, though the current political situation makes this uncertain. Tanzania (0.13% by weight, 0.22% by value) produced 220,000 carats worth \$25.5 million in 2005 and will probably stay at this level. Estimates for annual Brazilian production (including informal production) have been up to 1 Mct in the past, according to U.S. sources, but Kimberley Process data for 2005 put it at 300,000 carats worth \$21.85 million. Including Guyana and Venezuela, South America currently accounts for 700,000 carats worth \$57 million, which is only 0.4% by weight and 0.5% by value of global production. Similarly, annual production for China was estimated at 1.1–1.2 Mct by U.S. sources, but was only 71,764 carats worth \$1 million for 2005 by Kimberley Process data. Other minor producers in 2005 were India (60,000 carats worth \$98 million) and Indonesia (17,557 carats worth \$5 million).

Worldwide. Global production for 2005 was 176.7 Mct, a staggering amount compared to earlier years: 1.9 Mct in 1900; 4.2 Mct in 1925; 15.2 Mct in 1950; 41.6 Mct in 1975; and 126 Mct in 2000 (though the number for 2000 represented a dip because of the decrease in Australian production from 1997 to 2000; see above).

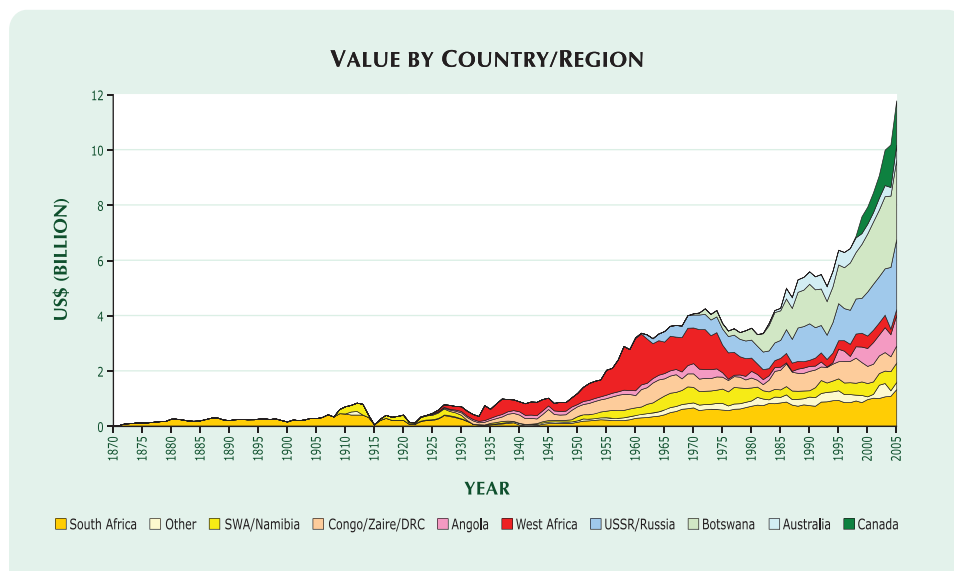
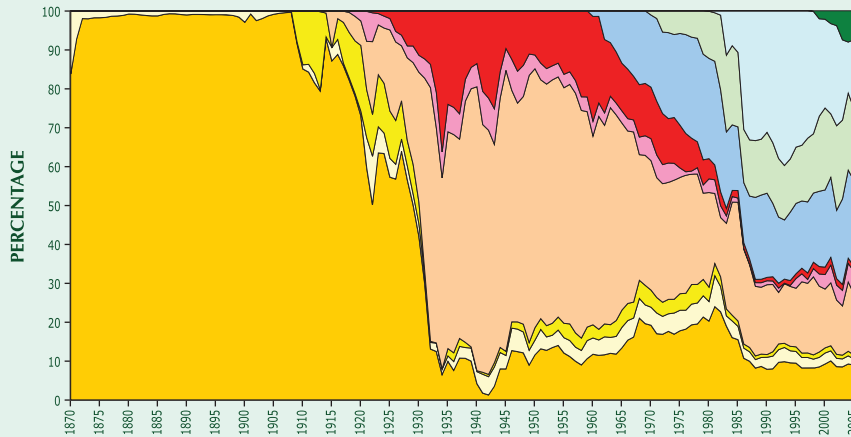


Figure 3. This chart shows production by (year 2000) U.S. dollar value for the same regions as in figure 2. Here, Congo/Zaire/DRC production for the most part is much less important than that of the higher-value alluvial diamonds from West Africa, and Australia's production is no longer as significant as that from Russia and Botswana.

PERCENT CARAT WEIGHT BY COUNTRY



PERCENT VALUE BY COUNTRY

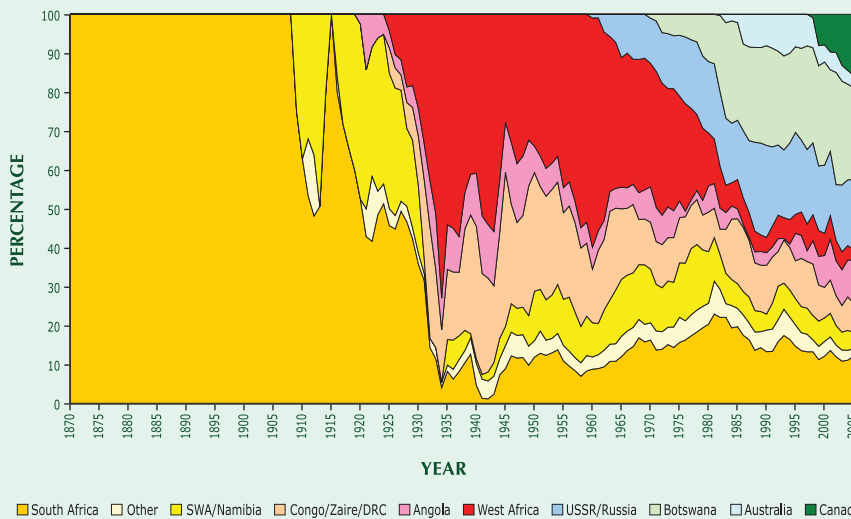


Figure 4. These charts compare the data in figures 2 and 3 as percentages of world production by country. The early dominance of Congo/Zaire/DRC production is clear when considered by carat weight (top), again giving way to Australia, Russia, and Botswana. Considered by dollar value (bottom), however, the alluvial production from West Africa is dominant from 1935 to the early '70s, while the lower value of Australia's production greatly reduces its impact.

By Value. The graph for annual values of production, based on year 2000 U.S. dollars (figure 3), shows quite different features compared to the graph for carat weight. The significant value of the South-West Africa production from 1910 to 1913 is quite distinct. In contrast, the band for Congo/Zaire/DRC from 1930 to 2005 is narrower due to the low value per carat. Angola shows an increase during the last decade, but the thickness of the band for West Africa from 1935 to 1975 is quite remarkable due to the high value of the diamonds from Sierra Leone and Guinea. The greatest contrast is shown by Australia: The band from 1985 to 2000 for value is very thin compared to that for carat weight (again, see figure 2), due to the low average value and the large quantities of diamonds produced.

RELATIVE PERCENTAGES FOR EACH COUNTRY BY WEIGHT AND VALUE

The annual production data have also been plotted as percentages of total production by weight and value for the same groups as in figures 2 and 3. This gives a better understanding of the relative significance of the producing countries. Figure 4 (top) shows the dominance of South African production by weight from 1870 to about 1930. A small shift occurred in 1909, when production from the coastal deposits in South-West Africa commenced, but a dramatic shift occurred after 1930, when most diamonds came from alluvial operations in the Belgian Congo and West Africa. The proportion from those two regions had started to decline by 1970, after production first from the USSR and then from Botswana entered the

market, with another big shift occurring when Australia's Argyle mine came on stream in 1986.

The percentages for value (figure 4, bottom) also show the dramatic shift after 1930, but here we see the greater impact of the higher value per carat brought by the rough from South-West Africa and especially West Africa. The shift after 1985, when Australian production commenced, is less pronounced, because the value of Australian rough is low, especially as compared to the diamonds from Botswana.

RELATIVE PERCENTAGES BY TYPE OF DEPOSIT

The relative proportions of diamonds produced from pipes (primary kimberlite or lamproite deposits), alluvials (secondary deposits formed by erosion and subsequent river transport), or beach (littoral deposits, discharged from river mouths into the ocean) have varied greatly over time. The two graphs in figure 5 show the percentages of annual production by weight and value represented by these three types of deposits.

By Weight. Although the earliest diamonds to enter the marketplace came from alluvial deposits in India (from antiquity to the mid-18th century) and

Brazil (from the 1720s onward), truly commercial quantities did not become available until the discovery of diamonds related to kimberlite pipes in South Africa starting in the late 1860s (see, e.g., Janse, 1995). Diamond production rose from tens of thousands of carats in the late 1860s to more than one million carats in 1872, almost all produced from the pipes at Kimberley (figure 6). During this period, only minor production came from alluvial deposits in Brazil and South Africa. From 1872 to 1909, pipe production reigned supreme.

For the next 50 years, 1910–60, the relative proportions of diamonds produced from primary versus alluvial and beach deposits shifted dramatically. Large beach and alluvial deposits were discovered, first along the coast of South-West Africa and later in the Belgian Congo, Angola (figure 7), West Africa, and South Africa (along the coast of Namaqualand and inland near Lichtenburg). By 1935, pipe production had dropped to less than 4% of the total versus 95% alluvial production (the remainder representing beach production). The sudden rise in alluvial production and dip in beach production (from German-occupied South-West Africa) in 1915 are anomalies due to WWI. Otherwise, production from beach deposits is significant from 1909 to 1925 and reached peaks of 12% in 1912 under German administration (SWA), and 16% in 1920 under the new administra-

Figure 5. Shown here are the trends in global diamond production by type of deposit, as percentages of the total. In carat weight (left), pipe production from South Africa constituted the bulk of world production until alluvial deposits from West Africa and Central Africa (the Belgian Congo and Angola) came on stream in the 1930s. With the discovery of large primary deposits in Russia, Botswana, Australia, and (most recently) Canada, pipe production has made a comeback since the 1960s. The trends by value (right) are similar, although South-West Africa/Namibia's beach production (and its high-value diamonds) are more significant, and the dominance of pipe production since the 1970s is not as pronounced, in large part because of the low-value diamonds from Australia's Argyle deposit.

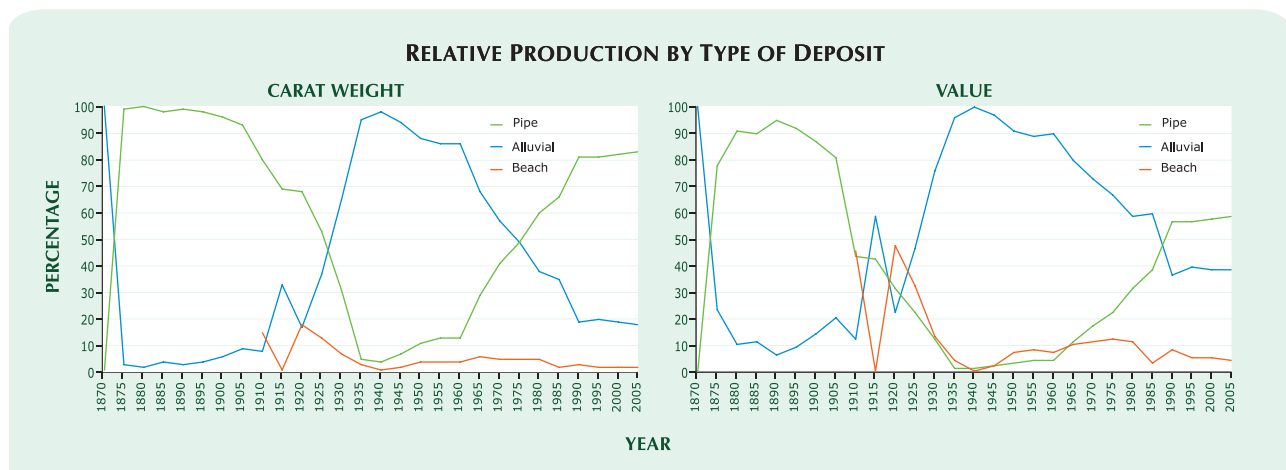




Figure 6. This 1872 photo shows the chaotic conditions that existed at the Kimberley pit in South Africa shortly after diamond mining there began in earnest. Annual world production by this point had already leaped from a few tens of thousands of carats to over a million. Photo © Bettmann/Corbis.

tion of the Consolidated Diamond Mines of South Africa, after which it declined in proportion to the rise in alluvial production.

Pipe production started to make a comeback in the 1960s, when modern methods of prospecting (stream sampling surveys for indicator minerals and airborne magnetic surveys) resulted in the discovery of large kimberlite pipes in South Africa (Finsch), Botswana (Orapa; figure 8), and Siberia (Mir and Udachnaya), which came on stream from the middle of the decade into the early 1970s. By 1990, with

numerous additional discoveries, production of primary deposits represented 80% of the total, and this number has continued to creep upward since then. Although these discoveries reestablished the dominance of pipe production, they also began to shift the focus away from Africa. Before 1960, African countries accounted for nearly all the world's diamonds (again, see figure 4). In 1980, however, African pipe, alluvial, and beach deposits combined accounted for 70% of the total, with 25% from Siberia (virtually all pipe), and 5% from others (mainly alluvial).

Figure 7. The discovery of alluvial deposits elsewhere in Africa signaled a shift from pipe mining to alluvial mining that persisted until the middle of the 20th century.

The rich alluvial deposits in Angola are worked by both large mechanized mining operations and small groups of artisanal diggers, such as these miners in Lunda-Norte Province in northwest Angola. Photo © 2007 Olivier Polet/Corbis.





Figure 8. Discovered in 1967 (and shown here in 2005), the Orapa mine in Botswana is one of the largest kimberlite deposits ever developed. Though later eclipsed in value by the Jwaneng mine (discovered in 1973), it remains a key element in Botswana's diamond industry. The discovery of large mines there and in Russia through modern prospecting methods helped reestablish the dominance of pipe production in the 1960s and 1970s. Photo by Robert Weldon.

The percentages shifted again when the Argyle AK1 lamproite pipe was discovered in 1979 and came on stream in 1986. Argyle is the world's largest single deposit in terms of production by weight, and at its peak in 1994 it yielded up to 40% of world production (though only 7% by value); that year, most of the remaining diamonds came from Russia (15%) and Africa (42%). Production from the Argyle pipe pushed global pipe production over 80%. Although Argyle's annual production had declined by 2000, it is likely that global pipe production will stay at this level due to recently discovered pipes in Canada, Russia, and Angola.

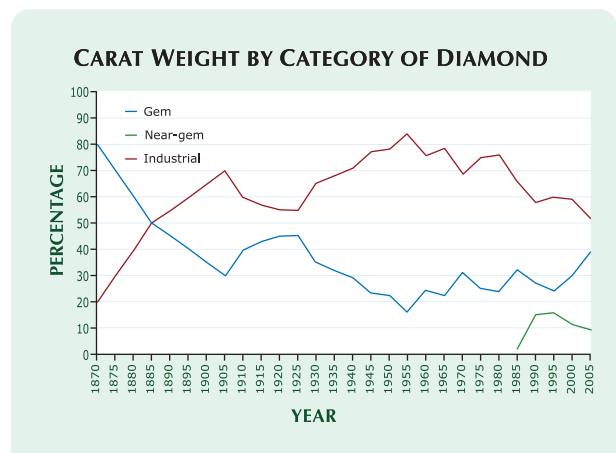
By Value. The annual production by value for each type of deposit shows a pattern similar to that for carat weight, except that the dominance of alluvial production from 1925 to 1980 is more pronounced. It clearly demonstrates the high value of beach deposits during their active years for the periods 1910 to 1930 and 1960 to 1990, though tapering off toward 2005. After 1980, the Argyle pipe is far less dominant because of the low value of its diamonds, while the high value of African alluvial production has retained its importance.

RELATIVE PERCENTAGES BY CATEGORY OF DIAMOND

The production data given thus far have included all qualities of diamond, gem and non-gem. Figure 9 shows the division into gem, industrial, and (over the last two decades) near-gem diamonds.

Before 1870, the percentage of gem-quality diamonds was high because all production was derived from alluvial deposits, and primitive mining methods were geared to recovering larger, good-looking stones. In the early days of pipe mining, recovery was still

Figure 9. The shifts in type of production (gem, industrial, and near-gem) in large part mirror the changes in technology and the types of deposits being mined. Early mining methods were not geared for the recovery of industrial diamonds, but this changed as modern pipe mining evolved. The peak in industrial production during the middle of the century reflects the large input of low-value diamonds from the Congo/Zaire. This began to fall as higher-value diamonds from Russia and other sources came on stream. Only since 1985, with the opening of the Argyle mine, is near-gem production indicated.



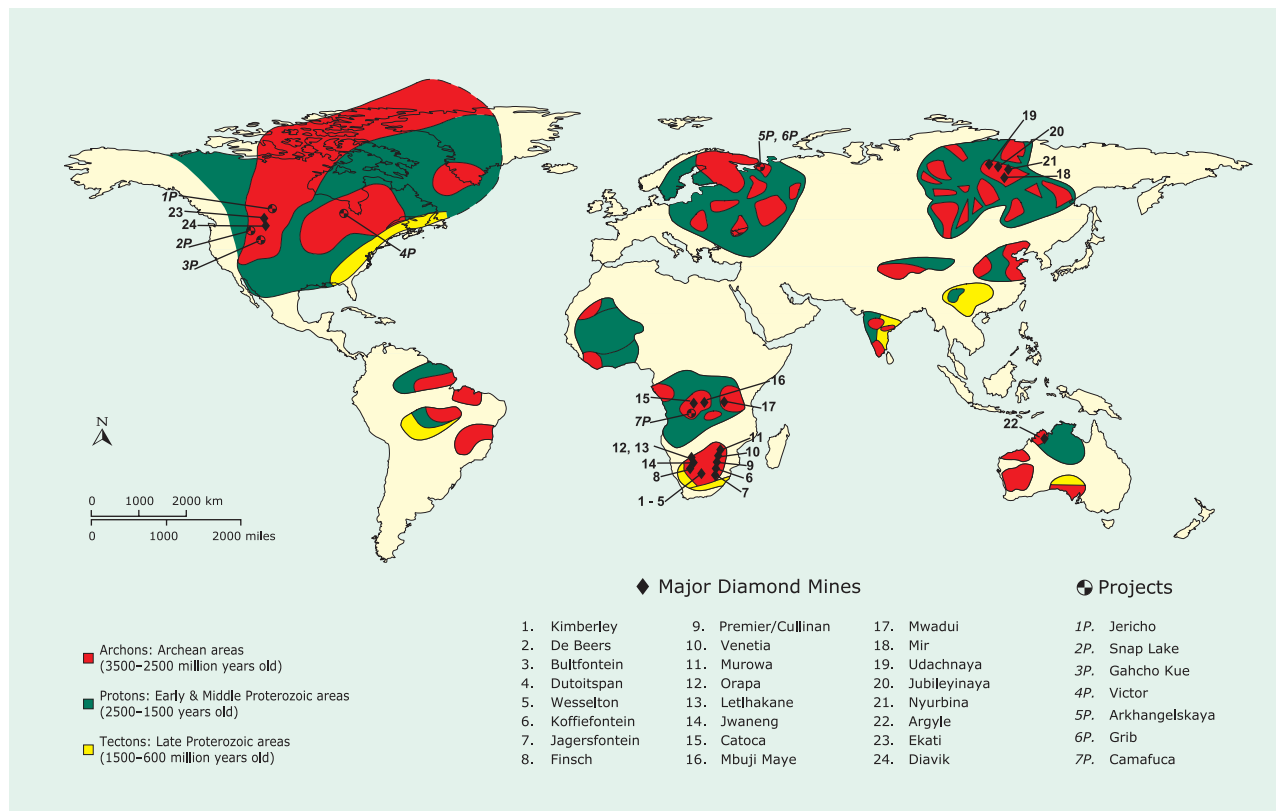


Figure 10. This map shows the tectonic location of 24 major diamond mines and seven advanced diamond projects. All major mines developed on kimberlite pipes are located within the boundaries of an archon, while those developed on lamproite pipes are located on a proton.

carried out by jiggling, sieving, and hand sorting, and this tendency continued until about 1885. When recovery from the pipe mines became more mechanized, there was a progressive increase in the percentage of smaller stones and industrial diamonds, so that the proportion of gem-quality rough dropped gradually from 50% in 1885 to 30% in 1905. After this point, the gem percentage increased to 45% from 1910 to 1925 because of the emergence of the beach deposits, which yield mainly gem-quality stones. It declined again from 1925 to 1955 due to the large output from the Mbuji Maye mines in the Belgian Congo, which have a high percentage of small and industrial diamonds. From 1960 to 2000, gem diamonds varied between ~20% and ~30% of total production, but since then the proportion has increased because of the new Canadian mines, which have a high percentage of gem-quality diamonds, and the decreasing output from Argyle. The Argyle mine—and the corresponding development of a low-cost cutting industry in India to fashion small stones from rough that once would have been used for industrial purposes—is also responsible for the relatively new category, “near-gem” diamonds. Between 1985 and

1995, “near gems” represented as much as 17% of total production.

As would be expected, gem-quality diamonds are responsible for almost all production by value. Only in the last 20 years has the near-gem category had any significance. Between 1985 and 1995, it rose to represent as much as 10% of the total value of diamonds produced. With the declining production at Argyle, however, it had dropped to less than 4% by 2005.

THE MAJOR DIAMOND MINES

The world’s 24 major diamond pipe mines (both historical and currently active) and seven (eight if Argyle’s underground operation is included) advanced projects are plotted on figure 10, which shows the three tectonic crustal elements according to the Janse (1994) terminology—archons, protons, and tectons—which was developed from Clifford’s Rule that kimberlites are restricted to cratons older than 1,500 million years (Clifford, 1966). Thus far, all major diamond mines developed on kimberlite pipes are located within the boundaries of an archon,



Figure 11. The Argyle diamond mine in northern Australia is the world's largest single producer of diamonds by weight, though the open pit is nearing the end of its active life. Argyle is also the only major mine situated on a lamproite pipe. Photo © Roger Garwood and Trish Ainslie/Corbis.

while those developed on lamproite pipes are located on a proton. Even though only one major diamond mine is underlain by a lamproite pipe (Argyle in Australia; figure 11), several small diamond mines on lamproite pipes and other occurrences of diamond-bearing lamproites (not shown on figure 10) are also located on protons and hence support this view. Figure 10 also shows that to date major dia-

mond mines (other than Argyle) have clustered into three regions of the world: southern Africa, Siberia, and western Canada.

Data for ownership, location, size, annual production, ore reserves, value, and "life" for the 24 mines are compiled in table 1. Included is the status as of 2005 for 16 major active pipe mines. For comparison, historical data for seven important but inactive De Beers mines and the Mir open pit mine (closed in 1998; figure 12) are also provided. Table 1 comprises 15 columns, some of which are discussed in more detail below.

Name of Mine (Col. 1). Most of the mines are developed on a single pipe bearing the same name. In recent years, however, it has been found that an economically viable "mine" can be established by combining the volumes of several small pipes. Five such mining areas are included here: (1) Murowa, which draws ore from four small pipes; (2) Mbuji Maye, which includes production from the kimberlite pipes of Tshibua and its derived secondary deposits, as well as additional smaller pipes nearby; (3) Argyle, which for some periods (1983–1985; 1989–2002) drew up to 20% of its production from nearby alluvial deposits; and (4) Ekati and (5) Diavik, which draw ore from, respectively, five and two (increasing to four) pipes.

Majority Owner (Col. 2). Most of the older mines are (or were) owned outright by De Beers (in South Africa) or by De Beers in joint venture with local governments, such as Debswana (50% Botswana) and Mwadui (25% Tanzania). The Canadian mines are also jointly owned: Ekati (BHP 80%; Charles Fipke and Stewart Blusson, the original prospectors, 10% each) and Diavik (60% Rio Tinto, 40% Aber Resources; figure 13). Catoca is owned by a consortium of four entities: Endiama (an Angolan parastatal [government-owned] company) 32.8%, Alrosa 32.8%, Odebrecht (a Brazilian company) 16.4%, and Dau-monty Finance Corp. (a Lev Leviev company) 18%.

Size (Col. 4). It should be noted that in several cases only part of the total volume of a pipe is mined. For example, at Argyle the southern part—with a surface outcrop of 12 hectares—has been mined for most of its life, while only in the last two years has mining progressed to shallow northern parts of the pipe. The size given for Mbuji Maye is for Tshibua pipe 1 only.

TABLE 1. Historic and production data for 24 major diamond mines discovered since 1869.^a

Col. 1	Col. 2	Col. 3	Col. 4	Col. 5	Col. 6	Col. 7	Col. 8	Col. 9	Col. 10	Col. 11	Col. 12	Col. 13	Col. 14	Col. 15
Name of mine	Majority owner	Country	Size (ha) ^b	Year of discovery	Year of opening	Annual production (kct/yr) ^c	Grade (cpht) ^d	Current value (\$/ct) ^d	Current value (\$/t)	Annual value (M\$/yr) ^e	Total production (Mct) ^f	Total production (M\$) ^g	Past life (yr)	Future life (yr)
Bultfontein ^h	De Beers	South Africa	9.7	1869	1901	874	54	75	40	66	24.5	1,838	105	Closed (2005)
Dutoitspan ^h	De Beers	South Africa	10.8	1869	1905	540	32	140	45	76	20	2,800	100	Closed (2005)
Jagersfontein ^h	De Beers	South Africa	10	1870	1902	363	12	200	24	73	9.5	1,900	60	Closed (1971)
Koffiefontein ^h	De Beers	South Africa	10.3	1870	1898	110	7	250	18	28	12	3,000	98	Closed (2005)
De Beers ^h	De Beers	South Africa	5.1	1871	1871	600	72	100	72	60	36.4	3,640	68	Closed (1960)
Kimberley ^h	De Beers	South Africa	3.7	1871	1871	500	200	80	160	40	32.7	2,900	44	Closed (1914)
Wesselton ^h	De Beers	South Africa	8.7	1891	1897	576	37	90	33	52	28.5	2,565	99	Closed (2005)
Premier/Cullinan	De Beers	South Africa	32.2	1902	1903	1,250	40	75	30	94	146	10,950	103	5
Finsch	De Beers	South Africa	17.9	1961	1965	2,000	36	75	27	150	113	8,475	41	21
Venetia	De Beers	South Africa	12.7	1980	1991	6,800	122	90	110	612	68	6,120	15	11
Mwadi	De Beers	Tanzania	146	1940	1942	317	11	145	16	46	19	2,755	64	5
Orapa	Debswana	Botswana	118	1967	1971	16,000	95	50	48	800	222	11,100	35	23
Letlhakane	Debswana	Botswana	11.6	1968	1976	1,100	29	200	58	220	22	4,400	30	7
Jwaneng	Debswana	Botswana	45	1973	1982	15,600	140	110	154	1,716	238	26,180	24	23
Murrowa	Rio Tinto	Zimbabwe	4	1997	2004	250	90	65	60	16	0.3	20	1	19
Mbuji Maye	MIBA	DRC	18.6	1946	1924	9,000	500	15	75	135	500	7,500	90	20
Catoca	consortium	Angola	66	1985	1997	6,000	45	75	34	450	23	1,725	9	20
Mir ⁱ	Alrosa	Russia	6.5	1955	1957	4,000	300	80	240	320	90	7,200	42	20 ^j
Udachnaya	Alrosa	Russia	27	1955	1976	20,000	120	55	66	1,100	540	29,700	31	20 ^j
Jubileynaya	Alrosa	Russia	50	1989	1997	10,000	56	45	25	450	50	2,250	9	20
Nyurba	Alrosa	Russia	nd	1998	2004	5,000	90	55	50	275	6	330	2	20
Argyle	Rio Tinto	Australia	46	1979	1985	30,476	310	13	40	396	700	9,100	21	10 ^j
Ekati	BHP Billiton	Canada	11	1992	1998	6,000	100	140	140	840	32	4,480	7	13
Diavik	Rio Tinto	Canada	5	1994	2003	8,475	372	88	327	746	21	1,848	2	20

^a Sources: De Beers Consolidated Mines (1880–2005); Wagner (1914); Hamilton (1994); Wilson and Anhaeusser (1998); Government of the Northwest Territories (2001–2005); Even-Zohar (2002, 2007); BHP Billiton (2007); Rio Tinto Diamonds (2007a,b); and author's files.

^b Values for sizes of pipes are modified from Janse (1996) and author's files; 1 ha (hectare) = 2.47 acres.

^c Annual production figures are in thousands of carats (kct/yr); for the first seven mines listed and for the Mir open pit (all of which are now inactive), see notes "h" and "i."

^d Values for grade in cpht (carats per hundred tonnes) and \$/ct (U.S. dollars per carat) are approximate and vary from year to year as different types of ore are mined. Except for the first seven mines listed and for Mir (see notes "h" and "i"), the latest robust values are from 2003 and are extrapolated to 2005 by the author.

^e Figures for annual value (in millions of U.S. dollars) were calculated by multiplying annual production (col. 7) by \$/ct (col. 9).

^f Total production figures (in millions of carats) were estimated by adding annual production figures, including from tailings, for the years of the life of the mine (col. 14).

^g Total production values to date (in millions of U.S. dollars) are calculated by multiplying total production (col. 12) by value per carat (col. 9).

^h The annual data for the five old Kimberley mines, Jagersfontein, and Koffiefontein (shaded in gray) are values chosen by the author from typical years of production throughout the life of the mine. Figures for grade were chosen likewise, and comparative values for \$/ct were recalculated taking the De Beers mine as \$/ct=\$100.

ⁱ The Mir open pit closed in 1998; the figures for annual production, grade, and \$/ct are derived from an average year in the 1980s.

^j Future production for Argyle, Mir, and Udachnaya is for underground workings only.

Years of Discovery and Opening (Cols. 5 and 6). In general, the time between discovery and commencement of mining varies from six to 10 years. This time frame has expanded in recent decades, as several stages of studies—e.g., scoping, pre-feasibility, feasibility, water use, and environmental and social

impact—are required before authorities will issue permits and banks will lend money. The dates for Mbuji Maye appear to conflict because mining on associated alluvial deposits commenced in 1924, but the kimberlite deposits were not recognized until 1946 [Magnée, 1946].



Figure 12. The Mir pit in Yakutia, which ceased open-pit mining in 1998, was the first major diamond mine to be developed in what was then the Soviet Union. The discovery of Mir and several other large kimberlite pipes in this region represented the first meaningful non-African production to enter the world market in over 100 years. Photo taken in 1995 by James Shigley.

Annual Production (Col. 7). This figure is reported in thousands of carats recovered during 2005, except for the first seven mines listed and for the Mir open pit (all now inactive), for which—for comparison to currently active mines—a production value was chosen by the author from a past year that appeared typical. Annual productions vary through time and generally increase when the mine plants are expanded and decrease as the deposit is depleted. In some cases, the open pit becomes too deep and the

pit walls need to be reconstructed (as happened to Argyle in 1999, when annual production fell from nearly 41 Mct/yr to 27 Mct/yr; see figure 2), or the mining method switches from open pit to underground (e.g., figure 14).

Grade (Col. 8). Grade—the yield of carats per 100 tonnes (cpht)—is the quotient of carats recovered during the year divided by tonnes (metric tons) of ore mined. It varies considerably between pipes. Grades



Figure 13. Canada's dramatic rise up the rankings in world diamond production has been the result of rich mines such as Diavik, shown here in a September 2006 image. A large dike had to be constructed to hold back the waters of Lac de Gras and allow safe open-pit mining of the A154 South and A154 North kimberlite pipes in the foreground. Just left of the A154 open pit, work has begun to expose the A418 pipe; production from that pipe is expected to begin in late 2007 or early 2008. Photo by Jiri Hermann, courtesy of Diavik Diamond Mines Inc.

also vary within a pipe. In many cases, the near-surface weathered rocks are higher in grade than the deeper rocks. For example, at Kimberley the grade was well over 200 cpht for the first 250 m of mining, but it had decreased to 40 cpht at closure in 1914 and averaged just over 100 cpht for the life of the mine (Janse, 1996).

Current Value (Cols. 9 and 10). Data for the average value per carat are not publicly listed by many mining companies, but they can be derived from the reports on sales of parcels of diamonds mined during the year and from estimates from diamond valuers and diamantaires who have inspected the run-of-mine product.

In some mines, such as Jagersfontein and Koffiefontein, the grade was very low (below 12 cpht), but the \$/ct was high (over \$200/ct); thus, the mines were viable. At Argyle the initial grade was very high (600 cpht) but the value per carat for the first production was very low (\$7/ct), and the mine would only be viable if operating costs could be kept low. This was done primarily by mining large volumes of ore, which kept the average cost per tonne down. In some mines—such as Jwaneng (Botswana), Mir (Siberia), Ekati (Canada), and Diavik (Canada)—both the grade and \$/ct are high, making them very profitable. Value per carat is influenced not only by the quality but also by the average size of the diamonds recovered. Generally, this is between 0.4 and 0.5 ct; diamonds over 2 ct are rare, amounting to only about 7% by weight (but 44% by value) of world production (Even-Zohar, 2002).

The product of multiplying the current grade (col. 8) by dollar value per carat (col. 9) gives the average value per tonne in the ground (\$/t; col. 10), which is one of the major factors in deciding if a project is economically viable. The second major factor is revenue, that is, the quotient of the value per tonne in the ground divided by the cost of mining it. Very approximately, this figure needs to be above one to make a viable mine, but several other factors (such as the time value of money, political risks, and environmental restrictions) must be factored into the decision to proceed with construction. In general, the \$/t varies between 30 and 100. Because data on mining cost per tonne are usually not publicly available, a column for revenue is not included.

Grade, value per carat, value per tonne, and ore reserves (see Past and Future Lives below) are all interrelated. Grade is typically a result of the recovery plant's cut-off screen size. If the bottom screen



Figure 14. Open pit mines eventually reach a depth at which the costs of further recovery by open-pit mining exceed the revenue produced. The mine will either close or shift to underground mining if there are sufficiently valuable reserves to make it economic. This miner working underground in the De Beers Finsch mine is using an automatically synchronized operated multiple drill in preparation for planting explosives to blast out another mass of kimberlite. Photo © Hervé Collart/Sygma/Corbis.

size is small (0.2 mm), many very small diamonds will be recovered in addition to commercially sized diamonds (1.5 to 2 mm) and the grade is high (as are ore reserves), but the cost of recovery goes up and the value per carat goes down because of the large quantity of small diamonds recovered from a tonne of ore. In general, most mines use bottom cut-off screen sizes between 1.5 and 2 mm, as the revenue from recovering more small diamonds usually does not compensate for the higher cost of recovery. However, this is a purely economic decision that has to be considered for each deposit on its own. Some mines have recently lowered this cut-off to 0.85–1.2 mm (see Tahera Diamond Corp., 2007), since the market for smaller rough has grown as cutters (mainly in Indian cottage industries) have become adept at manufacturing very small stones (Even Zohar, 2002). Raising the bottom cut-off, as Argyle did in 1994 (from 0.4 mm to 1.5 mm), lowers the grade, lowers ore reserves, decreases cost, but increases the value per carat and thus revenue. Likewise, costs increase when the top screen size is set high in order to recover possible large diamonds, but the revenue from these diamonds can compensate for the higher costs if the mine produces enough

of them. A top size of 25 mm is most common, but for some mines that have historically produced large diamonds, such as Premier/Cullinan, the top screen size is 36 mm.

Past and Future Lives (Cols. 14 and 15). Several active mines—such as Murowa, Catoca, Jubileynaya, Nyurba, Ekati, and Diavik—have existed for less than 10 years, and this affects the data for total amount of diamonds recovered and their value, which are too low to give a representative rank. Therefore, those mines for which reliable data on future ore reserves are available (all except Jubileynaya and Nyurba) are included in the table for advanced projects (table 2). Most major mines, except those based on several small pipes, have life expectancies of 50–100 years (e.g., the Kimberley mines and Premier/Cullinan). However, most mining companies and analysts do not attempt to calculate ore reserves, and thus life, beyond 20 years because such estimates eventually become too speculative.

ADVANCED DIAMOND PROJECTS

During the last few years, four of the old underground De Beers mines in Africa have been closed, and several open-pit mines—Argyle in Australia and

Mir (and possibly others, such as Udachnaya) in Russia—have reached or come close to their economic depth limit. It is therefore important to be aware of the development of advanced projects, which will contribute to the future supply of rough diamonds. It is hoped that data on planned underground mines in Russia eventually will also become available to complete these estimates.

Data for seven major advanced diamond projects and one planned underground mine are compiled in table 2. In contrast to many established mines, most companies now developing advanced projects publish data, updated regularly, on their capital cost of construction, year of projected opening, ore reserves, grade, value per carat, planned annual production, and life expectancy. This is because—in contrast to bygone times—many governmental or stock exchange regulations now require this information to protect shareholders and control wild fluctuations in stock prices. Such data also help government regulatory agencies draw up regional development plans. Note, however, that this is not the case for some countries, such as Russia in the recent past, where these data are traditionally considered privileged information and not disclosed, or for others where such regulations do not exist or are not enforced. Because pre-mine data for four young mines in table 1 are available (Ekati, Diavik,

TABLE 2. Historical and production data for eight advanced diamond projects and four young mines.^a

Col. 1	Col. 2	Col. 3	Col. 4	Col. 5	Col. 6	Col. 7	Col. 8	Col. 9	Col. 10	Col. 11	Col. 12	Col. 13	Col. 14
Name of project/mine	Majority owner	Country	Size (ha)	Year of opening	Capital cost (M\$)	Ore reserves (Mt)	Grade (cpht)	Reserves (Mct)	Value (\$/ct)	Value (\$/t)	Value (M\$)	Projected production (Mct/yr)	Projected life (yr)
Jericho	Tahera	Canada	3	2006	90	2.6	120	3.1	90	108	280	0.4	8
Snap Lake	De Beers	Canada	3	2007	580	23	146	33	76	111	2,500	1.5	20
Victor	De Beers	Canada	16	2008	750	27.4	23	6.3	450	105	2,850	0.6	12
Gahcho Kué	De Beers	Canada	3	2012	745	14.4	164	23.6	77	126	1,800	1	20
Grib	ADC/AGD	Russia	14	nd	nd	98	68	67	79	53	5,300	4	20
Arkhangelskaya	Severalmaz	Russia	15	2006	400	110	52	57	48	25	2,740	3	20
Camafuca	Endiama	Angola	160	2006	25	13	40	5.2	117	47	608	0.2	5
Argyle UG	Rio Tinto	Australia	12	2008	800	100	370	370	13	48	1,200	16	10
Ekati	BHPB	Canada	11	1998	880	78	109	85	84	92	7,100	5	17
Diavik	Rio Tinto	Canada	5	2003	1,170	27	395	107	62	245	6,300	8	20
Murowa	Rio Tinto	Zimbabwe	4	2004	61	19	90	17	70	63	1,200	0.5	17
Catoca	consortium	Angola	66	1997	nd	271	70	189	75	53	14,000	8	20

^aSources: Hamilton (1994); De Beers Consolidated Mines (2001–2005); Government of the Northwest Territories (2001–2005); Even-Zohar (2002, 2007); Tahera Diamond Corp. (2006); BHP Billiton (2007); De Beers Group (2007a,b,c); Rio Tinto Diamonds (2007a,b,c); Severalmaz (2007); and author's files. All figures for reserves, grade, \$/ct, and annual production are derived from bankable feasibility studies and will probably change during actual mining. Abbreviations used here are the same as for table 1; "nd" means no data are available. The rows shaded in blue—Ekati, Diavik, Murowa, and Catoca—are recently opened mines, included for comparison.

Murowa, and Catoca), they have been included here for comparison.

The above notwithstanding, these figures must be viewed with some caution. In general, when a project becomes a mine, it is often found that estimated costs of construction are too low, so ore reserves are calculated on the low side to be safe. Further, grade and value per carat can prove to be quite different when mining has actually progressed during the first year or so, and the life of a mine is often extended as additional ore reserves are discovered while the mine is in operation.

Table 2 comprises 14 columns, some of which are described here in more detail.

Name of Prospect (Col. 1). Jericho is a small mine developed on a small pipe, but neighboring small pipes may be mined in the future. The data in this table are for Jericho pipe 1 only. (Jericho data are placed in this table even though it opened in August 2005, because it only came into actual production in March 2006; Tahera Diamond Corp., 2006). Snap Lake is not a near-vertical pipe but rather a shallowly inclined (about 15°) dike. Victor is a complex of three coalescing pipes that have different ore reserves, grades, and values per carat; data values are averaged over the whole pipe system. Gahcho Kué is a complex of four neighboring small pipes. The Arkhangelskaya pipe is the first of a group of five large pipes in the Lomonosov cluster to be developed into a mine. Camafuca is an elongated pipe (or the fusion of five pipes in a line) underneath the bed of the Chicapa River. Consequently, Camafuca I (the first stage of operation) will be developed as a dredging operation, lasting five years. "Argyle UG" represents data for the underground mine, which is planned to go into production in 2008.

Majority Owner (Col. 2). Three of the four advanced projects in Canada are owned by De Beers Canada. Development of the Russian Grib project has halted because of protracted litigation involving future ownership. This was to be vested in a new company, Almazny Bereg, in which the equities would be ADC (Canada-based Archangel Diamond Corp.) 40% and AGD (Arkhangelskgeodobycha) 60%, but AGD has so far refused to transfer title to the new company. Arkhangelskaya is 97% controlled by Severalmaz, a subsidiary of Alrosa; the rest is held by local authorities. De Beers once held an interest in this project, but it sold its equity to Severalmaz several years ago. Camafuca is owned by a consor-

tium of Endiama (an Angolan parastatal company) 51%, Welox (a Lev Leviev company) 31%, and SouthernEra Diamonds (a Canada-based company) 18% free carried. (*Free carried* interest means that the company has equity in the development of the project, but does not have to contribute to the cost of development. Such interest either ends at the "decision to mine," when the risk has virtually disappeared, or lasts to the commencement of mining, after which the cost of contributing can be subtracted from the profit from mining.)

Size (Col. 4). The size given for Snap Lake is arbitrary; while its surface footprint is quite small, the dike extends underground for an as-yet-undetermined distance of at least 2 km down dip. The sizes of Gahcho Kué, Ekati, Diavik, and Murowa are a total for several small pipes, not all of which are currently mined (but are likely to be mined in the future).

Year of Opening (Col. 5). The scheduled year of opening for the Grib pipe cannot be given, again because of the litigation over ownership. Arkhangelskaya started overburden stripping in 2003; actual mining began on a small scale in 2006.

Capital Cost (Col. 6). This figure, often called *capex* (capital expenditure), represents construction costs only. Thus, the capital costs for Grib cannot be stated, as no mine construction has taken place. The capital costs for Arkhangelskaya are for the first stage of mining the pipe itself. The second stage, constructing a larger plant and a larger open pit in which the Arkhangelskaya pipe and the adjacent Karpinskaya 1 and 2 pipes will be mined, will begin in late 2007. The capex for Diavik is high because the pipes are located under water in Lac de Gras, which was too large to simply drain. Thus, development of Diavik required the construction of large encircling dikes (again, see figure 13), which were expensive to construct because of severe climatic conditions and environmental issues. In contrast, the first stage for Camafuca is a dredging operation, which is relatively simple and has a low cost compared to open-pit mining. Murowa is on land in an area of easy access and requires only small open pits; both African sites (unlike the Canadian mines) have comparatively low labor costs.

Ore Reserves (Col. 7). Given here in millions of tonnes (Mt), reserves are determined by sampling, which usually involves drilling many holes over a

TABLE 3. Historical and contemporary production data and rankings for 27 diamond producing countries: Totals to 2005.^a

Country	Year 1st diamond ^b	Year 1st kimberlite ^b	Year 1st mining ^c	Total prod. (to 2005) (Mct) ^d	Total prod. (2001–05) (Mct) ^d	% World prod. (to 2005) ^e	% World prod. (2001–05) ^e	Rank in world prod. (to 2005)	Rank in world prod. (2001–05)	Value/ct (to 2005) (\$/ct) ^f	Value/ct (2001–05) (\$/ct) ^f
South Africa	1867	1870	1870	614	65	15	9	4	5	95	90
SWA/Namibia	1908	1899	1908	94	8	2	1	8	8	373	373
Botswana	1959	1966	1970	485	148	12	19	5	3	90	90
Rhodesia/Zimbabwe	1903	1907	1913	1.5	0.3			20	19	145	145
Swaziland	1973	1973	1984	0.6	nd			24	25	90	90
Lesotho	1955	1939	1968	0.6	0.08			23	22	1,000	1,000
Southern Africa				1,196	221	29	29				
Angola	1912	1952	1916	111	31	3	4	7	7	155	155
Congo/Zaire/DRC	1907	1946	1913	991	114	25	15	1	4	20	20
Congo Republic	1932	nd	nd	30	nd						
Gabon	1939	1946	nd	4	nd						
CAR	1914	nd	1930	21	2	0.5		15	13	160	160
Tanzania	1910	1925	1925	20	1	0.5		14	16	120	120
Central Africa				1,177	148	29	20				
Guinea	1932	1952	1936	14	2.5			17	11	150	150
Sierra Leone	1930	1948	1932	57	2.5	1		9	10	220	220
Liberia	1910	1955	1955	21	0.5			13	17	100	100
Ivory Coast	1928	1960	1958	8	1.5			18	15	140	140
Ghana	1919	1994	1920	114	5	3	1	6	9	30	30
West Africa				214	12	5	2				
Brazil	1725	1973	1727	36	2.4	1		11	12	75	75
Guyana	1887	nd	1890	6	1.5			19	14	95	95
Venezuela	1883	1982	1913	16	0.3			16	19	60	60
South America				58	4	2					
Canada	1971	1948	1998	51	45	1	6	10	6	115	115
United States	1843	1885	1921	<1	nd			25	25	200	200
USSR/Russia	1829	1954	1960	684	175	16	23	3	1	55	60
Australia	1851	1972	1883	720	154	17	20	2	2	17	17
China	1870	1965	1980	13	0.4	1		12	18	20	20
India	antiquity	1870	antiquity	1	0.4			21	21	165	165
Indonesia	800	nd	800	1	0.01			21	23	280	280
Total global plus 10% illicit				4,115	761	100	100			67	65
				~4,500	~840					67	65

^aSources: The Mineral Industry (1870–1934); Mineral Resources of the United States (1870–1934); Wagner (1914); Minerals Yearbook (1934–2005); and Kimberley Process Certification Scheme (2004, 2005). Abbreviations used here are the same as for table 1; “nd” means no data are available.

^bSources: Janse and Sheahan (1995); Kjarsgaard and Levinson (2002).

^cNote that for several countries, mining began, closed, and sometimes reopened, e.g., Zimbabwe (Somabula, 1913–1930; River Ranch, 1992–1998; Murowa, 2004–present); Lesotho (Letseng, 1968–1982, reopened 2004); United States (Arkansas, 1921–1924; Kelsey Lake, 1995–1996); Russia (Urals, 1890–1917; Siberia, 1960–present); Australia (New South Wales, 1883–1948; Argyle, 1980–present).

^dCalculated by summing up each country’s annual production; illicit production is added as 10% of total global production.

specific grid pattern into a pipe to a certain depth and analyzing the number and value of the diamonds recovered from the drill cores (in some cases, trial mining may be used as well). The larger the diameter of the cores and the more numerous the holes, the better the ore-reserve calculation will be. Also, the deeper the holes, the more potential ore can be outlined (i.e., as a three-dimensional model of reserves) for further calculations. However, drill diameter and depth are constrained by practical and technical parameters, and there are strict guidelines

for the calculation of ore reserves. There is also a practical limit to the depth to which ore reserves can be calculated. Generally, a pipe narrows to a fissure at depth, which results in smaller volumes in cross-cut or plan and thus higher costs of mining; at some point, the mining costs will exceed the value per tonne of ore. Also, the deeper the reserves are projected, the less reliable the results are. Of course, the larger the pipe’s surface outcrop, the larger the cross-cut volumes at depth will be, so large pipes can have ore reserves calculated as deep as 500 m, which is

Total value (to 2005) (B\$) ^f	Total value (2001–05) (B\$) ^f	% World value (to 2005) ^e	% World value (2001–05) ^e	Rank in value (to 2005)	Rank in value (2001–05)
58	5.9	22	13	1	3
35	3	13	5	4	6
45	13.3	17	26	2	1
0.2	0.04			21	20
0.05				24	24
0.6	0.08			23	17
139	22	52	44		
17	4.8	6	10	7	5
21	2.3	8	5	5	8
3.3	0.3	1	1	11	11
2.5	0.1	1		12	15
44	7.5	16	15		
2	0.4	1	1	10	10
12.5	0.5	5	1	6	9
2	0.05	1		13	19
1	0.2			18	13
3.5	0.15	1		14	14
21	1.3	8	2		
3	0.2	1		15	12
1	0.1	0		19	16
1	0.02	1		16	21
5	0.3	2	1		
6	5.2	3	11	9	4
<0.1				25	25
38	10.5	14	21	3	2
12	2.6	5	5	8	7
0.3				17	23
0.2	0.07			20	18
0.3				22	22
266	49.5	100	100		

^eFigures in the percentage columns may not appear to add up correctly, as there are several countries in the list with less than 1%.

^fGiven as present-day values to compare the relative significance of countries only; they are not the values at the time of each year's production.

the case for the Arkhangelskaya pipe, where ore reserves were calculated down to 460 m. In practice, though, ore-reserve projections generally are not carried beyond 100–150 m below surface level.

Value (Cols. 10–12). The value per carat for Victor is very high, as the run-of-mine diamonds recovered thus far are remarkable for their white color, with very few brown or yellow diamonds. The value for Camafuca I is also high for pipe diamonds, but in this case the figures may include some proportion of

alluvial diamonds recovered in the dredging operation. The high overall value for Grib (\$5.3 billion) makes it clear why ADC persists in its legal battles to retain its part ownership in the project. The large Catoca mine has a very high potential value (\$14 billion), while Ekati and Diavik are outstanding at \$7.1 billion and \$6.3 billion.

The value for Arkhangelskaya (\$48/ct) multiplied by grade (52 cpht) gives a suspiciously low value per tonne: \$25/t. In general, new mines are not considered economic below \$40/t, which makes this figure an obvious discrepancy. Unofficial sources say that the value per carat of Arkhangelskaya is in fact similar to that for Grib (~\$80/ct), which would increase the figure to \$42/t, more in line with general economic considerations.

Projected Production (Col. 13). Grib and Arkhangelskaya should be significant mines. Projected annual production for Grib is 4 Mct. For Arkhangelskaya, plans call for a large recovery plant with a throughput of 5.6 Mt annually; if the grade (52 cpht) applies to all three pipes projected to be mined, then an annual production of about 3 Mct can be assumed, which will commence in 2010. Catoca is still increasing its annual production, which may eventually reach 8 Mct. Argyle UG will have a very high annual production, though with a comparatively low total value of \$1.2 billion.

Projected Life (Col. 14). The Jericho mine is projected to be relatively short lived, at eight years, but additional reserves may be discovered in neighboring pipes. The five-year life for Camafuca I is only for the dredging operation, during which time the reserves and a mining plan covering all or part of the pipe will be established, for a projected life of at least 20 years.

THE TWENTY-SEVEN DIAMOND PRODUCING COUNTRIES

Data and statistics for 27 diamond-producing countries (for both total production and 2001–2005) are listed in table 3. Not included are countries for which the occurrence of diamonds or kimberlite/lamproite has been recorded but no diamonds are mined (e.g., Algeria, Finland, Greenland, Kenya, Mali, Mauritania, Mozambique, and Thailand), or for countries from which diamond exports are recorded but no diamond mines are known (e.g., Burkina Faso, Guinea-Bissau, Nigeria, Rwanda,



Figure 15. Not all diamond production has come from organized mining. A significant—though difficult to quantify—percentage has come from informal, or “illicit,” mining by artisanal means. This 1996 photo taken in Sierra Leone shows local diggers using primitive methods to extract diamond-bearing gravels. The diamonds produced are often smuggled out of mining areas to avoid taxes or to obtain higher prices. Photo © Patrick Robert/Sygma/Corbis.

Senegal, and Uganda). The Republic of Congo (Congo-Brazzaville) and Gabon are partially included in the list, as their diamond outputs are recorded in *Minerals Yearbook* for some years, but alleged production for both has been included in the total for the Congo/Zaire/DRC in calculating percentages, rank, and value.

Illicit Mining. It is important to note again that the amount of illicit or informal production can be estimated only very broadly, since it results from the work of artisanal diggers (again, see figure 7, and figure 15), who are typically unlicensed and unregulated by official governmental agencies, and work

mainly on alluvial deposits or on the surface portions of pipes or fissures (dikes). Their output may be purchased by diamond buyers (who also may or may not be licensed) on the spot, but more often it is smuggled to another country to avoid paying taxes or to obtain a higher price in a more stable currency (Even-Zohar, 2002). The amount of illicit digging has varied greatly over time. It was high in Sierra Leone in the 1950s (Laan, 1965; Hall, 1968) and very high in Angola, Zaire/DRC, and Sierra Leone in the 1990s, often far outstripping the official or formal production (Partnership Africa Canada, 2004a,b, 2005a,b, 2006). In the 1990s, a large part of the proceeds of illicit production was used to purchase arms and supplies to equip rebel forces, which often occupied the alluvial diamond fields in these countries and engaged in mining by forced local labor. (This type of illicit production gave rise to the terms *blood diamonds* or *conflict diamonds*, further discussion of which is beyond the scope of this article.) The percentage of illicit digging is high in some places, anywhere from 20% to 100%, while in more regulated countries (such as Canada) it is low or nearly nonexistent. Consequently, a modest (and *arbitrary*) 10% figure for illicit digging has been added to total global production.

Historical Production. As noted earlier, historical production before 1870 was minor in today’s terms and was restricted primarily to India and Brazil, with some production from Indonesia. Information on diamond mining before the mid-1800s can be found in Lenzen (1970), Levinson et al. (1992), and Janse (1996), among other authorities. Diamond mining began in India in antiquity (and was first recorded in a Sanskrit text, the *Arthashastra*, written by Kautilya in the late fourth century BC; Rangarajan, 1992), with minor production from Borneo beginning about 800 AD (Legrand, 1980). Diamonds only became important in the world economy with the commencement of mining in Brazil in the mid-1700s (Lenzen, 1970).

The most important historical producer was South Africa, which dominated the market from 1872 to 1932. Over the full period 1870–2005, it ranks fourth in carat weight and first in value because of its long history of production. South-West Africa/Namibia ranks eighth in carat weight but fourth in value due to the high quality of diamonds in the beach deposits (figure 16).

From 1932 to 1970, the Congo, Angola, and West Africa dominated diamond production. The Congo/Zaire/DRC ranks first in carat weight up to



Figure 16. Namibia's beach mines, despite their relatively small production by weight, have long been an important contributor to the world market because of the very high value of the diamonds they produce. The diamonds are recovered from crevices in the bedrock after the overlying sand has been removed, as shown here in 2005. Photo by Robert Weldon.

2005, but due to the low quality of diamonds from Mbuji Maye, it ranks only fifth in value. Sierra Leone and Guinea rank ninth and 17th in carat weight, but sixth and 10th in value due to the high quality of their diamonds. Ghana ranks sixth in carat weight and 14th in value, again due to the relatively small size and consequent low value of its diamonds. Angola ranks seventh in both carat weight and value over the life of mining there.

From 1970 to 1985, legitimate production from Zaire and West Africa declined because of political upheavals, while newly commenced production from kimberlite pipes in Siberia and Botswana, and increasing production in South Africa, became dominant. The Soviet Union/Russia ranks third in both carat weight and in value, while Botswana ranks fifth in carat weight and second in value.

Production from Australia's Argyle diamond mine entered the market in 1986 and soon introduced a large volume of industrial diamonds. The market absorbed this amount partly by developing the near-gem category of diamonds and partly by scaling back production in South Africa. Consequently, while Australia ranks second in carat weight, it reaches only eighth in value. Canada's production of high-quality diamonds entered the market in 1999, and its rank of 10th in carat weight and ninth in value are low only because of its recent entry.

Brazil dominated world production from 1750 to 1870, but it has been far less significant since that period. Virtually every major river system in Brazil

contains alluvial diamonds, but the country currently has no diamond mines developed on a kimberlite or lamproite pipe. All major production has come from alluvial localities in Minas Gerais and Bahia, with lesser production from Roraima. Recently, the 30,000 ct/yr Chapada alluvial project in Mato Grosso commenced mining, while prospecting for economic kimberlites in Bahia, Minas Gerais, and Rondonia has shown promising results. Brazil's total historical production, as compiled from the U.S. source publications used, is 55 Mct, but Barbosa (1991) estimated diamond production up to 1985 as 100 Mct (too neat a figure for this author's liking). As about 20 Mct were produced from 1985 to 2005, the total production for Brazil would be 120 Mct if Barbosa's figure is accepted. (Note: This illustrates the uncertainty involved in compiling the totals of individual countries, but it does not significantly affect the global total of 4.5 Bct.) Brazil ranks 11th in lifetime carat weight, but would replace Angola as sixth if the higher figure was valid.

Other minor producers include British Guiana (now Guyana) and Venezuela, which commenced production in the late 1890s; the Central African Republic and Tanzania, beginning in the 1930s; and China in the 1980s; however, their combined production has never reached more than 1% by weight and 2% by value of modern global production.

Contemporary Production. Data for 2001–2005 give a modern perspective to the relative significance of

the producing countries. Russia now ranks first in carat weight and second in value, while Botswana is first in value though third in carat weight, just behind Australia. In the future, Botswana will probably exceed Australia in carat weight, since its production is still increasing while Australia's is declining as Argyle switches to underground production. Botswana will probably stay first in value, as Russia has to overcome a gap of nearly \$5 billion to catch up. South Africa has not changed much, with its rank of fifth in carat weight and third in value, but the new success story is Canada, which after only a few years is fourth in value and sixth in carat weight and may overtake South Africa in the near future.

The DRC is now fourth in carat weight and eighth in value and will probably maintain these rankings, since production is likely to increase as its civil disorders have diminished. Also, with the western and eastern Kasai being intensively prospected, new discoveries are likely to be made. Angola ranks seventh in carat weight and fifth in value and is climbing through the ranks, as production from the large Catoca pipe mine is still increasing and additional pipe mines (Camafuca, Camatchia, and Camagico; data for the last two have not been released) will come on stream in the future. Namibia ranks eighth in carat weight and, despite a modest 8 Mct, sixth in value due to the quality of its diamonds. Likewise, the high value of diamonds from Sierra Leone gives this country a rank of ninth in value for a carat weight of 2.5 Mct. The unknown player is China, for which no robust data are available. According to the Kimberley Process figures, its total production has been only 2.5 Mct, and it thus has a very low rank in weight and value. However, diamonds are being aggressively sought in China, and an important discovery could change the situation greatly.

Global production for 2001–2005 was 840 Mct

with a value of \$55 billion, for an average value per carat of \$65.

CONCLUSION

The history of modern diamond production spans 135 years. Although alluvial deposits have been known since antiquity, diamond production from primary deposits (kimberlites and lamproites) commenced only in the 1870s and has increased by leaps and bounds ever since to a staggering total of 4.5 billion carats.

It is interesting to note that nearly 20% of this total was produced during the last five years. During the last 10, nine new mines have commenced production or come very close: Nyurba and Arkhangel'skaya (Russia); Ekati, Diavik, and Jericho (Canada); Murowa (Zimbabwe); and Catoca, Camafuca, Camatchia, and Camagico (Angola). Four additional advanced projects are waiting in the wings: Snap Lake, Victor, and Gahcho Kué (Canada); and Grib (Russia). This will more than counterbalance the closing of seven old mines. As it is predicted that demand for rough will outstrip production during the next five years, and a gap of \$20 million in supply and demand by 2015 has been quoted (Even-Zohar, 2007), this new production can easily be accommodated in the diamond market.

Primary deposits were first discovered in South Africa and exploration spread from there to identify diamond-producing pipes in Tanzania (1940s), Siberia (1950s), Botswana (1960s), Angola (1970s), Australia and northwest Russia (1980s), and Canada and northwest Russia (1990s). Thus, it appears that at least one major diamond mine or field has been discovered every 10 years since the 1940s. If this trend continues, then a major new discovery is imminent. This may perhaps be in China, where prospecting for diamonds is being vigorously pursued at present.

ABOUT THE AUTHOR

Dr. Janse (archonexpl@iinet.net.au) is a diamond exploration consultant living in Perth, Western Australia.

ACKNOWLEDGMENTS

Dona Dirlam and her staff at the Richard T. Liddicoat Gemological Library and Information Center at GIA in

Carlsbad are thanked for access to many books and publications. CAD Resources, Carine, Western Australia, were helpful in constructing the diagrams that accompany the text. The author is also very grateful to the four reviewers—Dr. Jeff Harris, Dr. Melissa Kirkley, Russell Shor, and one who asked to remain anonymous—for their careful work, which made this article more readable and comprehensible.

REFERENCES

- Barbosa O. (1991) *Diamante no Brasil: Histórico, Ocorrências, Prospecção e Lavra*. [Diamonds in Brazil: History, Occurrences, Prospecting and Workings]. CPRM [Companhia de Pesquisa de Recursos Minerais], Rio de Janeiro, 136 pp.
- BHP Billiton (2007) About Ekati. ekati.bhpbilliton.com/about_ekati [date accessed: 06/06/07].
- Boyajian W.E. (1988) An economic review of the past decade in diamonds. *Gems & Gemology*, Vol. 24, No. 3, pp. 102–121.
- Cilliers J., Dietrich C., Eds. (2000) *Angola's War Economy*. Institute for Security Studies, Pretoria, South Africa, 370 pp.
- Clifford T.N. (1966) Tectono-metallogenic units and metallogenic provinces of Africa. *Earth and Planetary Science Letters*, Vol. 1, pp. 421–434.
- De Beers Consolidated Mines (1880–2000). *De Beers Consolidated Mines Annual Report*, Kimberley, South Africa (1880–1980)/London (1980–2000).
- De Beers Consolidated Mines (2001–2005) *De Beers Consolidated Mines Annual Review*, London.
- De Beers Group (2007a) Gahcho Kué. www.debeersgroup.com/debeersweb/about+de+beers/de+beers+world+wide/canada/gahcho+kué.htm [date accessed: 06/06/07].
- De Beers Group (2007b) Snap Lake. www.debeersgroup.com/debeersweb/about+de+beers/de+beers+world+wide/canada/snap+lake.htm [date accessed: 06/06/07].
- De Beers Group (2007c) Victor. www.debeersgroup.com/debeersweb/about+de+beers/de+beers+world+wide/canada/victor.htm [date accessed: 06/06/07].
- Even-Zohar C. (2002) *From Mine to Mistress*. Mining Journal Books, London, 555 pp.
- Even-Zohar C. (2007) *From Mine to Mistress*, 2nd ed. Mining Communications, London, 943 pp.
- Government of the Northwest Territories (2001–2005) Diamond Facts. www.iti.gov.nt.ca/diamond/diamond_facts2005.htm.
- Hall P.K. (1968) *The Diamond Fields of Sierra Leone*. Bulletin 5, Geological Survey of Sierra Leone, Freetown, 133 pp.
- Hamilton R. (1994) Diamond mines: 25 years on. In R. Louthean, Ed., *Australian Diamond Hand Book*, Resource Information Unit, Perth, p. 20.
- Janse A.J.A. (1994) Is Clifford's Rule still valid? Affirmative examples from around the world. In H.O.A. Meyer and O. Leonardos, Eds., *Proceedings of the Fifth International Kimberlite Conference 2, Diamonds: Characterization, Genesis and Exploration*, Departamento Nacional da Produção Mineral, Brasília, pp. 215–235.
- _____. (1995) A history of diamond sources in Africa: Part I. *Gems & Gemology*, Vol. 34, No. 4, pp. 228–255.
- _____. (1996) A history of diamond sources in Africa: Part II. *Gems & Gemology*, Vol. 35, No. 1, pp. 2–30.
- _____. (2006a) Global rough diamond production from 1870 to 2005. *Gems & Gemology*, Vol. 42, No. 3, p. 136.
- _____. (2006b) Major diamond mines of the world: Tectonic location, production, and value. *Gems & Gemology*, Vol. 42, No. 3, pp. 148–149.
- Janse A.J.A., Sheahan P.A. (1995) Catalogue of world wide diamond and kimberlite occurrences: A selective and annotative approach. *Journal of Geochemical Exploration*, Vol. 53, No. 1–3, pp. 77–111.
- Janse B. (2005) The search for diamonds. *Mining Journal*, Aug. 19, pp. 18–25.
- Kimberley Process Certification Scheme (2004) Annual global summary: 2004 production, imports, exports and KPC counts. www.kimberleyprocess.com/images/stories/docs/Global_Summary-2004.pdf.
- Kimberley Process Certification Scheme (2005) Annual global summary: 2005 production, imports, exports and KPC counts. www.kimberleyprocess.com/images/stories/docs/Global_Summary-2005.pdf.
- Kjarsgaard B.A., Levinson A.A. (2002) Diamonds in Canada. *Gems & Gemology*, Vol. 38, No. 3, pp. 208–238.
- Laan H.J. van der (1965) *The Sierra Leone Diamonds: An Economic Study Covering the Years 1952–1961*. Oxford University Press, London, 234 pp.
- Legrand J., Ed. (1980) *Diamonds: Myth, Magic and Reality*. Crown Publishers, New York, 287 pp.
- Lenzen G. (1970) *The History of Diamond Production and the Diamond Trade*. Barrie & Jenkins, London, 230 pp.
- Levinson A.A., Gurney J.J., Kirkley M.B. (1992) Diamond sources and production: Past, present, and future. *Gems & Gemology*, Vol. 28, No. 4, pp. 234–254.
- Magnée I. (1946) Présence de kimberlite dans la zone diamantifère de Bakwanga [Presence of kimberlite in the diamantiferous zone of Bakwanga]. *Bulletin of the Belgian Geological Society*, Vol. 56, No. 1–2, pp. 97–108.
- The Mineral Industry (1893–1932)* The Scientific Publishing Co., New York.
- Mineral Resources of the United States (1883–1922)* U.S. Bureau of Mines, U.S. Geological Survey, Washington, DC.
- Minerals Yearbook (1934–2005)* U.S. Bureau of Mines, U.S. Geological Survey, Washington, DC.
- Partnership Africa Canada (2004a) Diamond Industry Annual Review: Republic of Angola. www.pacweb.org/e/images/stories/documents/angola_ev4.pdf.
- Partnership Africa Canada (2004b) Diamond Industry Annual Review: Sierra Leone. www.pacweb.org/e/pdf/sierraleone_e.pdf.
- Partnership Africa Canada (2005a) Diamond Industry Annual Review: Republic of Angola. www.pacweb.org/e/images/stories/documents/angola%20review,%20june%202005-english%20(web%20version).pdf.
- Partnership Africa Canada (2005b) Diamond Industry Annual Review: Democratic Republic of the Congo. www.pacweb.org/e/images/stories/documents/ar-rdc%202005-eng-web.pdf.
- Partnership Africa Canada (2006) Diamond Industry Annual Review: Sierra Leone. www.pacweb.org/e/images/stories/documents/annual%20review%20sl%202006.pdf.
- Rangarajan L.N. (1992) *The Arthashastra by Kautilya*. Penguin Books India, New Delhi, 898 pp.
- Rio Tinto Diamonds (2007a) Argyle rough diamonds. www.riotintodiamonds.com/what-we-do/products/default.asp [date accessed: 06/06/07].
- Rio Tinto Diamonds (2007b) Diavik rough diamonds. www.riotintodiamonds.com/what-we-do/products/diavik.asp [date accessed: 06/06/07].
- Rio Tinto Diamonds (2007c) Murowa rough diamonds. www.riotintodiamonds.com/what-we-do/products/murowa.asp [date accessed: 06/06/07].
- Severalmaz (2007) Description of the deposit. www.severalmaz.ru/edeposit.htm [date accessed 06/06/07].
- Shigley J.E., Chapman J., Ellison R.K. (2001) Discovery and mining of the Argyle diamond deposit, Australia. *Gems & Gemology*, Vol. 37, No. 1, pp. 26–41.
- Shor R. (2005) A review of the political and economic forces shaping today's diamond industry. *Gems & Gemology*, Vol. 41, No. 3, pp. 202–233.
- Tahera Diamond Corp. (2006) Annual Report. www.tahera.com/Theme/Tahera/files/.Tahera_AR06_BW.pdf.
- Tahera Diamond Corp. (2007) First Quarter Report. www.tahera.com/Theme/Tahera/files/Tahera%20Diamond%20Corporation%202007%20Q1%20Report%20-%20FINAL.pdf.
- Wagner P.A. (1914) *Diamond Fields of South Africa*. The Transvaal Leader, Johannesburg, 347 pp.
- Wilson M.G.C., Anhaeusser C.R., Eds. (1998) *Mineral Resources of South Africa*, 6th ed. Council for Geosciences, Pretoria, South Africa, 740 pp.

DURABILITY TESTING OF FILLED EMERALDS

Mary L. Johnson

Researchers treated 128 emeralds with nine emerald fillers—Araldite 6010, cedarwood oil, paraffin oil, unhardened and surface-hardened Opticon, a mixture of cedarwood oil and Canada balsam, surface-hardened Norland Optical Adhesive 65, and the solid fillers Gematrat and Permasafe—and then exposed them (along with 14 unfilled emeralds) to common conditions of wear and cleaning. All emeralds were held for about six years, and most were then subjected to one of the following durability tests: exposure to long-wave UV radiation (a component of sunlight), to mild heat and incandescent light in a display case, to five chill-thaw cycles, and to a desiccation environment; ultrasonic cleaning with either warm water or BCR; and cleaning with steam or mild chemical solvents. Changes were evident in about 35% of the filled emeralds after the mild exposure tests (i.e., time, UV radiation, display case); those with liquid fillers were especially susceptible. The desiccation environment made fissures visible in a majority of emeralds. Hard fillers damaged their host emeralds by expanding cracks during durability testing, while chill-thaw cycling extended cracks in both filled and unfilled emeralds. Emeralds with liquid fillers were most susceptible to appearance changes due to ultrasonic cleaning and exposure to ethanol or acetone. Some observations on the effectiveness of different fillers on emerald appearance are also provided.

The finest emeralds are renowned for their saturated, slightly bluish green color (figure 1). However, this beauty comes with disadvantages. Compared to diamonds, sapphires, and rubies, emeralds are softer and more brittle; they also are almost invariably included. As a result, emerald inclusion scenes are commonly romanced as *jardins*—the French word for “gardens”—by the retail world. Because inclusions and, especially, surface-reaching fissures detract from emerald’s transparency and distinctive color, emeralds have been oiled—or *filled*—for centuries (see, e.g., Jennings et al., 1993; Weldon, 1997) to make these features less obvious.

In addition, open fissures in emeralds can collect polishing compounds, skin oils, and dirt. Internal fluid inclusions can break open (see, e.g., Koivula, 1980); likewise, solid inclusions can be plucked out during fashioning. Consequently, the vast majority of fashioned emeralds in the market today have some type of filling.

Over the last few decades, different sources and trading centers have tended to use different fillers for emeralds: cedarwood oil and Canada balsam in

Colombia, paraffin oil (mineral oil) in Zimbabwe and Zambia, and Opticon in Brazil (see, e.g., Ringsrud, 1983; Kammerling et al., 1991; Koivula et al., 1993, 1994a; Kennedy, 1998; for more on the history of emerald filling, see the *G&G* Data Depository at www.gia.edu/gemsandgemology). Although these practices require disclosure, for many years fillers were used to enhance the appearance of emeralds without much public comment. In the 1990s, however, controversies erupted over the use of epoxies and similar substances to fill emeralds, as little was known about their durability and they were considered synthetic or “unnatural” by some in the trade. When these controversies were brought to the attention of consumers (see, e.g., Costanza, 1998; “Jewelry scene...,” 1998), most of whom did not know that emeralds are customarily filled, the emerald market plummeted (see, e.g., Drucker, 1999).

See end of article for About the Author and Acknowledgments.
GEMS & GEMOLOGY, Vol. 43, No. 2, pp. 120–137.
© 2007 Gemological Institute of America



Figure 1. Their saturated slightly bluish green color makes emeralds such as the Colombian stones in this suite quite popular with consumers. However, emeralds are commonly filled, and consumer and seller alike should be aware of potential durability problems under conditions of normal wear and care. Necklace (46.5 ct) and earrings (17.5 ct) courtesy of Grando, Inc., Los Angeles; photo by Harold & Erica Van Pelt.

In the late 1990s, GIA began a systematic study of emerald fillers. The goal was to understand what these filling substances were, how to distinguish them from one another, and how to characterize their effects on emeralds. The first article, Johnson et al. (1999), examined 39 possible filling substances and characterized their physical, optical, and spectroscopic properties. The second article, McClure et al. (1999), showed how to determine the extent to which an emerald is filled (an important factor in evaluating the quality of the emerald). The present article examines the changes in filled emeralds with time and with consumer-focused durability testing.

The durability and stability of 36 gem materials, including emerald, were reviewed by Martin (1987). Previous studies of filler durability were made by Kammerling et al. (1991) on cedarwood oil, Canada balsam, and surface-hardened Opticon in emeralds

and other types of beryl; by Koivula et al. (1989) and Kammerling et al. (1994) on fracture filling in diamonds; and by C. M. Ou Yang on polymer-impregnated jadeite (see, e.g., Johnson and Koivula, 1996). Some specific durability tests were performed on emeralds with the solid fillers Gematrat and Permasafe ("New emerald process...", 1997; Ringsrud, 1998; Weldon, 1999), but information on these tests is limited.

BACKGROUND

What makes an emerald filler "ideal"? Participants at the First World Emerald Congress (held in Bogotá, Colombia, in 1998) agreed that it should be colorless and stable within the emerald (Lurie, 1998). It should also be permanent under routine conditions of wear and care, and yet easily removed if the emerald needs

to be evaluated for recutting (Federman, 1998a).

Physical properties used to discriminate among fillers include their solid or liquid nature (liquids ooze out of fissures or move when approached by a hot point), viscosity, scent, and other properties not easily ascertained within an emerald, such as specific gravity. Optical properties include color and refractive index (RI); the latter determines how visible a filled feather is and whether it shows a “flash effect.” Clues to the identity of the filling substance may also be provided by Fourier-transform infrared (FTIR) and Raman spectroscopy. For more on these properties, see Johnson et al. (1999) and Notari et al. (2002).

For the purpose of the present study, nine fillers were chosen to represent four important classes of commercial filling substances.

1. *Soft (liquid) fillers*: Araldite 6010 (sometimes called “palma”), cedarwood oil, unhardened Opticon, and paraffin oil
2. *Semi-hard (slow-flowing and possibly solidifying) fillers*: the 50:50 mixture of cedarwood oil and Canada balsam
3. *Surface-hardened fillers*: Norland Optical Adhesive 65 (a long-wave UV-setting adhesive, typically used fully hardened, but surface-hardened in this study) and Opticon
4. *Hard fillers*: Gematrat (Johnson and Koivula, 1997; Federman, 1998b) and Permasafe (“New type...,” 1998; Michelou, 1999; Weldon, 1999)

This study did not include any of the less common fillers from Johnson et al. (1999), colored fillers such as green Opticon or Joban oil, or fillers developed since this study began, such as Groom’s ExCel or ExCel 1.52 (see, e.g., Roskin, 2002, 2003; Gomelsky, 2003; “Myth of the month...,” 2006). In addition, this study did not test the claim that emeralds become more brittle after treatment under pressure, the ease of removal of the filler and subsequent refilling, or the properties of emeralds that had been enhanced by more than one filler. The main objective was to determine whether the appearance of an emerald treated with a specific filler changed with time, exposure to a variety of environments, or cleaning.

MATERIALS AND METHODS

Samples. The study collection consisted of 142 fashioned emeralds, ranging from 0.16 to 4.24 ct and averaging slightly less than 1 ct. All important gem sources were represented: 49 from Colombia, 23 from

Zambia, 12 from Brazil, and six from Zimbabwe. The remaining 52 were from unknown sources (see *G&G Data Depository*). These were mainly emerald cuts, but they also included cabochons and brilliant cuts of various shapes. Many of these samples were donated; the rest were taken from GIA collections. All had eye-visible, surface-reaching fissures, and most would have been graded as having moderate-to-significant enhancement after filling.

Most of the emeralds were cleaned (to remove preexisting stains or fillers in fissures) by Arthur Groom–Gematrat in New York, using a proprietary method. However, 16 emeralds filled with Permasafe and five filled with Gematrat were acquired already treated. Fourteen of the cleaned emeralds were retained unfilled for comparison purposes. Most of the remaining emeralds were treated at GIA using fillers acquired for Johnson et al. (1999) from sources listed in table 1 of that article. These fillers were: Araldite 6010 prepolymer resin; Merck cedarwood oil for clearing; Opticon 224 prepolymer resin, both without its catalyst and with surface hardening; Schroeder paraffin oil; a 50:50 mixture of cedarwood oil with Sigma Canada balsam; and Norland Optical Adhesive (NOA), type 65. The physical, optical, and spectroscopic properties of these fillers can be found in Johnson (1999). Most samples were filled at GIA using either a “Mini Oiler” (see, e.g., Koivula et al., 1994b) or a “Color Stone Oiling Unit” (again, see Johnson et al., 1999).

Fourteen emeralds were filled with NOA 65 and then exposed to long-wave UV radiation; however, leakage from some samples showed that the filler had not solidified below the surface. Hence, NOA 65 is considered a surface-hardened filler throughout this article, although it may not be so for other gem materials (or other emeralds). This incomplete hardening of the filler may have been due to the experimental procedure used here, as the output intensity of the long-wave lamp may not have reached the energy density recommend by Norland Optical. (Although NOA type 65 was used for this study based on information received from the emerald trade, the company currently recommends that type 71 be used for gemstone filling.)

Fifteen emeralds used in this study were filled with paraffin oil in vacuum chambers by Colgem Ltd. Eighteen were filled with a 50:50 mixture of cedarwood oil and Canada balsam by Ron Ringsrud using heat, vacuum, pressure, and refrigeration to approximate processes used in Colombia. Fourteen were filled with Opticon and then surface hardened

TABLE 1. Types of filled emeralds subjected to the 10 durability tests.

Filler type	Time only ^a	Long-wave UV	Display case	Chill-thaw cycling	Desiccation	Ultrasonic cleaning in water	Ultrasonic cleaning in BCR	Steam	Ethanol and acetone	Totals
None	2	1	2	2	2	1	1	1	2	14
Araldite 6010	1	2	1	2	2	1	1	2	1	13
Cedarwood oil	3	2	1	1	2	1	1	1	1	13
Unhardened Opticon	3	2	2	2	1	1	1	1	2	15
Paraffin oil	4	1	2	2	1	1	1	1	2	15
Canada balsam mixed with Cedarwood oil	4	2	1	2	2	1	2	2	2	18
Norland Optical Adhesive 65	2	2	2	2	1	1	1	1	2	14
Surface-hardened Opticon	2	2	2	2	2	1	1	1	1	14
Gematrat	1	1	2	1	1	1	1	1	1	10
Permasafe	2	2	2	2	2	1	1	2	2	16
Totals	24	17	17	18	16	10	11	13	16	142

^a Although all samples were stored for about 6 years, two samples were examined for both the time test and a different durability test (nos. 4477 and 4481). These two additional samples are not included in the "Time only" total.

by Ray Zajicek. Details of their methods are provided in the *G&G* Data Depository. Five emeralds were filled with Gematrat by Arthur Groom–Gematrat. Twenty-one emeralds, mentioned above, were obtained pre-filled with Permasafe or Gematrat. All filling work was performed in 1998 and early 1999.

The filled emeralds were rechecked after treatment for standard gemological properties (such as RI, specific gravity, and weight), and 57 stones with larger fissures were selected for FTIR characterization of their fillers. Macrophotographs of 110 emeralds were taken and then the emeralds were set aside to await durability testing. These durability tests were performed in 2004–2006, following a period of about six years to allow for changes of the fillers with time.

Durability Testing. Ten tests were chosen to assess the durability of the various commercial emerald fillers: time alone (~6 years), exposure to long-wave UV radiation (a component of sunlight), exposure to heat and incandescent light in a display case, multiple chill-thaw cycles, one year in a desiccation environment, ultrasonic cleaning with either warm water or buffing compound remover (BCR), and cleaning with steam or two mild organic solvents. These tests, which are described in detail in box A, were selected to mimic likely causes of changes in the appearance of filled emeralds in retail and consumer environments. Note that all 142 samples were exposed to the passage of time and, where photos were available, checked against those photos before further durabili-

ty testing. Detailed observations of changes with time alone were made of 26 samples treated with the different fillers or left untreated and then classified into four degree-of-change categories: obvious, slight, very slight, and no changes observed (see below). The degrees of change due to time in the remaining samples were not categorized but were assessed for their appropriateness for additional durability testing. Then, 118 emeralds were each subjected to an additional exposure or cleaning test (again, see box A).

Durability tests are typically conducted by cutting each sample into multiple parts and testing each part (see, e.g., Johnson and Koivula, 1996). However, the fissures in the emeralds were not evenly distributed throughout the stones, and a goal of this study was to monitor the effect of the durability tests on the overall appearance of fashioned emeralds. Therefore, this study took a different approach, and instead compared emeralds to photographs.

The original emerald-filler study began with 181 emeralds, and at least two emeralds were intended for each filler and each durability test. However, after the original filler study (Johnson et al., 1999), some samples were set aside for other experiments. The remaining 142 samples discussed here were examined and allocated such that each filler was represented in each test (table 1); however, the most-changed samples were allocated to the time test (with the rest randomly distributed among the remaining tests).

Imaging Protocol. Usable photos were taken of 115

BOX A: DURABILITY TESTING

For this study, 10 tests were conducted—five representing exposure during normal wear, display, and storage of emerald-set jewelry; and five representing techniques that might be encountered in cleaning an emerald—as described below.

1. Exposure to the passage of time

Goal: There is anecdotal evidence that some emerald fillers deteriorate or leak out with time, which this test sought to investigate.

Test description: The best method for assessing the impact of time is, simply, to allow time to pass. In an examination of tests for archival materials in other disciplines, we found no other test that exactly duplicated time's effects (see, e.g., "Rate of paper degradation ...," 2001). The sample emeralds were kept in a sealed container (a zippered plastic bag) in ambient conditions (usually in the dark, but occasionally exposed to fluorescent lighting, in an office in southern California with heating/air conditioning on workdays only). This also provided a standard for comparison for changes from more active tests.

After noting how much time had passed since filling, 26 of the emeralds were compared against a photo of their appearance immediately following filling.

2. Exposure to long-wave UV radiation

Goal: Long-wave UV (at about 365.4 nm) may have an effect on filled emeralds (as previously shown for fracture-filled diamonds; see, e.g., Kammerling et al. 1994). This type of radiation is also found in sunlight, so long-wave UV testing mimics one aspect of long-term exposure to sunlight. (Short-wave UV was not used, because it is not a significant component of sunlight.)

Test description: Seventeen emeralds were placed face-up, about 2.5 cm away from the filtered source of long-wave UV radiation from a GIA four-watt long-wave/short-wave unit, within a viewing cabinet. Emeralds were exposed for 200 hours (corresponding to 3,400 hours [~9 months] of exposure to

sunlight, according to Kammerling et al., 1994). After this time, the emeralds were reexamined.

3. Exposure in a display case

Goal: The appearance of a filled emerald may change over time in the light and mild heat of a display environment. This test was an attempt to monitor that effect.

Test description: A display case was set up with a black velvet background and placed under three 50-watt halogen lights (using the manufacturer's recommendation for distance of 4 feet, [-1.2 m]); temperatures of 25.9–26.3°C were recorded in the case. Seventeen emeralds were arranged in the center of the case (directly under a light), and exposed to 720 hours of illumination (equivalent to thirty 24-hour days) in 128-hour continuous intervals, then reexamined.

4. Exposure to chill-thaw cycling

Goal: Temperature changes (such as might be caused by wear in cold climates) may affect filled emeralds. This test was also performed on fracture-filled diamonds by Kammerling et al. (1994).

Test description: Eighteen emeralds were placed in two layers of sealed clear plastic bags in aluminum foil (as barriers to humidity changes) sitting on ice in a refrigerator overnight (measured air temperature 9°C). The bags were removed and allowed to thaw for an hour or so, then the emeralds were examined while in their inner bags to check for drastic damage. The emeralds were wrapped again and rechilled, for a total of five chill-thaw cycles.

5. Exposure to dry air (desiccation)

Goal: There are many claims in the trade press that emerald fillers can "dry out." To test these reports, the filled emeralds were exposed to a desiccation environment (storage at ambient temperature in a dry chamber with a silica gel desiccant). This test was designed to simulate consumer storage (e.g., in a bank vault) and is relevant to wear in dry climates.

emeralds after cleaning and, as appropriate (since some were left unfilled), before filling; "before" photos were not available for 21 emeralds that were acquired already filled. Shortly after filling, 110 samples were photographed; 24 filled samples were photographed after six years had elapsed and before the durability

tests that followed. Due to other exigencies, not all samples could be photographed immediately before filling, after filling, or after the time test. Therefore, the comparison used to gauge the effect of the durability test on the emerald's appearance was either a photo taken immediately after filling or one taken six

Test description: Sixteen emeralds were placed on transparent glass dishes in a clear-windowed closed chamber with a desiccant (a 40 g unit of Hydro-sorbent silica gel that included indicator beads; see www.dehumidify.com). The emeralds were examined visually once a week through the windows of the chamber, and were removed and checked for damage monthly, then returned to the chamber. After one year, the emeralds were removed from the chamber and reexamined.

6. Cleaning: ultrasonic cleaning in water

Goal: Ultrasonic cleaners use vibration in a heated liquid (e.g., water or a jewelry cleaner) to loosen and “shake off” dirt particles. The combination of heat, vibration, and the immersion liquid may affect the appearance of a filled emerald.

Test description: Ten emeralds were placed loose in three batches in beakers with 40 mL of tap water in a Gesswein Ultrasonic Cleaner model 87 and allowed to “clean” for 30 minutes, while the temperature was monitored (it increased from 33°C to 63°C during the process). The emeralds were rinsed in tap water, dried in air, and reexamined.

7. Cleaning: ultrasonic with cleaning solution

Goal: Typical jewelry cleaning with a cleaning solution in an ultrasonic cleaner may have a greater impact on the appearance of a filled emerald than vibrating in water alone. This test was an attempt to monitor that effect.

Test description: Eleven emeralds were placed loose in three batches in beakers of common jewelry cleaner Oakite Buffing Compound Remover (BCR; see, e.g., <http://www.landainternational.com/catalog/prod226.shtml>) in a Gesswein Ultrasonic Cleaner model 87 and allowed to clean for 30 minutes, while the temperature was monitored (it increased from 39°C to 63°C during testing). The emeralds were rinsed several times in tap water, allowed to dry in air, and reexamined.

8. Cleaning: steam

Goal: Since jewelry is often steam cleaned (although this cleaning technique is usually not recommended

for emeralds), we wished to see whether steam cleaning affects the appearance of a filled emerald. These emeralds were cleaned for shorter times than tests involving filled diamonds (see, e.g., Koivula et al., 1989; Kammerling et al., 1994) or other beryls (Kammerling et al., 1991) due to the less durable nature of emeralds.

Test description: The tables of 13 emeralds were steam cleaned for 30 seconds, using a Gesswein portable steam generator, with the emeralds held in rubber-tipped tweezers. After drying in air, they were reexamined.

9. Cleaning: mild chemical solvent (ethanol)

Goal: Since fillers are carbon-based (i.e., organic) chemicals, often they can be dissolved by various alcohols (which are also organic chemicals). Hence, we wished to see whether exposure to a common mild solvent such as ethanol would affect the appearance of emeralds filled with the different substances.

Test description: Sixteen emeralds were placed in high-purity ethanol (denatured, high-purity liquid chromatography [HPLC] grade) in two beakers held for 24 hours in a fume hood. Room temperature was 21°C. The emeralds were removed from the ethanol, dried in air, and then reexamined.

10. Cleaning: stronger, but still relatively mild chemical solvent (acetone)

Goal: Ethanol is considered a very mild solvent for organic chemicals such as oils and resins. Hence, a slightly stronger common solvent may show a more pronounced effect on the appearance of filled emeralds, and it is common practice to try first with the weakest solvent. Acetone is also a component in fingernail polish remover, so this test might have bearing on some accidental damage in the home. Possibly, cleaning in acetone alone might have different results than cleaning in acetone after ethanol.

Test description: The 16 emeralds used in test 9 were examined (compared to macrophotographs to categorize their appearance) and then placed for 24 hours in two beakers filled with spectroscopic-grade acetone (Aldrich Chemical Company no. 15,459-8) in a fume hood at 22°C. The emeralds were then removed from the acetone, dried in air, and compared with the pretest images.

years after filling and immediately prior to the durability test. This protocol necessitated that we split the reporting of the data for each durability test into two categories: one in which the comparison includes the effects of time (i.e., “test + time”) and one in which the comparison photo already shows the effect of time

(i.e., “test”). In most cases, photos were also taken after the durability tests.

Although filled emeralds can look quite different owing to choices of lighting among the various photographers (e.g., figure 2) and the use of film (as in the earliest images) or digital (such as those taken



Figure 2. This emerald, filled with a mixture of cedar-wood oil and Canada balsam (no. 4728; left), had an obvious change due to ultrasonic cleaning in BCR (right). However, the appearance of the emerald in these photos, along with all the emerald photos, was influenced by changes in the choice of photos, intensity of light, film, and processing choices by the different photographers. Therefore, the fissures visible parallel to the long axis of the emerald are not as evident in the right image, and the emerald's color looks different.

Figure 3. Changes in emerald appearance after durability tests (before, left; after, right) were divided into four categories: obvious (no. 4706, 0.79 ct, ultrasonic cleaning in water); slight (no. 4633, 1.09 ct, ultrasonic cleaning in BCR); very slight (no. 4936, 2.95 ct, steam cleaning); and no observed changes (no. 4757, 0.46 ct, ethanol and acetone cleaning).



immediately before and after the durability testing), the positions of fissures did not change. In this article, the backgrounds have been made uniform to facilitate the comparisons and the color of some images has been adjusted to more closely match the actual color of the stone at the time of the observation. The images were not otherwise manipulated.

Observations of Overall Appearance. It was usually possible to reproduce the overall appearance of an emerald in a photo by holding the stone under a high-intensity incandescent lamp, shifting its position, and then comparing the appearance of the emerald itself to its archived image on a computer monitor. The following factors were noted: any change in visibility of fissures and other inclusions to the unaided eye; any discoloration or change in transparency of the filler; and overall changes in transparency and color distribution in the emeralds.

For comparison purposes, changes in emerald appearance (with the table up) due to durability testing were put into four categories (figure 3), listed here from greatest to least change:

- *Obvious:* The after-testing emerald differed from the before-testing image at first glance, and varying the lighting environment could not make the emerald match the photo.
- *Slight:* The after-testing emerald resembled the before-testing image at first glance, but further examination of the emerald showed some change.
- *Very slight:* Only subtle changes were seen in careful examination of the after-testing emerald and the before-testing image. These were confirmed by microscopic examination of the emerald.
- *No observed changes:* No changes were seen, even with careful examination. Note, however, that microscopic examination, or photography from a different direction (e.g., of the pavilion side), might have revealed differences in appearance.

Spectroscopy. Infrared spectra were taken in reflectance mode using a Nicolet Magna 550 Fourier-transform infrared (FTIR) spectrophotometer and its successors; details of spectral acquisition methods were published in Johnson et al. (1999). FTIR spectra were recorded for 57 emeralds (not all of which are included in table 1) with evident filled fissures. The goals were to see if quantitative measurements of filler loss could be made and to monitor any change in the FTIR spectra due to durability testing. All FTIR data are provided in the *G&G* Data Depository.

RESULTS


Initial Effectiveness of Emerald Fillings. Although this research did not focus on the effectiveness of the fillers, we did observe the changes in appearance they produced. The most dramatic examples for eight of the fillers—those that had the greatest impact on apparent clarity—are shown in table 2. It is possible that a professional filling laboratory would have been even more effective. The examples provided in table 2 show that the presence of a filler can improve the apparent color distribution in emeralds, by getting rid of “white” areas caused by air-filled feathers.

Durability Testing. The results for the durability tests are provided in table 3. The following types of changes were seen: Feathers were more evident, had opened up at the surface (cavities in the fissures were visible with magnification), leaked (oily fluid leaking out of fissures was visible with magnification), delaminated (a new opening along one side of the filler in the fissures was seen with magnification), extended (the length of the fissures increased), and new feathers were seen. Also, the filler deep within fissures could crystallize or turn cloudy. As expected, these durability tests had no observed impact on the unfilled emeralds, with one exception (no. 4806), which reacted to the chill-thaw cycles.

FTIR spectra proved not to be useful for tracking differences over time, since almost all filled emeralds tested had some filler left after several years, and we found that the amount of filler indicated in the spectra depended on the path light took through the emerald. In no case did we see any changes besides intensity in the spectral features of the filler.

Time. Thirteen of the 23 filled emeralds showed *no observed* change with time (see table 3). The emerald filled with Araldite 6010 showed a *very slight* change, a cloudy band throughout the stone (figure 4). *Slight* changes were seen in six emeralds: two filled with cedarwood oil (emptying of feathers), two filled with paraffin oil (whitening at the surface or crystallization at depth: figure 5), one filled with a mixture of cedarwood oil and Canada balsam (feather more evident), and one filled with surface-hardened NOA 65 (feathers leaking fluid onto their surface). Three emeralds showed *obvious* changes (feathers opening up) due to time alone—two filled with unhardened Opticon and one filled with paraffin oil (figure 6).

TABLE 2. Changes in emerald appearance according to filler type.^a

Filler/Sample no.	Before filling	After filling
Araldite 6010 No. 4508 ^b		
Cedarwood oil No. 4479 ^b		
Unhardened Opticon No. 4578 ^c		
Paraffin oil No. 4922 ^d		
A 50:50 mixture of Canada balsam and Cedarwood oil No. 4495 ^b		
Norland Optical Adhesive 65 No. 4710 ^e		
Surface- hardened Opticon No. 4923 ^d		
Gematrat No. 4708 ^e		

^a Due to lack of “before” images, emeralds filled with Permasafe are not included in this table. All photos in this table were taken by Maha Calderon. ^b From Colombia. ^c From Zambia. ^d From Zimbabwe. ^e From Brazil.

Exposure to Long-Wave UV Radiation. No changes were observed in 13 of the 16 filled emeralds with exposure to long-wave UV radiation, and none showed *obvious* changes. An emerald filled with

TABLE 3. Observed changes in the emeralds categorized according to durability tests and filler type.^a

Durability test	No filler	Soft (liquid) fillers				Semi-hard fillers
		Araldite 6010	Cedarwood oil	Unhardened Opticon	Paraffin oil	Cedarwood oil mixed with Canada balsam
Time only	No observed change (4477, 4502, 4596)	Very slight (4584)	No observed change (4481, 4719); Slight (4479, 4704)	No observed change (4515); Obvious (4763, 4799)	No observed change (4774); Slight (4599, 4640); Obvious (4747)	No observed change (4702, 4742, 4917); Slight (4800)
Long-wave UV	No observed change (4707*)	No observed change (4566); Very slight (4506)	No observed change (4744); Slight (4777)	No observed change (4585, 4937)	No observed change (4563)	No observed change (4598); Slight (4770)
Display case	No observed change (4477*, 4587)	No observed change (4574)	Slight (4638*)	No observed change (4486); Slight (4594*)	No observed change (4493); Very slight (4934)	No observed change (4492)
Chill-Thaw cycling	No observed change (4472*); Slight (4806)	No observed change (4950*); Slight (4508)	No observed change (4481*)	No observed change (4500); Slight (4478)	No observed change (4511*, 4801)	No observed change (4751); Obvious (4505)
Desiccation	No observed change (4755, 4919)	No observed change (4570*); Slight (4775)	Very slight (4507); Slight (4920)	Obvious (4807*)	Very slight (4593)	Slight (4470, 4715)
Ultrasonic cleaning in water	No observed change (4568)	Slight (4931)	Obvious (4576*)	Obvious (4706)	Slight (4739)	Slight (4495)
Ultrasonic cleaning in BCR	No observed change (4930)	Obvious (4600)	Obvious (4804)	Slight (4722)	Obvious (4484)	Slight (4633); Obvious (4728)
Steam	No observed change (4636)	No observed change (4592); Slight (4938)	Very slight (4513*)	No observed change (4918)	Slight (4952*)	No observed change (4483*, 4569)
Ethanol	No observed change (4720, 4786)	Obvious (4797)	Obvious (4735)	Obvious (4578, 4814)	Slight (4922); Obvious (4716)	Slight (4639); Obvious (4773)
Ethanol + Acetone	No observed change (4720, 4786)	Obvious (4797)	Obvious (4735)	Obvious (4578, 4814)	Obvious (4716, 4922)	Obvious (4639, 4773)

^aSample numbers are given in parentheses. Note that although all samples showed the effect of time, some samples only had comparison photos that were taken prior to the time exposure, so the changes reported reflect both the effect of time and the additional test (i.e., test + time). However, some samples had comparison photos taken only after the time exposure, so the changes reported reflect only the difference seen with the additional durability test (i.e., test only, as indicated by an asterisk).

Araldite 6010 showed a *very slight* change, with a feather near the tip slightly more evident. Two emeralds showed *slight* changes: One filled with cedarwood oil and one with a mixture of cedarwood oil and Canada balsam had feathers open up.

Display Case Environment. Nine of the 15 filled emeralds showed *no observed* change. Two emeralds showed *very slight* changes: One filled with paraffin oil showed crystallization similar to that

seen in figure 5, while feathers looked more evident in a Permasafe-filled emerald. Three emeralds had *slight* changes: Feathers were more evident in a cedarwood oil-filled emerald, a surface feather had opened up in an emerald filled with unhardened Opticon, and a deep feather appeared to be opening up in an NOA 65-filled emerald. One of the two Gematrat-filled emeralds showed an *obvious* change (figure 7), with feathers opening up at the surface.



Figure 4. A 1.48 ct emerald filled with Araldite 6010 (no. 4584; left, immediately after filling) showed a *very slight* change with time (center): a cloudy band throughout the stone that became more evident (right; magnified 15×).

Surface-hardened fillers		Hard fillers—rigid solids	
Norland Optical Adhesive 65	Surface-hardened Opticon	Gematrat	Permasafe
No observed change (4733); Slight (4573)	No observed change (4586, 4785)	No observed change (5347)	No observed change (5583, 5587)
No observed change (4772, 4794)	No observed change (4504, 4575)	No observed change (5344)	No observed change (5586, 5589*)
No observed change (4565); Slight (4494)	No observed change (4567, 4622)	No observed change (4473*); Obvious (4708)	No observed change (5585); Very slight (5574)
No observed change (4810, 4949*)	No observed change (4942*); Slight (4745)	Obvious (4816*)	No observed change (5578, 5579)
No observed change (4796)	No observed change (4805); Very slight (4923)	Obvious (91843)	No observed change (5582); Slight (5452*)
Slight (4444*)	Very slight (4475)	No observed change (5357*)	No observed change (5573)
Slight (4710)	Very slight (4729*)	Slight (5356)	No observed change (5581)
No observed change (4749)	Very slight (4936)	Slight (5350*)	No observed change (5588); Very slight (5580)
No observed change (4581, 4757)	No observed change (4721)	Slight (4795)	Very slight (5575); Slight (5576)
No observed change (4757); Slight (4581)	Slight (4721)	Slight (4795)	Very slight (5575); Obvious (5576)

Chill-Thaw Cycles. One of the two unfilled emeralds showed a *slight* change in appearance, with more extended fractures. Eleven of the 16 filled emeralds had *no observed* change. Three filled emeralds showed *slight* changes: Feathers were slightly more evident in an emerald filled with Araldite 6010, there was a fresh-looking feather on the bezel of an emerald filled with unhardened Opticon, and filler was oozing out of an emerald filled with surface-hardened Opticon. An emerald filled with a mixture of cedar-

wood oil and Canada balsam (figure 8) had an *obvious* appearance change, with a glassy feather on the pavilion now visible through the crown. Feathers had extended and cracked further in an emerald filled with Gematrat, causing an *obvious* change in appearance (figure 9). The changes in this last emerald and the unfilled one that was altered are particularly significant in that the emeralds themselves—not just the fillers—were damaged.

Desiccation. Four of the 14 filled emeralds had *no observed* changes. Three emeralds showed *very slight* changes: One filled with cedarwood oil and one filled with surface-hardened Opticon showed very slightly more evident feathers; and one that was filled with paraffin oil showed surface feathers opening up subtly. Five emeralds showed *slight* changes: One filled with Araldite 6010, one filled with Permasafe, and two filled with a mixture of cedarwood oil and Canada balsam showed slightly more evident feathers; while one that was filled with cedarwood oil showed feathers appearing to open up at depth. Two filled emeralds—one with unhardened Opticon (figure 10) and one with Gematrat—showed *obvious* changes, in the form of more prominent feathers.

Ultrasonic Cleaning in Water. The two emeralds filled with Gematrat or Permasafe had *no observed* changes. The emerald filled with surface-hardened Opticon had a *very slight* change, with feathers open at the surface. Four emeralds showed *slight* appearance changes: Surface-reaching feathers were opened up more in the emeralds filled with Araldite 6010 and paraffin oil; and fissures were more evident in the emerald filled with a mixture of cedarwood oil and Canada balsam and the one filled with NOA 65. The emerald filled with cedarwood oil (figure 11) not only had *obvious*, open fissures, but with magnification it also revealed material leaking onto its surface. Similarly, several feathers had



Figure 5. A 0.74 ct emerald filled with paraffin oil (no. 4599; left, after filling) showed a slight change with time (center); crystallization at depth (right, magnified 35x).



Figure 6. This 3.57 ct emerald filled with paraffin oil (no. 4747; left) showed obvious changes due to time alone (center). Feathers, especially to right of center, were observed as more open (right, magnified 40 \times).

opened up in the unhardened Opticon-filled emerald (again, see figure 3), an obvious change.

Ultrasonic Cleaning in BCR. All the filled emeralds except the one that was filled with Permasafe showed changes with this test. The emerald filled with surface-hardened Opticon showed a *very slight* change, with open feathers more cleaned out at depth. Four emeralds showed *slight* changes: One filled with unhardened Opticon, one filled with a mixture of cedarwood oil and Canada balsam (again, see figure 3), and one filled with Gematrat (figure 12) had feathers emptied out. An emerald filled with NOA 65 (figure 13) showed slightly more iridescent glassy feathers. Four filled emeralds showed *obvious* changes: One with Araldite 6010 (figure 14), one with cedarwood oil, one with paraffin oil, and one with a mixture of cedarwood oil and Canada balsam were partly emptied.

Figure 7. A 1.65 ct Gematrat-filled emerald (no. 4708; left, after filling) showed the most obvious change in the display-case test (right), with feathers opening up at the surface.



Figure 8. A 0.27 ct emerald (no. 4505; left, before filling), which was filled with a mixture of cedarwood oil and Canada balsam (center), had an obvious appearance change after five chill-thaw cycles (right): A glassy feather on the pavilion was visible through the crown.

Steam Cleaning. Perhaps because of the short time used in this test, differences in appearance were slight at most, and longer steaming may have resulted in further changes (see, e.g., Kammerling et al., 1991). Six filled emeralds had *no observed* changes. Three filled emeralds showed *very slight* changes: One with cedarwood oil had a little opening up of surface-reaching fissures; one with surface-hardened Opticon (again, see figure 3) had very slightly more evident feathers; and one with Permasafe had a very small crack forming at the end of a hollow tube. Three emeralds—one each filled with Araldite 6010, paraffin oil, and Gematrat—showed *slight* changes (i.e., more evident feathers).

Mild Chemical Solvents. As the same samples were used for both ethanol and acetone, the results will be provided together.

One emerald filled with NOA 65 had *no observed* changes after both tests. An emerald filled with Permasafe showed *very slight* changes, with one small fissure slightly emptied out. Three emeralds showed *slight* changes after acetone cleaning, with feathers open or more visible at the surface: one with NOA 65, one with surface-hardened Opticon (this sample had no observed change after ethanol cleaning), and one with Gematrat. Three emeralds showed *slight* changes with ethanol, but *obvious* changes with acetone, in which the filler was completely cleaned out relative to the post-ethanol appearance; these included ones filled with paraffin oil, a mixture of cedarwood oil and Canada balsam,

Figure 9. A 0.47 ct Gematrat-filled emerald (no. 4816; left, after filling) showed obvious changes after five chill-thaw cycles (center). The photomicrograph (magnified 40×) shows that some of the fissures have opened up and become more extensive.



Figure 10. This 0.95 ct emerald (no. 4807; left) was filled with unhardened Opticon (center) and showed an obvious change, in the form of more prominent feathers (right), after a year in a desiccation chamber.



Figure 11. A 1.09 ct emerald filled with cedarwood oil (no. 4576; left) showed an obvious change after 30 minutes of soaking in water in an ultrasonic cleaner (center). Examination with 30× magnification and reflected light shows the raised material leaking from the dark fissures (right).



and Permasafe (figure 15). The remaining six filled emeralds showed *obvious* changes (i.e., emptying) with ethanol alone; these included one filled with Araldite 6010 (figure 16) one filled with cedarwood oil, both filled with unhardened Opticon, one filled with paraffin oil, and one filled with a mixture of

cedarwood oil and Canada balsam (figure 17).

Although we did not specifically test for the ease with which a filler could be removed (or reapplied), the FTIR spectra confirmed that ethanol and acetone could remove some fillers such as Araldite 6010 and cedarwood oil (see *G&G* Data Depository).

Figure 12. A 1.49 ct emerald filled with Gematrat (no. 5356; left, after filling) showed a slight change following 30 minutes of ultrasonic cleaning in BCR (right), with feathers somewhat emptied out.



Figure 13. This 1.50 ct emerald filled with surface-hardened NOA 65 (no. 4710; left, after filling) showed a slight change—slightly more iridescent glassy feathers—after 30 minutes of ultrasonic cleaning in BCR (right).





Figure 14. The fissures in this 0.74 ct emerald filled with Araldite 6010 (no. 4600; left, after filling) had been partly emptied out following 30 minutes of ultrasonic cleaning in BCR, an obvious change (right).

DISCUSSION

What Conditions Affect the Appearance of Filled Emeralds? The results of the five exposure tests (time and exposure to long-wave UV [i.e., “sunlight”], the mild heat and light in a display case, chill-thaw cycling, and desiccation) and five cleaning tests (ultrasonic in water, ultrasonic in BCR, steam, and soaking in ethanol followed by soaking in acetone) give some guidance as to the safety of exposing emeralds to certain environmental conditions and to various cleaning techniques.

About 40% of the filled samples categorized (10 of 23) showed noticeable changes (from very slight to obvious) due to time alone. However, it should be noted that about half the samples in the time test were in the soft category, and that those emeralds had the most dramatic changes. Therefore, all categories of fillers are not equally represented in this statistic. A better gauge of the emerald fillers is that about 35% (19 of 54) of the filled emeralds changed in appearance without exposure to any particularly harsh conditions (i.e., with exposure only to time, long-wave UV, or the mild heat and light of a display case).

The exposure test that changed the highest percentage of samples was a year in a desiccation environment after the basic time test. Desiccation made feathers appear more evident in 10 of the 14 filled

emeralds, more than 70%. This suggests that filled emeralds, like opals and pearls, should not be kept in safe deposit boxes or other “dry” environments, and emeralds worn in dry climates may need to be clarity enhanced more frequently. The chill-thaw cycles led to permanent damage of two emeralds themselves (i.e., not just their fillers). Although this test did not have the highest percentage of emeralds that showed changes, it produced the most catastrophic changes. It is, therefore, important to avoid severe changes in temperature with any emerald, since this is the only test that affected an unfilled emerald used as a control sample.

Ultrasonic cleaning in either water or BCR, and soaking in solvents such as ethanol and acetone, affected the appearance of most of the filled emeralds (29 of 33; ~90%). Thus, cleaning filled emeralds risks changing their appearance. Steam cleaning is also risky, as noted by Kammerling et al. (1991), but it was done very gently in this study. In general, it should be considered potentially dangerous.

Grouping Fillers by Viscosity. Rather than treat all the fillers individually, it made sense to consider them in groups to see whether any results could be generalized. In Johnson et al. (1999), we grouped emerald fillers by their spectral properties; in this study, however, the changes seen involve fillers leaking, solidifying, or delaminating from feather walls (and sometimes cracking the emeralds). Therefore, these fillers were grouped by their viscous properties—that is, their ability to flow. (Although fillers can discolor and react with the atmosphere, these properties may not be associated with their viscosity.) The results by filler type are given in figure 18, which also suggests the probable durability behavior of untested fillers with similar viscosity.

Soft Fillers. Only soft fillers showed obvious changes with time (however, it is possible that changes in other emeralds in subsequent durability tests may

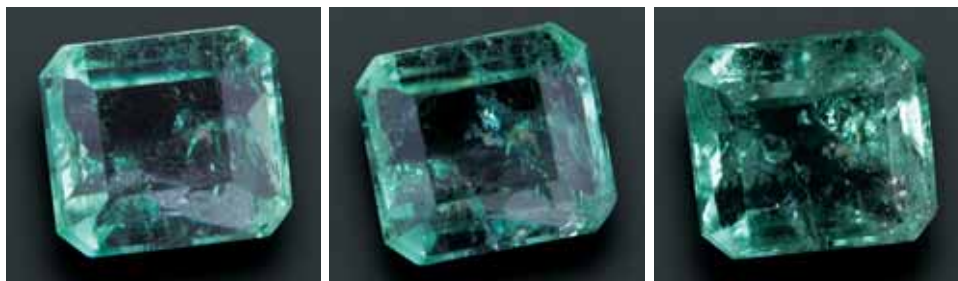


Figure 15. This 0.26 ct emerald filled with Permasafe (no. 5576; left, after filling) had a slight change after soaking in ethanol (center), but an obvious change after exposure to acetone (right).

Figure 16. A 0.80 ct emerald filled with Araldite 6010 (no. 4797; left) showed obvious changes following a day in ethanol (center). After a day in acetone (right), not only did the fissures look empty, but there was also no evidence of filler in the emerald's FTIR spectrum.



have been influenced by the time factor). In addition, emeralds with soft fillers showed obvious changes with desiccation, ultrasonic cleaning, and organic solvents. Soft fillers can crystallize (see, e.g., figure 5), leak out (see, e.g., figure 11), harden (i.e., become rigid), or evaporate. In general, fissures looked emptier with time and other exposure tests, and especially after cleaning in organic solvents. Of the soft fillers, unhardened Opticon showed the most instances of obvious changes with exposure tests (3 of 10 cases); but one of 10 emeralds filled with paraffin oil also showed an obvious change, due to time alone.

Semi-Hard Filler. The semi-hard filler (a 50:50 mixture of cedarwood oil and Canada balsam) showed better results than soft fillers during the exposure tests; with one of 11 samples showing an obvious change (when subjected to the chill-thaw cycles; figure 8). The feathers in this sample became more evident, and some filler leakage was noted. Obvious changes were seen with ultrasonic cleaning and soaking in organic solvents in three of the five samples. Although Canada balsam solidifies over decades (see, e.g., figure 19), there was no evidence of solidification in these samples over about six years.

Figure 17. This 1.00 ct emerald, filled with a mixture of Canada balsam and cedarwood oil, looks yellowish in fissures after filling (no. 4773; left), but much of this color went away (along with the filler) after soaking in ethanol (right).



Surface-Hardened Fillers. No obvious changes were seen in the emeralds with surface-hardened fillers, although several showed slight changes. For instance, filler was oozing out of emerald no. 4745 after chill-thaw durability testing, suggesting that the hard surface of the Opticon had cracked, which allowed the softer filler at greater depths to escape.

Solid Fillers. There were no obvious changes from time alone in emeralds treated with the hard fillers Gematrat and Permasafe; but three of 16 emeralds (all three filled with Gematrat) showed obvious changes with other types of exposure (display case, chill-thaw cycles, and desiccation). Feathers became more evident, showing separation of the filler from the emerald (i.e., delamination along the width; figure 20) and extension of fissures at the edges of the filled areas (again, see figure 9). Although slight changes in the samples treated with Permasafe were observed under these conditions, one emerald (no. 5587), which showed no macroscopic change over time, revealed fissures extending in length beyond the filled area when examined with the microscope. Thus, further fracturing of emeralds with both of these hard fillers was observed under various conditions, suggesting that hard fillers in general might cause such problems due to differential thermal expansion (like granite being cracked by ice).

One emerald treated with Permasafe showed obvious changes (partial emptying of fissures) after cleaning with ethanol and acetone (again, see figure 15). Otherwise, appearance changes related to the cleaning of emeralds with hard fillers were slight at most.

Nature of Appearance Changes and Damage in Emeralds. The changes that cause the greatest concern are those that damaged the emeralds themselves, by feather extension (again, see figure 9). (Fissure widening may also damage emeralds, but this study generally did not distinguish widening from fissures opening up, delaminating, or becoming more evident, all of which could be due to



Figure 18. The observed changes in the filled emeralds varied dramatically (from none to obvious) depending on the viscosity of the filler and the type of durability test. Generally, cleaning the filled emeralds led to much more noticeable differences in their appearance than the exposure tests.

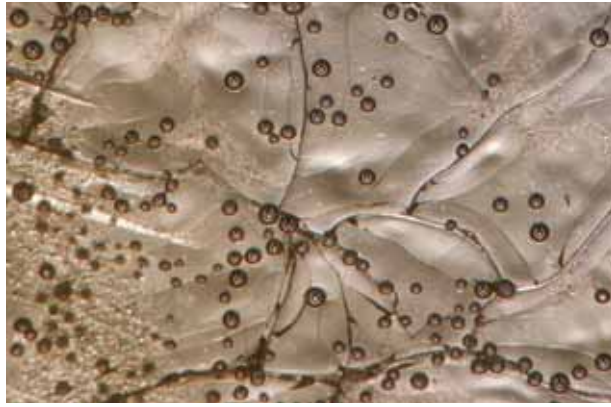


Figure 19. This magnified (20×) image of Canada balsam (poured on a slide in the mid-20th century) shows cracks, gas bubbles, and an irregular surface. Anecdotal evidence indicates that Canada balsam solidifies and gets darker over decades.

changes in the filler rather than the emerald.) The next level of concern is for changes that occur within filled fissures (cloudy or crystallizing filler), as the changed material invariably affects the apparent clarity of the emerald and may be hard to remove. Open, leaking, and more evident feathers also cause worries for jewelers since these are likely to dismay customers.

Most of the exposure conditions (e.g., the long-wave UV component of sunlight, mild heat and light [as approximated by a display-case environment], along with cold and temperature fluctuations [chill-thaw cycling]) did not significantly affect the appearance of most filled emeralds. However, repeated exposure to cold should be avoided, since this extended the fissures in two emeralds, and one sam-

Figure 20. Delamination, or separation of the filler in fissures from the host emerald, makes this fissure in a Gematrat-filled emerald (no. 4816) more obvious after chill-thaw testing. Photomicrograph by Shane F. McClure, magnified 25×.



ple showed the filler delaminating from the walls of the fissures (again, see figure 20).

Two emeralds filled with paraffin oil showed filler crystallization at depth (again, see figure 5) under mild conditions (time, display case exposure). Cloudy filler was seen in one sample filled with Araldite 6010 (figure 4); Johnson et al. (1999) noted that such resins form cloudy emulsions with water in emeralds, which might account for the change seen here. Since cloudy or crystallized material might require additional effort to remove from a filled emerald, these emeralds might need extra attention during refilling.

The most common exposure-related appearance change, with 16 cases, was the greater visibility of preexisting feathers. These changes apparently did not represent damage to the emerald (as seen by comparing “before filler” images to “after testing” images), but they exposed its natural (prefilled) state after the filler had leaked out or evaporated (again, see figures 8 and 10). Four cases of more evident fissures after testing involved surface-hardened or hard fillers; these represent some change besides leakage or evaporation. The most obvious explanation would be that the hard filler separated from the emerald surface, thus letting out filler (seen as leakage) or letting in air.

Another common change, with 11 examples seen in the exposure tests, was the apparent opening up of preexisting feathers. In most of these cases presumably the fissures were already open at the surface (again, see figure 6) so that fillers evaporated; but fissures opening wider is another possible cause for this change.

Four emeralds with more evident or open feathers after the exposure tests contained hard fillers: two with Gematrat (figure 7), and two with Permasafe. The changes occurred during the display-case and desiccation tests. As with sample no. 5587 mentioned above, which cracked microscopically over time, these samples suggest that hard fillers may cause appearance changes—or even damage emeralds—without being subjected to particularly harsh circumstances.

CONCLUSIONS

Durability testing was performed on 142 emeralds using nine fillers. About 35% of the filled emeralds changed in appearance due to rather mild durability testing. The desiccation test affected the highest percentage of the samples subjected to those condi-



Figure 21. Emeralds create memorable pieces of jewelry such as these two rings (left, 3.30 ct; right, 16.16 ct).

However, to help preserve their beauty, filled emeralds need to be treated with care and not subjected to extreme environments. Courtesy of Grando Inc., Los Angeles; photo by Harold & Erica Van Pelt.

tions, but the chill-thaw cycles led to the most damage to individual stones.

Every filler type showed changes with one or more types of exposure. In most cases after testing, the filled emeralds resembled their unfilled condition, with feathers that were opening or more visible. Emeralds with soft fillers were the most likely to be affected. Such changes might not damage the emeralds, but they could distress a customer who had not realized the emerald was filled. A few of the emerald fillers showed crystallization at depth (paraffin oil) or cloudiness (Araldite 6010). In other emeralds, many with hard fillers, the fissures appeared to have been extended or broadened. The surface-hardened fillers showed the least damage from exposure tests, with no obvious changes.

In the cleaning tests, a desirable filler would be durable during jewelry cleaning (e.g., ultrasonic tests), but easily removed with the “right” solvent. However, almost every filler that was easily removed (with either ethanol alone, or ethanol and acetone) was also easily changed by ultrasonic cleaning, which is probably the most common method used for cleaning jewelry. Surface-hardened and hard fillers were the most durable in jewelry cleaning.

The following limitations of this study should be made clear to the reader: (1) Only a limited

number of samples with each filler were tested; (2) the study did not include tests independent of the time factor; (3) it did not test any fillers first in use after 1998, such as the successors of Gematrat (the ExCel types), NOA 71, or “Perma”; and (4) the data for acetone are not independent of the ethanol results. Additionally, although this study dealt with emeralds that were filled after faceting, recent reports describe significant durability problems related to emeralds filled while in the rough or preformed state (Roskin, 2007). Finally, variations in locality of origin, prior filling history, and original clarity of the emeralds could also affect the outcome of these durability tests. It is clear that more work remains to be done.

Fillers add risk by hiding or disguising existing durability problems. There is also the risk involved in cleaning and filling the emerald—and removing damaged fillers. None of the fillers used for this study were stable to all the tests, but the results imply that the best candidate with regard to the durability of the filled emerald’s appearance under conditions of normal wear and care appears to be a surface-hardened liquid. Additional concerns apply, though. For example, surface-hardened liquids may be difficult to remove in the event of an appearance change, or a client’s desire to have an untreated stone; and viscous liquids usually require pressure if they are to be introduced into emeralds, creating additional risks in the filling process (see, e.g., Kennedy, 1998).

Although emeralds are often set with diamonds (figure 21), these results show that emeralds should not be treated in the same manner. Emerald appearance can be quite variable over time and quite susceptible to environmental conditions.

So what should a jeweler tell a client? The bottom line is that filled emeralds—which are most emeralds—require maintenance and disclosure. Here is a possible script:

“Like pearls, and unlike most diamonds, your emerald is a delicate stone. It has probably had its fissures filled and sealed in some fashion. You should clean it only with soap and water, and avoid ultrasonic cleaning or harsh chemicals. If you notice a change, bring it back and we will be happy to have it resealed (just as we would help you by cleaning your jewelry, or replacing watch batteries). If you are concerned about the extent to which it is enhanced, we can get a laboratory report for you.”

ABOUT THE AUTHOR

Dr. Johnson is the principal of Mary Johnson Consulting, San Diego, California. Most of the research on which this article is based was performed while she was manager of Research and Development at GIA in Carlsbad.

ACKNOWLEDGMENTS

The author wishes to thank the following individuals for sharing their knowledge of emerald enhancements: Ricardo Alvarez Pinzon, Luis Ernesto Vermudez, and others at Treatment World Emerald Gemológico Universal, Bogotá, Colombia; Dr. Rodrigo Giraldo, Centro Gemológico para la Investigación de la Esmeralda, Bogotá; Carlos Osorio, Mineralco, Bogotá; Jaime Rotlewicz, C. I. Gemtec, Bogotá; the staff of Alagecol (Asociación de Laboratorios Gemológicos), Bogotá; Darold Allen, Gemological Laboratory of Los Angeles, California; Kenneth Scarratt, AGTA Gemological Testing Center, New York City; Amnan Gad, Amgad Inc., New York City; Michael and Ari Gad, Gad International Ltd., New York City; Morty Kostetsky, Arigad Gems, New York City; Dr. Kumar Shah, Real Gems Inc., New York City.

The company Eichhorn (San Jose, California) donated emerald samples. Arthur Groom and Fernando Garzon (Arthur Groom-Gematrat, New York) provided emeralds, cleaning services, and Gematrat filling. David Kaassamani (Kaassamani and Co. Intl., South Lake Tahoe, California), Daniel Sauer (Amsterdam Sauer, Rio de Janeiro), Dr. R. Shah (Real Gems Inc., New York), Maurice Shire (Maurice Shire Inc., New York) provided emeralds. In New York, Abe Nassi provided useful insights. Many thanks also to the staff of Proexport Colombia (Bogotá), including Ana Maria Lleras and Cristina Montejó, for their hospitality while the author was in Colombia.

Colgem Ltd. (Ramat-Gan, Israel; through the help of Israel Eliezi), Ron Ringsrud (Constellation Colombian Emeralds, Saratoga, California), and Ray Zajicek (Equatorian Imports, Dallas, Texas) filled some of the emeralds. Ray Zajicek also provided useful comments on this manuscript. Zamrot Ashalim Engineering Ltd. (Ramat-Gan, Israel) and Jairo Vaca Camacho (Bogotá) provided equipment to assist with the emeralds that were filled at GIA.

Dr. Henry Hänni, and J.-P. Chalain, SSEF Swiss Gemmological Institute, Basel, and Dr. Lore Kiefert, then with SSEF, provided hospitality and information about the identification techniques used in their laboratory. The author also thanks the organizers of the First World Emerald Congress in Bogotá for their warm hospitality.

Former senior research associate Sam Muhlmeister performed emerald filling at GIA in Carlsbad, with assistance from analytical equipment supervisor Shane Elen. Adolfo Miranda of Col Quimicos Ltda., Bogotá, provided data sheets on Ciba-Geigy Araldite 6010.

Many current and former GIA colleagues provided support for this project. Shane McClure, Maha DeMaggio, John Koivula, Dino DeGhionno, Kim Rockwell, and Jo Ellen Cole, GIA Carlsbad, determined gemological properties. Also in Carlsbad, early FTIR and Raman spectra were collected by Shane Elen and Sam Muhlmeister; recent spectra were taken by research scientist Dr. Christopher M. Breeding, who also provided helpful comments on parts of this manuscript. Steam cleaning was performed by staff gemologist Eric Fritz. Dr. Peter Buerki (former research scientist) provided useful comments and calculations; Mike Moon (former research technician) and Arizona research scientist Dr. Troy Blodgett helped set up the display case test. Margot McLaren of the Richard T. Liddicoat Gemological Library and Information Center, Carlsbad, located auction records; and Dr. James Shigley, Tom Moses, Dr. Ilene Reinitz, and Phil York gave suggestions that improved this manuscript. We also wish to thank the manuscript reviewers for their monumental efforts.

Unless otherwise noted in the figure captions, all photographs were taken by Maha Calderon (former staff gemologist in Carlsbad), Don Mengason and Shane McClure of the GIA Laboratory in Carlsbad, Elizabeth Schraeder (formerly of the GIA Laboratory in New York), Robert Weldon of the Richard T. Liddicoat Library and Information Center in Carlsbad, and the author.

GIA thanks Jewelers' Circular-Keystone, Radnor, Pennsylvania, and Kyocera Corp., Kyoto, Japan, for financial support of this research project. Michael Scott generously donated a Renishaw Raman microspectrometer to GIA, which was used in this research.

REFERENCES

- Costanza F.S. (1998) Undisclosed gem treatment airs on national TV show. *National Jeweler*, Vol. 42, No. 1, pp. 1, 42.
- Drucker R.B. (1999) Venue and value: The wide-ranging prices of sapphires and emeralds. *JCK*, Vol. 170, No. 3, pp. 174–176, 178, 180–181.
- Federman D. (1998a) Fair play. *Modern Jeweler*, Vol. 97, No. 2, p. 108.
- Federman D. (1998b) Inside story. *Modern Jeweler*, Vol. 97, No. 6, p. 17.
- Gomelsky V. (2003) Emerald is back, say dealers. *National Jeweler*, Vol. 97, No. 8, p. 28.
- Jennings R.H., Kammerling R.C., Kovaltchouk A., Calderon G.P., El Baz M.K., Koivula J.I. (1993) Emeralds and green beryls of Upper Egypt. *Gems & Gemology*, Vol. 29, No. 2, pp. 100–115.
- Jewelry scene: Coming clean (1998) *Modern Jeweler*, Vol. 97, No. 1, pp. 9–10, 12.
- Johnson M.L., Elen S., Muhlmeister S. (1999) On the identification of various emerald filling substances. *Gems & Gemology*, Vol. 35, No. 2, pp. 82–107.
- Johnson M.L., Koivula J.I., Eds. (1996) Gem news: Durability of polymer-impregnated (B-type) and natural jadeite. *Gems & Gemology*, Vol. 32, No. 1, pp. 61–62.
- Johnson M.L., Koivula J.I., Eds. (1997) Gem news: A new emerald filler. *Gems & Gemology*, Vol. 33, No. 2, pp. 148–149.
- Kammerling R.C., Koivula J.I., Kane R.E., Maddison P., Shigley J.E., Fritsch E. (1991) Fracture filling of emeralds: Opticon and traditional "oils." *Gems & Gemology*, Vol. 27, No. 2, pp. 70–85.
- Kammerling R.C., McClure S.F., Johnson M.L., Koivula J.I., Moses T.M., Fritsch E., Shigley J.E. (1994) An update on filled diamonds: Identification and durability. *Gems & Gemology*, Vol. 30, No. 3, pp. 142–177.
- Kennedy H.F. (1998) Brazilian emeralds: Oiling at the source. *National Jeweler*, Vol. 42, No. 10, pp. 36, 38, 42, 46, 48, 50, 52.
- Koivula J.I. (1980) Fluid inclusions: Hidden trouble for the jeweler and lapidary. *Gems & Gemology*, Vol. 16, No. 8, pp. 273–276.
- Koivula J.I., Kammerling R.C., Fritsch E., Fryer C.W., Hargett D., Kane R.E. (1989) The characteristics and identification of filled diamonds. *Gems & Gemology*, Vol. 25, No. 2, pp. 68–83.
- Koivula J.I., Kammerling R.C., Fritsch E., Eds. (1993) Gem news: Apparatus for fracture filling gems. *Gems & Gemology*, Vol. 29, No. 1, pp. 62–63.
- Koivula J.I., Kammerling R.C., Fritsch E. (1994a) Emeralds from Brazil. *Gems & Gemology*, Vol. 30, No. 1, pp. 49–50.
- Koivula J.I., Kammerling R.C., Fritsch E. (1994b) Gem news: New emerald treatment/polishing systems from Israel. *Gems & Gemology*, Vol. 30, No. 2, pp. 129–130.
- Lurie M. (1998) Emerald congress spotlights Colombian industry. *Colored Stone*, Vol. 11, No. 3, pp. 1, 84–89.
- Martin D.D. (1987) Gemstone durability: Design to display. *Gems & Gemology*, Vol. 23, No. 2, pp. 63–77.
- McClure S.M., Moses T.M., Tannous M., Koivula J.I. (1999) Classifying emerald clarity enhancement at the GIA Gem Trade Laboratory. *Gems & Gemology*, Vol. 35, No. 4, pp. 176–185.
- Michelou J.-C. (1999) Nouvelles de Bogota. *Revue de Gemmologie*, No. 136, pp. 8–9.
- Myth of the month: Excel & Gematrat are the same? (2006) *The Eternity Report*, Vol. 3, January 2006, p. 4.
- New emerald process developed (1997) *Jewellery News Asia*, No. 157, September 1997, pp. 1, 113–114.
- New type of epoxy resin. (1998) *Jewellery News Asia*, No. 172, December 1998, p. 60.
- Notari F., Grobon C., Fritsch E. (2002) Observation des émeraude traitées en luminescence U-VISIO. *Revue de Gemmologie*, No. 144, pp. 27–31.
- Rate of paper degradation: The predictive value of artificial aging tests (2001) *Abbey Newsletter*, Vol. 24, No. 6, pp. 107–108.
- Ringsrud R. (1983) The oil treatment of emeralds in Bogotá, Colombia. *Gems & Gemology*, Vol. 19, No. 3, pp. 149–156.
- Ringsrud R. (1998) Enhancement process under review. *Jewellery News Asia*, No. 161, pp. 52–53.
- Roskin G. (2002) C.E.L. renames Gematrat emerald filler. *JCK*, Vol. 173, No. 2, p. 44.
- Roskin G. (2003) New Excel enhancement: R.I. = 1.52? *JCK*, Vol. 174, No. 3, pp. 40, 42.
- Roskin G. (2007) "Emerald crack-up." *JCK*, Vol. 178, No. 6, pp. 288–292.
- Weldon R. (1997) Renewing trust in emeralds. *JCK*, Vol. 168, No. 9, September 1997, pp. 80–84.
- Weldon R. (1999) New emerald treatment at the source. *Professional Jeweler*, Vol. 2, No. 4, p. 45.

CONTINUITY AND CHANGE IN CHINESE FRESHWATER PEARL CULTURE

Doug Fiske and Jeremy Shepherd

The great majority of Chinese freshwater cultured pearls are produced by implanting tissue pieces in the mantle of *Hyriopsis cumingii* mussels. Farmers have experimented with bead nucleation, but until recently the methods tried did not produce the quantity or quality necessary for economic success. In the late 1990s, Chinese researchers imported *H. schlegelii* mussels from Japan, began propagating them in hatcheries, and started cross-breeding them with native *H. cumingii* mussels. Using the two pure species and the hybrid, Chinese farmers produce tissue-implantation-only cultured pearls and have developed a method called coin-bead/spherical-bead nucleation. This method has yielded significant quantities of jewelry-quality baroque shapes and lesser quantities of jewelry-quality rounds and near-rounds. Continued experimentation is expected to increase the percentage of rounds and near-rounds.

In April 2007, the authors traveled to some of the freshwater pearl culturing provinces in China. One author (DF) had visited the area in 1998, and the other (JS) had visited several times a year since 1996. The authors' purposes were to gather information for the revision of the GIA *Pearls* course (DF) and for the online forum Pearl-Guide.com (JS), and to buy commercial quantities (JS) of Chinese freshwater cultured pearls (CFCPs). The authors found that, like virtually everything in China, freshwater cultured pearl production is changing rapidly. This

article reviews the current situation and describes some of the changes. Unless otherwise indicated, the information came from interviews with Chinese pearl farmers, processors, and dealers, and from the authors' observations while visiting pearl farms in Anhui, Jiangsu, and Zhejiang provinces.

PAST AND PRESENT

Since about 1970, when small "rice" pearls first appeared internationally, the overwhelming majority of CFCPs have been produced by implanting tissue pieces from donor mussels in the mantles of host mussels, waiting several years, and harvesting the resulting cultured pearls. At an unknown time after the introduction of this process, farmers began producing a far smaller volume of bead-nucleated CFCPs. Over the years, they experimented with various means of bead nucleation.

Tissue Pieces Only. Today, the great majority of CFCPs are produced by implanting donor-mussel tissue pieces in the mantles of *Hyriopsis cumingii* (triangle shell, *san jiao fan bang* in Mandarin Chinese) mussels, waiting three to five years, and harvesting the resulting cultured pearls. For 2006, the most frequently cited volume was 1,500 metric tons (J. Chan, T. Shou, F. Tian, and W. Zhan, pers. comms., 2007). About 800 metric tons were suitable for use in jewelry (J. Chan, pers. comm., 2007), some of superior quality (figure 1).

See end of article for About the Authors and Acknowledgments.
GEMS & GEMOLOGY, Vol. 43, No. 2, pp. 138–145.
© 2007 Gemological Institute of America



Figure 1. These round (6.5–7.5 mm), natural-color, exceptional-quality Chinese freshwater cultured pearls were grown with tissue implantation only. They were not treated in any way. The authors were not present at the harvest and could not identify the mussel that produced them. Courtesy of PearlParadise.com; photo by Kevin Schumacher.

Bead Nucleation. Akamatsu et al. (2001) reported three bead-nucleation methods then used in Chinese freshwater pearl culture. Of these, the present authors found only “bead nucleation by direct operation” still being practiced by some Chinese freshwater pearl farmers. To understand this method and its results, it is helpful to use the terms *first generation* and *second generation*.

With direct operation, first generation is the implantation of tissue pieces as mentioned above. Generally, the mussel mortality rate at first-generation harvest is 90% (W. Zhan, pers. comm., 2007). At that time, technicians assess the health of the surviving mussels and the quality of the cultured pearls produced. They return some mussels to the water to create second-generation cultured pearls. Technicians implant some of the original pearl

sacs with a spherical bead nucleus or a nucleus of one of several other shapes. They leave other pearl sacs empty to produce what Chinese farmers call “keshi”^{*} pearls. The ensuing pearl-growth period is three to four years (W. Zhan, pers. comm., 2007).

With the direct-operation method, second-generation cultured pearl quality is worse than first generation, and there is a lower incidence of rounds and near-rounds. The second-generation harvest contains many buttons and baroques, some with tails (J. Chan, Y. Lou, and W. Zhan, pers. comms., 2007).

RECENT DEVELOPMENTS

During our trip, we learned of two important developments in Chinese freshwater pearl culture. One involved the introduction of a non-native mussel, its hybridization with a native mussel, and the evident use of both pure species and the hybrid in pearl culture. The other development was an innovative bead-nucleation process.

***H. schlegelii* in China.** Some Chinese pearl farmers reported that *H. cumingii* is still the only mussel

^{*}As used by Chinese freshwater cultured pearl farmers, processors, and dealers, the term *keshi* does not fit the CIBJO definition, which refers to a similar product but restricts it to saltwater pearl culture. This article reflects Chinese usage, which defines *keshi* as a second-generation cultured pearl created in a pearl sac that formerly held a cultured pearl or shell bead of any shape.



Figure 2. When the CBSB-nucleated freshwater cultured pearls known as “fireballs” first appeared on the wholesale market in 2002, luster and surface quality were poor, as this strand (10–11 mm) shows. Courtesy of PearlParadise.com; photo by Kevin Schumacher.

they use to culture freshwater pearls. However, a large pearl-farming company in Zhuji said that 80% of its mussels are *H. cumingii* and 20% are *H. schlegelii* (pond butterfly shell, *ci die bang* in Mandarin Chinese). That company estimated that generally in China, 70% of the freshwater cultured pearl production is from *H. cumingii*, while 30% is from *H. schlegelii*. In Japanese, “pond butterfly” is *ikecho*, also called the Biwa pearly mussel.

M. Fujita began culturing freshwater pearls in *H. schlegelii* at Lake Biwa, Japan, in 1914 (*Pearl Museum*, 1998). Freshwater pearl culture continues at Lake Biwa to this day, although pollution has severely reduced the volume (Pawasarat, 2007). Due to their colors and quality, Japanese Biwa cultured pearls have achieved something of a legendary status in pearling circles.

Evidence indicates that some Chinese freshwater pearl farmers have been culturing pearls in *H. schlegelii* and in the *H. cumingii* × *H. schlegelii*



Figure 3. The CBSB-nucleation method recently produced these four baroques and one “keshi” (center). They were sieve-sized at 13–14 mm. Excellent luster and variable color are often seen in CBSB-nucleated pearls harvested today. Courtesy of Sea Hunt Pearls; photo by Kevin Schumacher.

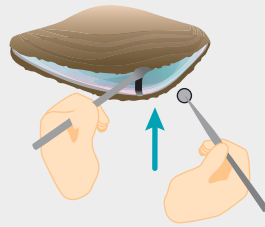
hybrid for several years. A search of the Chinese-language scientific literature reveals a strong presence of *H. schlegelii* in China, its superiority to *H. cumingii* as a pearl-bearing mussel, and the superiority of its hybrid with *H. cumingii* to either pure species with respect to pearl culture (e.g., Lei, 2005; Xu et al., 2005; Xie et al., 2006).

Coin-Bead/Spherical-Bead (CBSB) Nucleation. This method involves implanting a coin-shaped bead and tissue piece at first generation, and often only a spherical bead at second generation. The process produces the CFCPs called “fireballs” (figure 2), other baroque shapes, “keshis,” “coin pearls,” and rounds and near-rounds. The volume is significant and growing rapidly, but producers will not give specifics (J. Chan and W. Zhan, pers. comms., 2007). Rounds range from 10 to 15.5 mm, while baroques can measure up to 25 mm long. Natural colors include “lavender,” purple, “peach,” “gold,” blue, and white (see, e.g., figure 3). Several colors often appear in the same cultured pearl. We believe this method (figure 4) is used with *H. cumingii*, *H. schlegelii*, and the *H. cumingii* × *H. schlegelii* hybrid.

Fireballs first appeared on the wholesale market in 2002. They and other CBSB pearls have been mentioned and shown in some trade publications, and the production method has been touched upon, but not explored in detail (Federman, 2006; Wong, 2006). In standard pearl terminology, fireballs are baroques. They come in an infinite variety of shapes. What they have in common is a bulb somewhere in the cultured pearl and, sometimes, a spiked tail stretching from it. As noted above,

Coin-Bead/Spherical-Bead (CBSB) Nucleation and Alternatives

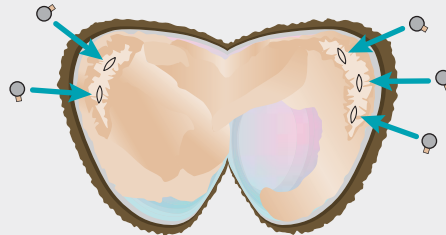
Process begins when the *Hyriopsis cumingii* mussel measures about 14 cm in diameter and is three to four years old.



- ◊ Incision
- ▣ Tissue piece
- Coin bead
- Empty pearl or "keshi" sac
- "Coin pearl"
- "Keshi"
- Spherical bead
- CBSB round pearl
- CBSB baroque pearl

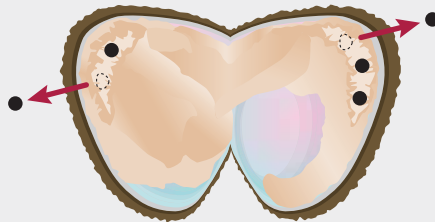
Shells are shown open for illustration purposes only.

1 Implant coin beads and tissue pieces in posterior ventral margin of each valve.



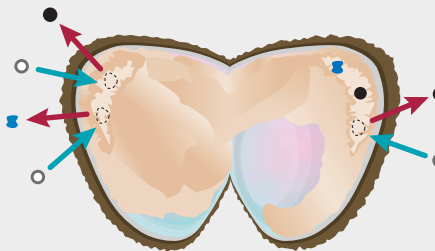
2 Wait one year.

3 Leave "coin pearls" in mantle to grow, or harvest "coin pearls" and return mussel to water to grow "keshis." Choice varies within each mussel and among all mussels.



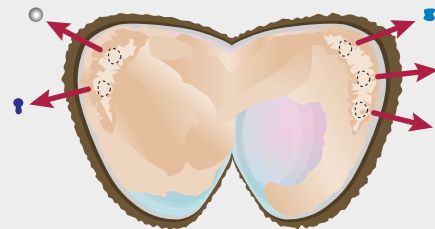
4 Wait one year.

5 Harvest "coin pearls" or "keshis," and implant spherical beads in existing pearl sacs. Or don't harvest "coin pearls" or "keshis," and let either or both continue to grow. Choice varies within each mussel and among all mussels.



6 Wait one or two years.

7 Harvest CBSB pearls and/or "coin pearls" and "keshis."



Total pearl-growth period is three or four years. Mussel is six to eight years old at final harvest. Alternatives are shown in one mussel and can vary among mussels.

Figure 4. Illustrated here are the various options for coin-bead/spherical-bead nucleation in *H. cumingii* as practiced on some freshwater pearl farms in China. Evidence indicates the method is also used with *H. schlegelii* and the *H. cumingii* × *H. schlegelii* hybrid. Illustration by Karen Myers.



Figure 5. These “coin pearls” and “keshis” were harvested prematurely for demonstration purposes about 17 months after coin beads were implanted. One year after implantation, the farmer left these “coin pearls” in the mussels to continue to grow. At that time, he harvested other “coin pearls” and returned the *H. cumingii* mussels to the water to let them develop “keshis.” The “keshis” shown are about five months old. Courtesy of He Jainhua; photo by Valerie Power.

however, other pearls cultured by the same means are round or near-round.

When Chinese freshwater pearl farmers use *H. cumingii* to start the process that yields fireballs and other shapes, the mussel measures about 14 cm in diameter and 19 cm laterally. At that size, it is between three and four years old. Technicians implant two or three coin-shaped shell beads, each accompanied by a 1-mm-square donor-mussel tissue piece, in the posterior ventral margin of each

valve. The low number of beads helps ensure bigger and better-quality cultured pearls. The unusually small tissue piece helps minimize or eliminate the tail on the resulting “coin pearl” (J. He, pers. comm., 2007).

After one year, farmers decide on one of two steps to take next. First, their technicians can harvest the “coin pearl” and return the mussel to the water for another year to produce an often petal-shaped “keshi” pearl. Second, they can let the “coin pearl” continue to grow for an additional year (figure 5).

After the second year, farmers make one of three choices for each pearl sac. First, their technicians can harvest the “coin pearl” or “keshi” and place a 9–12.5 mm spherical bead in each of the empty pearl sacs. Second, they can let the existing “coin pearl” continue to grow. Third, they can let the existing “keshi” continue to grow. After the choice is made, technicians return the mussel to the water for one or two additional years. At this stage, a two-year pearl-growth period produces bigger and better-quality cultured pearls (J. He, pers. comm., 2007).

X-radiography at the GIA Laboratory in Carlsbad revealed the internal features of the three different kinds of cultured pearls produced by this method (figure 6). X-ray fluorescence and EDXRF testing of the beads in round and baroque samples proved they were of saltwater-mollusk origin (figure 7). Beads used in saltwater pearl culture and the direct-operation freshwater pearl culture method

Figure 6. The photograph (left) and composite X-radiograph (right) are of the same CBSB-nucleated cultured pearls and are configured in parallel. The top sample shows a spherical bead nucleus, the one on the left shows a coin bead nucleus, and the one on the right is a “keshi” with no nucleus. The samples were sieve-sized at 12–14 mm. Courtesy of Sea Hunt Pearls; photo by Kevin Schumacher, X-radiograph by Cheryl Wentzell.

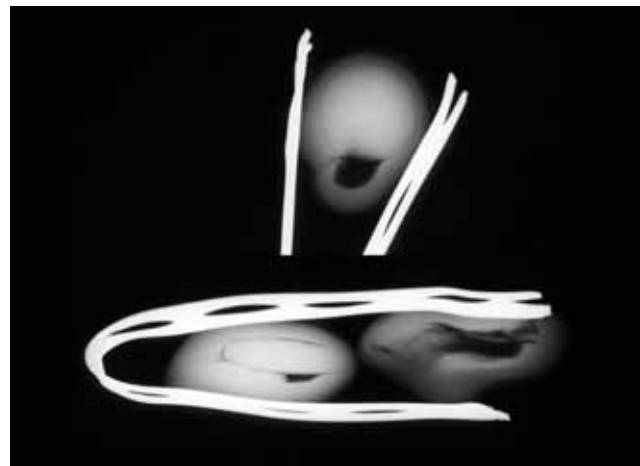




Figure 7. A 13.4 mm CBSB-nucleated round pearl sawn in half on the drill-hole axis revealed a 10.7 mm shell bead (left). An 11 × 23 mm CBSB-nucleated baroque pearl sawn in half on the long axis revealed a 9 mm shell bead (right). X-ray fluorescence and EDXRF tests proved the beads to be of saltwater origin. Courtesy of Sea Hunt Pearls; photos by Kevin Schumacher.

described above are virtually always of freshwater-mussel origin.

During the final CBSB one- or two-year pearl-growth period, *H. cumingii* typically deposits 0.5–0.75 mm of nacre per year on the “coin pearl,” on and often adjacent to the spherical shell bead, and on the “keshi.” In two years, a 12 mm spherical bead can become a 15 mm round or near-round cultured pearl, or a baroque cultured pearl with or without a tail (J. He, pers. comm., 2007).

How the tail develops or why it does not is not precisely known. Speculation centers on what happens when a technician places a spherical bead in a coin-shaped pearl sac. The result depends on the size of the spherical bead and sac, where in the sac the technician presses the spherical bead, the elasticity of the sac, and how the mantle tissue reacts. The technician’s skill and his or her possible introduction of random epithelial cells can also affect the final product (J. He and G. Latendresse, pers. comms., 2007).

The incision that permits removal of a coin bead and insertion of a spherical bead is lateral and faces the technician. If the mussel accepts the spherical bead and heals the incision, the pearl sac closes and the mantle tissue deposits nacre. If the mussel expels the spherical bead, a “keshi” pearl forms in the sac and becomes whatever shape the sac adopts after the incision heals.

If the pearl sac completely conforms to the spherical bead (figure 8), it deposits nacre only on the bead, and a round or near-round cultured pearl results. If the pearl sac does not conform to the spherical bead, it deposits nacre on the bead and in

any void that remains in the sac. In that case, a baroque cultured pearl results, with or without a tail. Baroques occur more frequently than rounds and near-rounds.

Figure 8. This spherical bead in an *H. cumingii* mussel was on its way to becoming a CBSB-nucleated cultured pearl. The cultured pearl would probably have been round or near-round when harvested, because the formerly coin-shaped pearl sac had conformed closely to the spherical bead. A technician implanted the spherical bead about five months before the photo was taken, along with other spherical beads that had been removed at the time of photography. Photo by Valerie Power.





Figure 9. The 12–14 mm baroque CFCPs in these strands were produced using the CBSB-nucleation method. Those in the multicolored strand are natural color, while those in the white strand were bleached. A 15 mm bleached round CFCP is shown for comparison. The authors could not identify the mussel that produced these CFCPs. Courtesy of Sea Hunt Pearls; photo by Kevin Schumacher.

CONCLUSION AND PROJECTION

Chinese freshwater pearl farmers are creative, industrious, and resourceful people. They originated pearl culture about 800 years ago by creating blister pearls in *Cristaria plicata* mussels. In the 1960s and 1970s, they flooded the market with wrinkled, oddly shaped “rice” pearls, also grown in *C. plicata*. In the 1980s, farmers switched to *H. cumingii* mussels, maintained a huge volume, and began improving their product in every value factor. In the late 1990s, Chinese researchers imported *H. schlegelii* from Japan, propagated the species in hatcheries, and produced a hybrid with *H. cumingii*. We believe

farmers later began using *H. cumingii*, *H. schlegelii*, and the hybrid to grow tissue-only and CBSB-process cultured pearls (figure 9).

The CBSB method is the latest in a long chain of successes that have resulted from constant experimentation. Some observers now predict that within two years, Chinese freshwater pearl farmers will discover how to control shape using the CBSB method (J. Lynch, pers. comm., 2007), will continue to improve quality, and will consistently produce rounds, near-rounds, and whatever other shapes and quantities the market demands and can absorb.

ABOUT THE AUTHORS

Mr. Fiske (dfiske@gia.edu) is a writer/editor in the Course Development department at GIA in Carlsbad, California. Mr. Shepherd is the founder of PearlParadise.com Inc. and Pearl-Guide.com in Los Angeles.


ACKNOWLEDGMENTS

The authors gratefully acknowledge Jack Lynch of Sea Hunt Pearls in San Francisco for supplying Chinese freshwater cultured pearl samples for examination and photography, and You Hong Qing of Xuwen Jinhui Pearl Co. in Xuwen, China, for research assistance. Special thanks to Faye Tian of Holy City Pearl Co. in Zhuji, China, for being a gracious guide and host. The authors thank Cheryl Wentzell, Sam Muhlmeister, and Dino DeGhionno of the GIA Laboratory in

Carlsbad for the X-radiographs/X-ray fluorescence testing, EDXRF analysis, and sawing, respectively. The authors are grateful to Gina Latendresse of The American Pearl Company in Nashville, Tennessee, for her expertise. The authors are especially grateful to pearl farmers Cai Shui Miao, He Jinhua, and Yang Jinlong of Zhejiang Province; to Joyce Pan, Shao Wei Huan, Wang Jian, and Zhan Wei Jiang of Grace Pearl Co. in Zhuji and Hong Kong; to Lou Yongqi and Shou Tian Guang of Shanxiahui Pearl Group Co. in Zhuji; to Lu Ling Hong of Heng Feng Jewellery Craft Factory and Zhou Hai Lin of Joint Venture Pearls Cultivation Holding Co. in Weitang, Jiangsu Province; and to Johnny Chan of the Hong Kong Pearl Association. Thanks also to Melissa Wong of Jewellery News Asia in Hong Kong for her generous assistance.

REFERENCES

- Akamatsu S., Li T., Moses T., Scarratt K. (2001) The current status of Chinese freshwater cultured pearls. *Gems & Gemology*, Vol. 37, No. 2, pp. 96–109.
- Federman D. (2006) Fireball cultured pearls. *Modern Jeweler*, Vol. 105, No. 6, pp. 51–52.
- Lei S. (2005) Aquaculture varieties: *Hyriopsis schlegelii* artificial breeding. *Journal of Beijing Fisheries*, No. 4, pp. 62–63.
- Mikimoto Pearl Island (1998) *Pearl Museum*. Toba City, Japan.
- Pawasarat C. (2007) Biwa on the edge. *Colored Stone*, Vol. 20, No. 3, pp. 26–30.
- Wong M. (2006) Production of bead-nucleated freshwater pearls on upward trend. *Jewellery News Asia*, No. 261, p. 62.
- Xie N., Li Y., Zheng H., Wang G., Li J., Oi N., Yuan W. (2006) Comparison of culture and pearl performances among *Hyriopsis schlegelii*, *Hyriopsis cumingii* and their reciprocal hybrids. *Journal of Shanghai Fisheries University*, Vol. 15, No. 3, pp. 264–269.
- Xu X., Qiu Q., Sun X., Luo J., Hu G., Jiang Y. (2005) A comparative study of *Hyriopsis schlegelii* and *H. cumingii* mussels in pearl production. *Jiangxi Fishery Sciences and Technology*, No. 1, pp. 39–41.



Give the gift of knowledge.

Whether it's the young family member just starting their gemology education or the client you've done business with for decades, we're sure there's someone on your list who would love a gift subscription to *Gems & Gemology*. Order now and we'll even include this personalized gift card. And if you've got a long gift list, ask about our special rates for bulk subscription orders.

GEMS & GEMOLOGY.
The Quarterly Journal That Lasts A Lifetime

To order, visit www.gia.edu/gemsandgemology and click on *Gift Subscriptions*.
Call 800-421-7250 ext. 7142 within the U.S., or 760-603-4000 ext. 7142.

YELLOWISH GREEN DIOPSIDE AND TREMOLITE FROM MERELANI, TANZANIA

Eric A. Fritz, Brendan M. Laurs, Robert T. Downs, and Gelu Costin

Four similar-appearing yellowish green samples from Block D at Merelani, Tanzania, were identified as diopside and tremolite. The gems are identical in color, but their standard gemological properties are typical for calcic pyroxene and amphibole. The identification of the diopside was made with Raman spectroscopy, while single-crystal X-ray diffraction and electron-microprobe analyses were used to confirm the amphibole species as tremolite. Absorption spectroscopy (in the visible–mid-infrared range) revealed that the two gem materials are colored by V^{3+} , Cr^{3+} , or both.

At the 2006 Tucson gem shows, Steve Ulatowski showed one of the authors (BML) some yellowish green crystals that he purchased as diopside while on buying trips to Tanzania in August and November 2005. The material was reportedly produced during this time period from Block D at Merelani, in the same area that yielded some large tsavorite gem rough (see Laurs, 2006). Mr. Ulatowski obtained 1,200 grams of the green crystals, mostly as broken pieces ranging from 0.1 to 50 g (typically 1–5 g). More recently, in May 2007, he obtained some additional pieces of gem-quality material weighing 0.1–2 g. The “mint” green color is quite attractive, but most of the rough is not cuttable due to the presence of cleavage planes and, in some cases, the flat morphology of the crystal fragments.

In 2006, Mr. Ulatowski was informed by a few of his customers that the flatter crystals might be tremolite, rather than diopside. This was consistent with the diamond-shaped cross-section of these crystals (typical of an amphibole), which was distinct from the blocky cross-section

(typical of diopside, which is a pyroxene) shown by other crystals in the parcels.

Mr. Ulatowski loaned one example of both types of crystals to GIA for examination (figure 1), and we also

Figure 1. These yellowish green crystals were recovered from Block D at Merelani in the latter part of 2005. A blocky morphology is shown by the diopside crystal (1.6 cm tall; left and bottom), whereas the tremolite crystal has a flattened, diamond-shaped cross-section. Photos by Robert Weldon.



See end of article for About the Authors and Acknowledgments.

GEMS & GEMOLOGY, Vol. 43, No. 2, pp. 146–148.

© 2007 Gemological Institute of America



Figure 2. This diopside (3.39 ct) and amphibole (probably tremolite, 0.63 ct) were cut from two yellowish green crystals recovered from Merelani. Photo by Robert Weldon.

studied two gemstones (0.63 and 3.39 ct) that were cut from Mr. Ulatowski's stock (figure 2). Gemological properties and various types of spectra (visible–near-infrared, Raman, and energy-dispersive X-ray fluorescence [EDXRF]) were collected on the faceted stones at GIA by one of us (EAF). Electron-microprobe analyses (Cameca SX50 instrument, 15 kV accelerating voltage, 10 nA current, 10 mm defocused beam, natural mineral standards) and single-crystal X-ray diffraction analysis were performed on the amphibole crystal at the University of Arizona; this sample was donated by Mr. Ulatowski for inclusion in the RRUFF Project (ID no. R070422 at <http://rruff.info>).

Results and Discussion. The gemological properties of the cut stones are shown in table 1. Their optical properties and SG values are consistent with those reported for calcic pyroxene (larger stone; see Deer et al., 1978) and calcic amphibole (smaller stone; Deer et al., 1997), but further work was needed to determine the particular mineral species. Raman analysis of the pyroxene (faceted stone as well as crystal) identified it as diopside, and the RI values indicated that it contained very little iron. The specific amphibole species could not be identified by Raman analysis, but single-crystal X-ray diffraction and electron-microprobe analyses of the crystal proved that it was tremolite. Although the cut amphibole was not analyzed by these techniques, its properties are consistent with tremolite.

EDXRF spectroscopy of the faceted amphibole showed major amounts of Si, Mg, Ca, and Al, and traces of Mn, Fe, V, Ti, K, and Cr. However, since there is overlap in the EDXRF peaks for V and Cr (as well as for Na and Zn), and since this technique is only qualitative, there are some uncertainties regarding the presence of the minor/trace elements that were detected in the cut stone. Using an electron microprobe, wavelength-dispersive X-ray spectroscopy (WDS) of the tremolite crystal showed the presence of Si, Mg, Ca, Al, Na, K, V, and F (listed in order of relative peak intensity). An average of 15 point analyses of the same sample by electron microprobe provided the fol-

lowing composition (wt.%): SiO₂=52.34, Al₂O₃=6.70, MgO=21.81, CaO=13.05, Na₂O=0.73, K₂O=0.67, V₂O₅=0.32, F=0.47, and total 96.05; this corresponds to the chemical formula: $(\square_{0.74}\text{Na}_{0.15}\text{K}_{0.11})_{\Sigma=1}(\text{Ca}_{1.96}\text{Na}_{0.04})_{\Sigma=2}(\text{Mg}_{4.55}\text{Al}_{0.41}\text{V}_{0.04})_{\Sigma=5}(\text{Si}_{7.33}\text{Al}_{0.67})_{\Sigma=8}\text{O}_{22}[(\text{OH})_{1.80}\text{F}_{0.20}]_{\Sigma=2}$. The elements Cr, Ti, Fe, Mn, and Zn did not show detectable peaks in the WDS scan, so their concentrations (if present) are at or below the detection limits of the electron microprobe. Since the faceted stone was not cut from the same crystal that was analyzed by microprobe, differences in the presence of Mn, Fe, Ti, and Cr in these samples may be attributed to natural chemical variations in the material. By comparison, EDXRF spectroscopy of the faceted diopside showed major amounts of Si, Ca, and Mg, and traces of Mn, Fe, V, Cr, Ti, Zn, and Al.

Visible–near-infrared spectroscopy of the two cut stones showed similar absorption features, with broad peaks at 434/455 and 652 nm that are related to V³⁺ or Cr³⁺, or both (figure 3). Similar absorptions were documented by Schmetzer (1982) in green tremolite from Lualenyi, Kenya, and in green diopside from Merelani. A shoulder at ~690 nm in both samples is due to Cr³⁺ (see, e.g., Cr-diopside spectra at <http://minerals.gps.caltech.edu/files/visible/pyroxene/index.htm>). The yellowish green color of both the diopside and the tremolite appears to be related to the presence of trace amounts of V³⁺ and Cr³⁺ in the octahedral sites; Na and K enter the structure by a coupled substitution such as V³⁺ (or Al³⁺) + Na⁺ (or K⁺) ↔ Mg²⁺ + Mg²⁺.

The yellowish green color of these stones is unusual in amphiboles and pyroxenes, although a comparable color appearance has been reported for amphiboles (pargasite and edenite) from China and Pakistan (see Kanaan, 2002; Blauwet et al., 2004; Lu et al., 2006). A similar diopside was documented by Koivula and Kammerling (1991) from the Lelatema Hills of Tanzania; its properties were

TABLE 1. Properties of yellowish green diopside and tremolite from Merelani, Tanzania.

Property	Diopside	Tremolite
Weight	3.39 ct	0.63 ct
Color	Yellowish green	Yellowish green
Pleochroism	None seen	None seen
RI	1.670–1.700	1.610–1.635
Birefringence	0.030	0.025
SG (hydrostatic)	3.30	3.07
Chelsea filter reaction	None	None
UV fluorescence		
Long-wave	Very weak orange	Weak orange
Short-wave	Weak greenish yellow	Moderate greenish yellow
Spectroscope spectrum	No features visible	No features visible
Microscopic features	Only minor surface abrasions	Growth tubes and planar fluid inclusions

comparable to those of the diopside described here, except for somewhat different fluorescence behavior (weak reddish orange to long-wave UV, and strong yellow-green to short-wave). Fryer (1992) reported on a yellowish green diopside from Merelani that had a lower birefringence (0.019; RIs = 1.670 and 1.689) and an absorption spectrum typical of “chrome diopside.” A somewhat less distinct yellowish green bodycolor is shown by diopside (“Tashmirine”) from central Asia (Shor and Quinn, 2002).

Conclusion. Small amounts of gem-quality diopside and tremolite containing traces of V and possibly Cr have been recovered from Block D at Merelani. While pale green diopside is locally present in the Merelani area, the distinct yellowish green color of this diopside and tremolite is unusual. Future production of these

gems is uncertain, and will depend on the mineralization encountered during further mining for tanzanite, green grossular, and other gems at this famous locality.

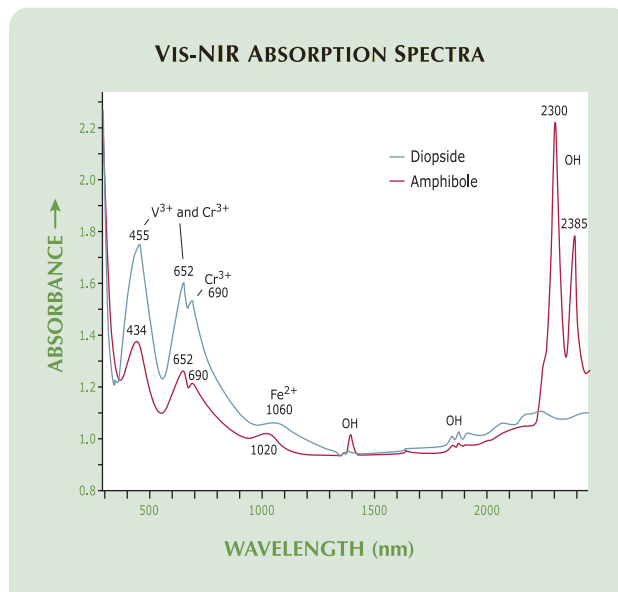
ABOUT THE AUTHORS

Mr. Fritz (eric.fritz@gia.edu) is staff gemologist in the Identification Department at the GIA Laboratory, and Mr. Laurs is editor of *Gems & Gemology*, at GIA in Carlsbad. Dr. Downs is a professor, and Dr. Costin is a research scientist, at the Department of Geosciences, University of Arizona, Tucson.

ACKNOWLEDGMENTS

The authors thank Steve Ulatowski (New Era Gems, Grass Valley, California) for bringing these gem materials to our attention and for loaning/donating samples for our research. Herb Obodda (H. Obodda, Short Hills, New Jersey) loaned the faceted diopside, and Shane McClure (GIA Laboratory, Carlsbad) supplied the cut tremolite.

Figure 3. The Vis-NIR spectra of the faceted yellowish green diopside and amphibole samples are dominated by absorption features related to V^{3+} and/or Cr^{3+} in the visible range and hydrous components in the infrared region (for the amphibole).



REFERENCES

- Blauwet D., Hawthorne F.C., Muhlmeister S., Quinn E.P. (2004) Gem News International: Gem amphiboles from Afghanistan, Pakistan, and Myanmar. *Gems & Gemology*, Vol. 40, No. 3, pp. 254–257.
- Deer W.A., Howie R.A., Zussman J. (1978) *Rock-Forming Minerals—Single-Chain Silicates*, Vol. 2A, 2nd ed. John Wiley & Sons, New York.
- Deer W.A., Howie R.A., Zussman J. (1997) *Rock-Forming Minerals—Double-Chain Silicates*, Vol. 2B, 2nd ed. The Geological Society, London.
- Fryer C.W., Ed. (1992) Gem News: Diopside from Tanzania. *Gems & Gemology*, Vol. 28, No. 2, p. 201.
- Kanaan S.-P. (2002) Gem News International: Pargasite from China. *Gems & Gemology*, Vol. 38, No. 1, p. 97.
- Koivula J.I., Kammerling R.C., Eds. (1991) Gem News: Attractive Tanzanian diopside. *Gems & Gemology*, Vol. 27, No. 4, p. 257.
- Laurs B.M. (2006) Gem News International: Tucson 2006. *Gems & Gemology*, Vol. 42, No. 1, pp. 62–63.
- Lu L., He X., Shen M. (2006) Gemmological study on Cr-bearing edenite. *Journal of Gems and Gemmology*, Vol. 8, No. 2, pp. 17–19.
- Schmetzer K. (1982) Absorption spectroscopy and colour of V^{3+} -bearing natural oxides and silicates—A contribution to the crystal chemistry of vanadium. *Neues Jahrbuch für Mineralogie, Abhandlungen*, Vol. 144, No. 1, pp. 73–106 [in German].
- Shor R., Quinn E. (2002) Gem News International: “Tashmirine”—Diopside from Central Asia. *Gems & Gemology*, Vol. 38, No. 3, pp. 261–262.

For regular updates from the world of **GEMS & GEMOLOGY**, visit our website at:

www.gia.edu/gemsandgemology

POLYMER-IMPREGNATED TURQUOISE

Kyaw Soe Moe, Thomas M. Moses, and Paul Johnson

A large “Persian” turquoise cabochon was impregnated with a material that was also present in cavities on its base. Raman spectroscopy identified the filler as a UV-hardened polymer. Although such polymers have been seen as fillers in other gems, especially emerald, this is the first time the GIA Laboratory has seen turquoise treated with this material.

Turquoise has a cryptocrystalline structure that is composed of very fine, randomly oriented groups of tightly stacked parallel growths of pseudo-rhombohedral crystals (see King, 2002), which contributes to the porous nature of the material. Turquoise is a relatively stable mineral, as evidenced by a necklace showing no sign of deterioration that was found on the skeleton of a Native American dated to 1350 AD (again, see King, 2002). However, because it is porous, turquoise is vulnerable to skin oils or dirt when used in jewelry, both of which can produce a change in color. It is well known that the appearance and durability of turquoise may be enhanced by plastic impregnation, in a process referred to in the trade as *stabilization*.

During the 2007 Tucson gem show, these contributors encountered a 19.08 ct cabochon represented as Persian

turquoise (figure 1). Although no treatments were disclosed, the sample had several small cavities and one large one in its base that were filled or partially filled with a transparent material (figure 1, right). Since this sample offered an excellent opportunity to characterize the material used for stabilization, we purchased it to conduct further studies in the laboratory. We collected standard gemological properties, as well as Raman spectra (using a Renishaw inVia Raman microspectrometer with a 514 nm laser at room temperature) and infrared spectra (using a Nicolet 6700 FTIR spectrometer equipped with a DRIFT accessory).

Results and Discussion. The spot RI was 1.60, and the SG (measured hydrostatically) was 2.48; the presence of the filler may be responsible for the relatively low SG value. With the desk-model spectroscope, the turquoise showed a 430 nm band (of moderate strength, due to iron absorption) and a weaker “smudge” at 460 nm. The turquoise was inert to long- and short-wave UV radiation, although the cavity edges fluoresced yellow to short-wave UV. There was no indication of dye when the sample was exposed to a thermal reaction tester (the color of any dye would be expected to bleed as the sample “sweated” next to the hot point). However, the transparent filler in the large cavity on the base of the cabochon emitted an acrid odor when tested with the hot point.

The characteristic bands in the Raman spectrum of the filler exposed on the base matched those of Norland

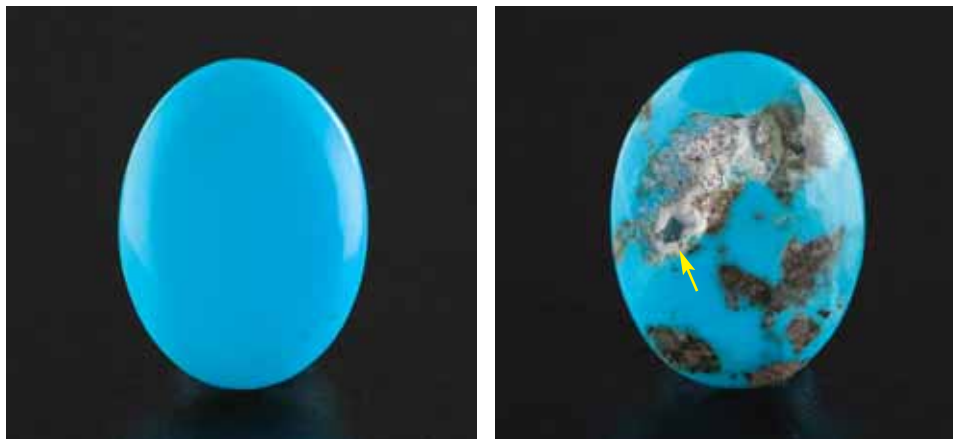


Figure 1. This 19.08 ct turquoise cabochon (top view on the left) was represented as “Persian,” with no treatment disclosed. A large cavity visible on the base (right) is partially filled with a clear polymer, and a whitish residue can be seen in the rest of the cavity. The arrow points to a small transparent lump of the polymer, through which the blue color of the turquoise can be seen.

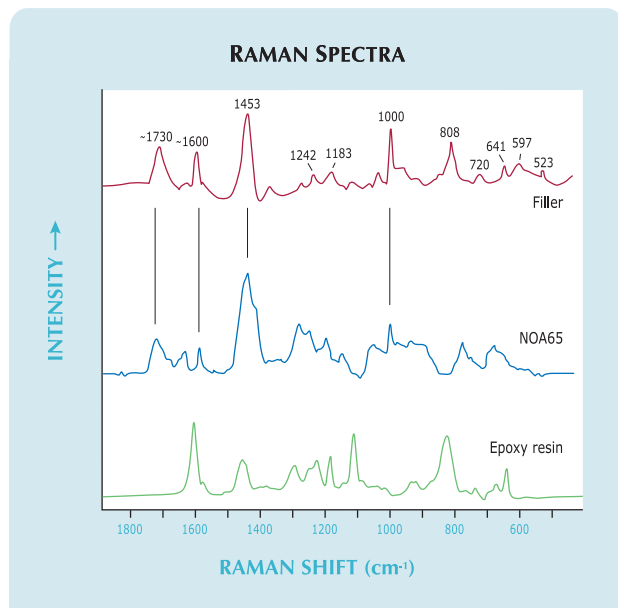


Figure 2. The Raman spectrum of the filling material exposed on the base of the turquoise cabochon shows bands that are characteristic of Norland Optical Adhesive 65. Some additional Raman bands (i.e., at 1242, 1183, 808, 720, 641, 597, and 523 cm^{-1}) suggest that this photopolymer may have been plasticized with other polymers. The Raman spectrum of epoxy resin, which is commonly used for gemstone impregnation, is shown for comparison.

Optical Adhesive 65 (NOA 65, figure 2). This spectrum is quite different from that of the polymers typically used for gemstone filling/impregnation in the trade (e.g., for emerald and jade), such as epoxy resin. Bands characteristic of NOA 65 were observed at ~ 1730 ($\text{C}=\text{O}$ stretching), ~ 1600 , 1453 (CH_3 -bending), and 1000 cm^{-1} (styrene phenyl ring; see Clarke et al., 1999; Miliani et al., 2002). In addition, strong bands in the 3100 – 2800 cm^{-1} region (not shown in the figure) are due to $\text{C}-\text{H}$ stretching, and their intensity is related to the alkyl group (see Nørbygaard and Berg, 2004).

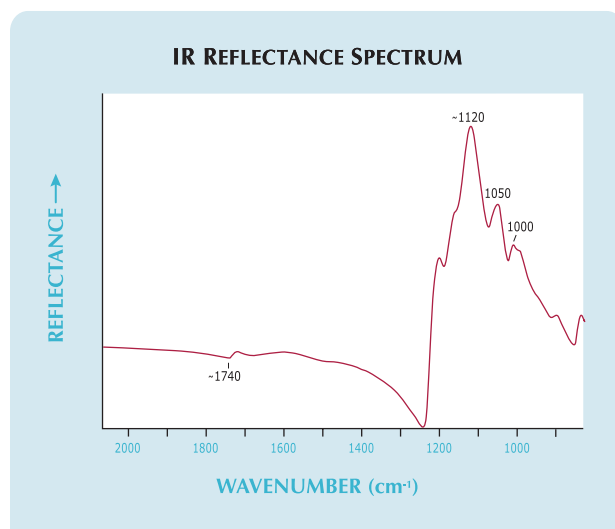
Raman spectroscopy of the top of the cabochon showed turquoise bands along with the major NOA 65 bands. This suggests that the NOA polymer was present throughout the stone, in addition to filling the cavities. Reflectance IR spectroscopy of the top of the cabochon (figure 3) showed turquoise peaks at ~ 1120 , 1050 , and 1000 cm^{-1} , as well as an absorption at ~ 1740 cm^{-1} that is the carbonyl band usually associated with polymers (see Learner, 1998; Fritsch et al., 1999). Since Raman spectroscopy eliminated the possibility of other types of polymers that can be identified by IR

spectral features in the 2700 – 3300 cm^{-1} region, figure 3 focuses instead on the 2000 – 1000 cm^{-1} region, where distinctive bands due to plastics/polymers have been documented in impregnated turquoise.

NOAs are colorless liquid photopolymers. After curing with UV radiation, they become solid and thus polishable. The main advantages of NOAs for gem treatment are transparency, lack of color, and color stability; they can also provide mechanical stabilization of porous materials, such as turquoise, due to their high tensile strength. According to the company's web site (www.norlandprod.com), the NOA photopolymers are inert to sulfuric acid but exposure to acetone, dimethyl formamide, and ethylene dichloride will cause them to swell or soften (based on one-hour exposure time). NOAs are widely used in optical lamination (e.g., optical lenses, safety windows, holographic displays, and flat panel displays) as relatively thin films, 3 μm to ~ 1 mm. Although uncommon, such UV-hardened polymers have been used in the gem trade (e.g., Johnson et al., 1999; www.norlandprod.com/ApplicationsPageAdhesives.asp).

In addition to the Raman bands that are characteristic of NOA 65, we observed some minute extra Raman bands at 1242 , 1183 , 808 , 720 , 641 , 597 , and 523 cm^{-1} . Thus, we cannot eliminate the possibility of other NOA adhesives in the filler or plasticization with other polymers. Although we could not conclusively identify the filling material(s) in this turquoise, the characteristic Raman bands suggest that it consists mainly of a UV-hardened polymer. IR absorption bands for plastic have been documented in impregnated turquoise at 1725 cm^{-1} (Lind et al., 1983), 1734 cm^{-1} (Dontenville et al., 1986), and at 1744 cm^{-1} (Pavese et

Figure 3. The reflectance IR spectrum of the cabochon in figure 1 reveals turquoise peaks at ~ 1120 , 1050 , and 1000 cm^{-1} . The absorption band at ~ 1740 cm^{-1} is caused by carbonyl, which is usually found in polymers.



See end of article for About the Authors and Acknowledgments.

GEMS & GEMOLOGY, Vol. 43, No. 2, pp. 149–151.

© 2007 Gemological Institute of America

al., 2005). These studies and the present work (i.e., the IR absorption band at $\sim 1740\text{ cm}^{-1}$) suggest that various polymers/plastics have been used for stabilizing turquoise.

Conclusion. The use of a UV-hardened polymer for impregnating/filling a turquoise cabochon was documented using Raman and FTIR spectrometry. While such polymers have been previously used in gem trade (e.g., to fill emeralds), this is the first time we have seen them applied to turquoise.

ABOUT THE AUTHORS

Mr. Moe and Mr. Johnson are research technicians, and Mr. Moses is senior vice president for Research and Identification, at the GIA Laboratory in New York.

ACKNOWLEDGMENTS

The authors thank two reviewers, Dr. Lore Kiefert and Dr. Mary Johnson, for their constructive comments and suggestions.

REFERENCES

- Clarke R.H., Londhe S., Premasiri W.R., Womble M.E. (1999) Low-resolution Raman spectroscopy: Instrumentation and applications in chemical analysis. *Journal of Raman Spectroscopy*, Vol. 30, pp. 827–832.
- Dontenville S., Calas G., Vervelle B. (1986) Étude spectroscopique des turquoises naturelles et traitées. *Revue de Gemmologie a.f.g.*, No. 85, pp. 8–10; No. 86, pp. 3–4.
- Fritsch E., McClure S.F., Ostrooumov M., Andres Y., Moses T., Koivula J.I., Kammerling R.C. (1999) The identification of Zachery-treated turquoise. *Gems & Gemology*, Vol. 35, No. 1, pp. 4–16.
- Johnson M.L., Elen S., Muhlmeister S. (1999) On the identification of various emerald filling substances. *Gems & Gemology*, Vol. 35, No. 2, pp. 82–107.
- King R.J. (2002) Turquoise. *Geology Today*, Vol. 18, No. 3, pp. 110–114.
- Learner T. (1998) The use of a diamond cell for the FTIR characterization of paints and varnishes available to twentieth century artists. *Postprints: IRUG², Infrared and Raman Users' Group meeting*, held September 12–13, 1995, Victoria & Albert Museum, London, www.irug.org/documents/irug2.pdf, pp. 7–20.
- Lind T., Schmetzer K., Bank H. (1983) The identification of turquoise by infrared spectroscopy and X-ray powder diffraction. *Gems & Gemology*, Vol. 19, No. 3, pp. 164–168.
- Miliani C., Ombelli M., Morresi A., Romani A. (2002) Spectroscopic study of acrylic resins in solid matrices. *Surface and Coatings Technology*, Vol. 151–152, pp. 276–280.
- Nørbygaard T., Berg R.W. (2004) Analysis of phthalate ester content in poly (vinyl chloride) plastics by means of Fourier transform Raman spectroscopy. *Applied Spectroscopy*, Vol. 58, No. 4, pp. 410–413.
- Pavese A., Proserpi L., Dapiaggi M. (2005) Use of IR-spectroscopy and diffraction to discriminate between natural, synthetic and treated turquoise, and its imitations. *Australian Gemmologist*, Vol. 22, No. 8, pp. 366–371.



Save the Date!

August 21-23, 2009 | San Diego, California

- > Advanced gemological research
- > World-renowned keynote speakers
- > Cutting-edge oral and poster presentations and panel discussions
- > International, multi-disciplinary participation
- > Field trips to gem pegmatite mines in San Diego County
- > *Gems & Gemology* 75th anniversary party

HOSTED BY



GIA
GEMOLOGICAL INSTITUTE OF AMERICA®

For future updates,
visit www.grc2009.gia.edu

Order Your
BACK ISSUES
 CHARTS & BOOKS
 Today!

GEMS & GEMOLOGY.

The Quarterly Journal
 That Lasts A Lifetime

Visit the Web:

www.gia.edu/gemsandgemology

Call Toll Free 800-421-7250 ext. 7142

or 760-603-4000 ext. 7142

Fax: 760-603-4070

E-Mail: gandg@gia.edu

or Write: G&G Subscriptions,
 P.O. Box 9022, Carlsbad, CA

92018-9022

USA

	U.S.	Canada	International
Single Issues	\$ 12	\$ 15	\$ 18
Complete Volumes* 1992-2006	\$ 40	\$ 48	\$ 60
Three-year set	\$ 115	\$ 135	\$ 170
Five-year set	\$ 190	\$ 220	\$ 280

*10% discount for GIA Alumni and active GIA students.

Limited issues from 1984-1991 are also available. Please call or visit our website for details on these and the 2007 issues as they are published.

Spring 2001

Ammolite from Southern Alberta, Canada
 Discovery and Mining of the Argyle Diamond Deposit, Australia
 Hydrothermal Synthetic Red Beryl

Summer 2001

The Current Status of Chinese Freshwater Cultured Pearls
 Characteristics of Natural-Color and Heat-Treated
 "Golden" South Sea Cultured Pearls
 A New Method for Imitating Asterism

Fall 2001

Modeling the Appearance of the Round Brilliant
 Cut Diamond: Fire
 Pyrope from the Dora Maira Massif, Italy
 Jeremejevitte: A Gemological Update

Winter 2001

An Update on "Paraíba" Tourmaline from Brazil
 Spessartine Garnet from San Diego County, California
 Pink to Pinkish Orange Malaya Garnets from Bekily,
 Madagascar
 "Voices of the Earth": Transcending the Traditional in
 Lapidary Arts

Spring 2002—Special Issue

The Ultimate Gemologist: Richard T. Liddicoat
 Portable Instruments and Tips on Practical Gemology in
 the Field
 Liddicoatite Tourmaline from Madagascar
 Star of the South: A Historic 128 ct Diamond

Summer 2002

Characterization and Grading of Natural-Color Pink Diamonds
 New Chromium- and Vanadium-Bearing Garnets from
 Tranoroa, Madagascar
 Update on the Identification of Treated "Golden" South
 Sea Cultured Pearls

Fall 2002

Diamonds in Canada
 "Diffusion Ruby" Proves to Be Synthetic Ruby Overgrowth
 on Natural Corundum

Winter 2002

Chart of Commercially Available Gem Treatments
 Gemesis Laboratory-Created Diamonds
 Legal Protection for Proprietary Diamond Cuts
 Rhodizite-Londonite from the Antsongombato Pegmatite,
 Central Madagascar

Spring 2003

Photomicrography for Gemologists
 Poudretteite: A Rare Gem from Mogok
 Grandidierite from Sri Lanka

Summer 2003

Beryllium Diffusion of Ruby and Sapphire
 Seven Rare Gem Diamonds

Fall 2003

G. Robert Crowningshield: A Legendary Gemologist
 Cause of Color in Black Diamonds from Siberia
 Obtaining U.S. Copyright Registration for the Elara Diamond

Winter 2003

Gem-Quality CVD Synthetic Diamonds
 Pezzottaite from Madagascar: A New Gem
 Red Beryl from Utah: Review and Update

Spring 2004

Identification of CVD-Grown Synthetic Diamonds
 Cultured Pearls from the Gulf of California, Mexico
 X-Ray Fingerprinting Routine for Cut Diamonds

Summer 2004

Gem Treatment Disclosure and U.S. Law
 Lab-Grown Colored Diamonds from Chatham
 The 3543 cm⁻¹ Band in Amethyst Identification

Fall 2004

Grading Cut Quality of Round Brilliant Diamonds
 Amethyst from Four Peaks, Arizona

Winter 2004

Creation of a Suite of Peridot Jewelry: From the Himalayas
 to Fifth Avenue
 An Updated Chart on HPHT-Grown Synthetic Diamonds
 A New Method for Detecting Beryllium Diffusion-
 Treated Sapphires (LIBS)

Spring 2005

Treated-Color Pink-to-Red Diamonds from Lucent Diamonds Inc.
 A Gemological Study of a Collection of Chameleon Diamonds
 Coated Pink Diamond: A Cautionary Tale

Summer 2005

Characterization and Grading of Natural-Color Yellow Diamonds
 Emeralds from the Kafubu Area, Zambia
 Mt. Mica: A Renaissance in Maine's Gem Tourmaline Production

Fall 2005

A Review of the Political and Economic Forces Shaping
 Today's Diamond Industry
 Experimental CVD Synthetic Diamonds from LIMHP-
 CNRS, France
 Inclusions in Transparent Gem Rhodonite from
 Broken Hill, New South Wales, Australia

Winter 2005

A Gemological Pioneer: Dr. Edward J. Gübelin
 Characterization of the New Malossi Hydrothermal
 Synthetic Emerald

Spring 2006

"Paraíba"-type Tourmaline from Brazil, Nigeria, and
 Mozambique: Chemical Fingerprinting by LA-ICP-MS
 Identification and Durability of Lead Glass-Filled Rubies
 Characterization of Tortoise Shell and Its Imitations

Summer 2006

Applications of Laser Ablation-Inductively Coupled Plasma-
 Mass Spectrometry (LA-ICP-MS) to Gemology
 The Cullinan Diamond Centennial
 The Effects of Heat Treatment on Zircon Inclusions in
 Madagascar Sapphires
 Faceting Transparent Rhodonite from New South Wales,
 Australia

Fall 2006—Special Issue

Proceedings of the 4th International Gemological Symposium
 and GIA Gemological Research Conference

Winter 2006

The Impact of Internal Whitish and Reflective Graining on the
 Clarity Grading of D-to-Z Diamonds at the GIA Lab
 Identification of "Chocolate Pearls" Treated by Ballerina Pearl Co.
 Leopard Opal: Play-of-Color Opal in Basalt from Mexico
 The Cause of Iridescence in Rainbow Andradite from Japan

EDITORS

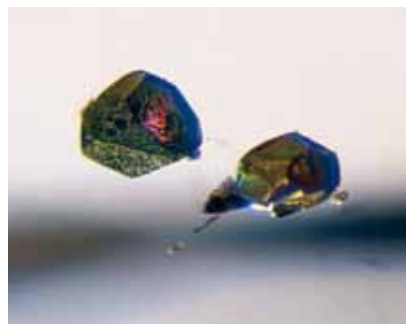
Thomas M. Moses and
Shane F. McClure
GIA Laboratory

DIAMOND With Bimineralic Inclusions

In the GIA Laboratory, diamond graders and staff gemologists examine thousands of diamonds each year to determine their grade, possible treatments, and their natural or synthetic origin. During this process, they often encounter mineral inclusions, the colors of which can cover the entire visible-light spectrum from violet to red as well as near colorless, with diaphaneity ranging from transparent to completely opaque.

Occasionally, these mineral inclusions may warrant further study. When they are close enough to the host dia-

Figure 1. A hint of underlying red color can be seen emanating from the largest of these otherwise opaque-looking inclusions. The visual appearance suggests an opaque sulfide coating over transparent color-change garnet. Magnified 25×.



mond's surface to be fully identified (for instance, by Raman microanalysis), the results may be surprising, as was the case with the blue sapphire inclusions we reported on recently (Summer 2006 Lab Notes, pp. 165–166). More often, though, interesting solid inclusions are too deep inside their host to be conclusively “identified” by other than visual means.

This was the situation we encountered with the two crystals shown in figure 1, which were observed in a light yellow 1.20 ct round brilliant-cut diamond. These inclusions were interesting because at first they appeared to be opaque, displaying a brassy metallic luster in reflected light as if they were sulfides such as pyrite or pyrrotite, both of which are known inclusions in diamond. Closer examination, however, revealed that the interiors of these inclusions were actually deep purplish red when viewed with incandescent light, and that the color shifted toward blue-green in fluorescent light. Using polarized light, and examining the crystals from several different viewing angles, we did not detect pleochroism in either inclusion, which suggests that they were optically isotropic.

The interior color of the inclusions was well masked by the sulfide-like coatings. Only a few gaps in the coatings allowed the bodycolor of the inclusions to be observed from certain viewing directions (again, see figure 1). As a result of this microscopic examination, we concluded that these inclusions were likely color-change garnets that were coated by an overgrowth of a sulfide or

sulfides at some point before they were completely sealed in the diamond.

While we have encountered change-of-color garnets in diamonds on rare occasions (see, e.g., Fall 1982 Lab Notes, p. 169; Winter 1989 Lab Notes, pp. 237–238), and have often observed sulfides as crusts (sometimes mixed with graphite) filling cracks around inclusions, this is the first time we have noticed what appeared to be opaque sulfides as thin coatings on otherwise transparent inclusions. Similar inclusions may have been overlooked in the past as more common sulfides, but we will now watch for them during future examinations.

John I. Koivula and Laura Dale

HPHT-Treated Type Ia Diamond With a Green Component Caused by the H2 Defect

High-pressure, high temperature (HPHT) treated type Ia diamonds are often yellow with a secondary green hue of varying saturation, which primarily results from fluorescence caused by

Editors' note: All items are written by staff members of the GIA Laboratory, East Coast (New York City) and West Coast (Carlsbad, California).

GEMS & GEMOLOGY, Vol. 43, No. 2, pp. 153–161
© 2007 Gemological Institute of America

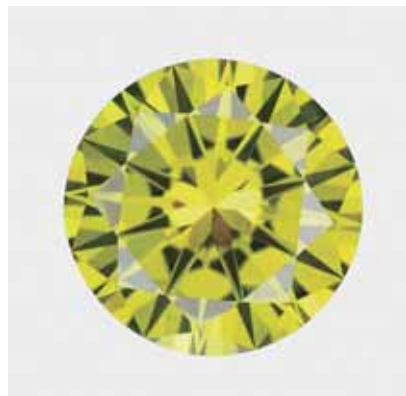


Figure 2. The strong green color component of this 5.82 ct Fancy Deep green-yellow HPHT-treated diamond is unusual due to a high concentration of H2 defects.

the H3 defect (503.2 nm; see, e.g., I. Reinitz et al., "Identification of HPHT-treated yellow to green diamonds," Summer 2000 *Gems & Gemology*, pp. 128–137). While the H2 defect (zero-phonon line at 986.3 nm) is also very common in HPHT-treated type Ia diamonds, its contribution to bodycolor, if any, is usually quite limited. However, in the East Coast laboratory, we recently examined an unusual diamond in which H2 absorption was the primary cause of the green color.

This known-HPHT-treated round-cut 5.82 ct diamond was color graded Fancy Deep green-yellow (figure 2). The color was evenly distributed except for an area of very weak brown that followed internal graining. Very small cloud-like features were seen at the center of the diamond, but it was otherwise free of inclusions. When exposed to long-wave ultraviolet (UV) radiation, it displayed a moderately strong greenish yellow fluorescence; to short-wave UV, it fluoresced a very weak greenish yellow. No phosphorescence was observed. In the DiamondView, moderate blue and greenish yellow fluorescent growth zones were seen, in addition to several nearly inert regions with a triangle shape (figure 3); these latter features are rarely observed on polished facets of untreated natural diamonds.

Infrared absorption spectra showed

that this diamond contained a high concentration of nitrogen as type Ia with a very low hydrogen content. In addition to a strong H2 absorption, the near-infrared spectra also revealed some unusual features in the 6500–4400 cm^{-1} region (6456.5, 5765.0, 5395.2, 4931.2, and 4397.8 cm^{-1} ; figure 4). The assignment of these absorptions is unknown, and to the best of the authors' knowledge they have not been previously reported. The UV-Vis-NIR spectrum also showed very strong N3, H3, and H2 absorptions (figure 5); very weak absorptions were observed at 536.1 and 575.9 nm. The side band of the H2 defect extended out to ~600 nm and efficiently blocked red and orange light. As a result, a transmission window in the 504–600 nm region was created, leading to the apparent green-yellow bodycolor.

Despite the high concentration of H3 defects in this diamond, only weak green luminescence to visible light was observed, which could not entirely explain the strong green component. In addition, the green color was more saturated and clearly darker than that of typical HPHT-treated green-

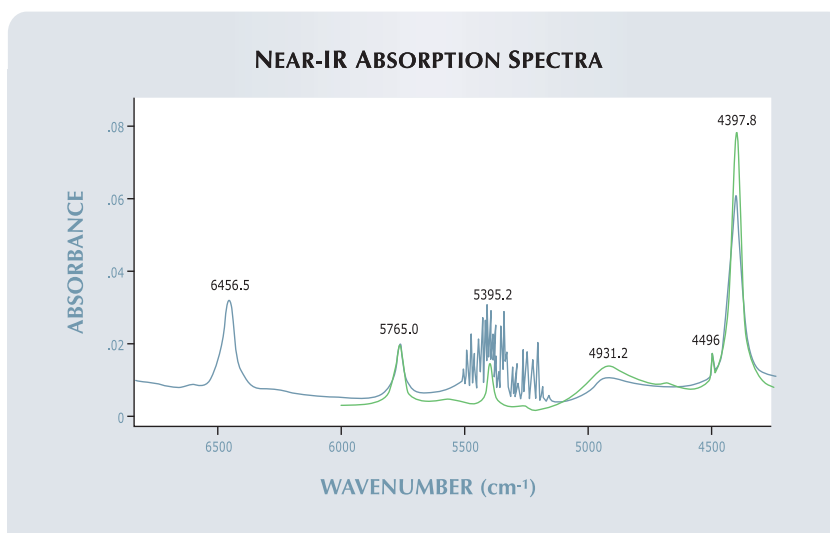


Figure 3. The nearly inert "trigons" in the blue fluorescing regions of this DiamondView image are rarely observed on polished facets of untreated natural diamonds.

yellow diamonds. All these observations strongly indicated that the H2 defect, along with more common defects, caused the attractive green-yellow hue of this rare diamond.

Wuyi Wang and Matthew Hall

Figure 4. The near-infrared absorption spectra of this diamond revealed some unusual features in the 6500–4350 cm^{-1} region. Assignment of these absorptions is unclear, and they have not been reported in other natural or treated diamonds, except for the sharp peak at 4496 cm^{-1} due to hydrogen. The two spectra were collected using different sources with different sensitivities.



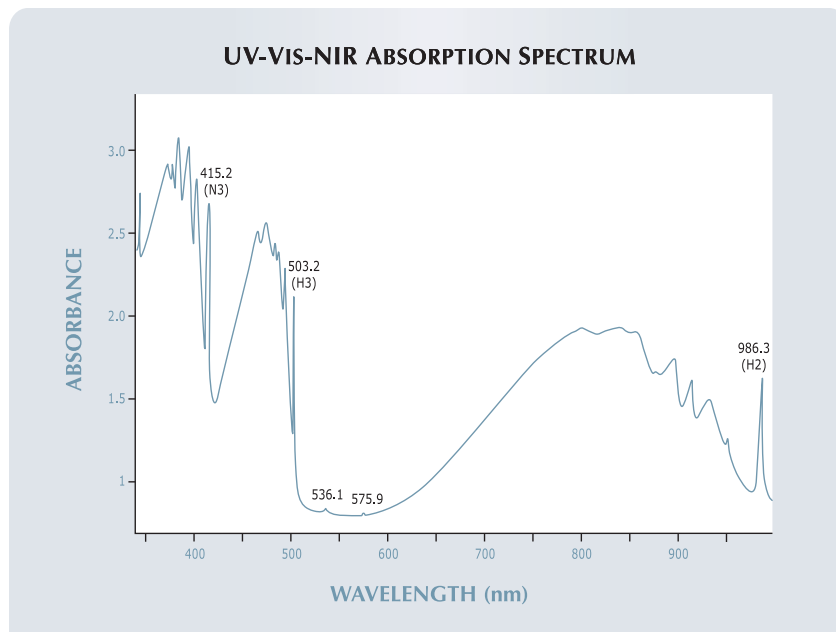


Figure 5. The UV-Vis-NIR absorption spectrum showed very strong absorptions of N3, H3, and H2 centers. The side band of the H2 defect extended well into the visible region, which induced the strong green color component.

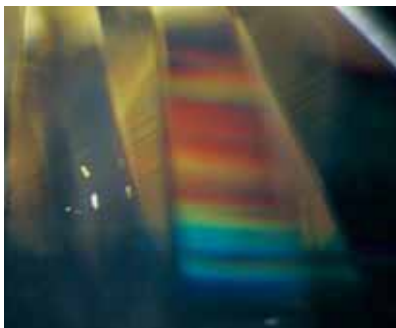
Diamond with Intense “Rainbow Graining”

Gemologists who grade diamonds are familiar with internal graining and how, in certain manifestations under current diamond grading standards, it can negatively impact the clarity grade of a diamond (see, e.g., J. M. King et al., “The impact of internal whitish and reflective graining on the clarity grading of D-to-Z color diamonds at the GIA Laboratory,” Winter 2006 *Gems & Gemology*, pp. 206–220). One type of internal graining referred to as *phantom* or *colorless graining* is typically just that, colorless and sometimes relatively difficult to see, though it is also the most common. Within this category, however, there is a most unusual type of phantom graining that is both very colorful and extremely rare. On the infrequent occasions that it has been reported, it has been referred to as *rainbow graining* (see, e.g., J. I. Koivula, *The Microworld of Diamonds*, Gemworld International, Northbrook, IL, 2000, p. 94; J. M. King et al.,

“Characterization and grading of natural-color yellow diamonds,” Summer 2005 *Gems & Gemology*, pp. 88–115, and figure 15 therein).

Phantom or colorless internal graining bands are actually contact zones or layers between competing growth planes in the diamond’s crystal structure; these cause a slight-to-heavy

Figure 6. This is the most intense display of “rainbow graining” in a diamond that we have encountered in the GIA Laboratory. Field of view approximately 2.1 mm.



distortion of the surrounding crystal lattice, making the grain area visible. It is also well known that diamonds often undergo plastic deformation, particularly in the {111} octahedral planes, which may result in numerous parallel internal phantom grain lines.

If the layers of phantom graining are sufficiently fine and numerous, then rainbow graining may be observed. However, in addition to possibly being the rarest form of internal graining, rainbow graining is also one of the most elusive and easily overlooked, in that it is highly directional and can thus be viewed only in specific directions in its host. In most directions, it looks like common colorless phantom graining, but a slight tilt of the diamond causes the grain layers to act as a diffraction grating, resulting in a spectral display of colors. This optical effect is essentially the same as that shown by iris agates and some transparent natural glasses that exhibit very fine growth layers (see also T. Hainschwang and F. Notari, “The cause of iridescence in “rainbow” andradite from Nara, Japan,” Winter 2006 *Gems & Gemology*, pp. 222–235, for a general discussion of this effect in gem materials).

Recently, while investigating the color origin of a light yellow round brilliant-cut diamond of over a carat in weight, we encountered the strongest and most vivid display of rainbow graining that we have ever seen (figure 6). It was fortunate that there were also a few small mineral inclusions to focus on while taking this photomicrograph, because rainbow graining does not have any specific focal point; as a result, photos of this type of graining can appear as if the entire image is out of focus.

John I. Koivula and Alethea Inns

Natural Color Hydrogen-Rich Blue-Gray Diamond

Prior to the 1990s, virtually all natural-color blue diamonds were thought to be type IIb and electrically conductive. Since then, the lab has seen, on rare occasions, nonconductive type Ia gray-

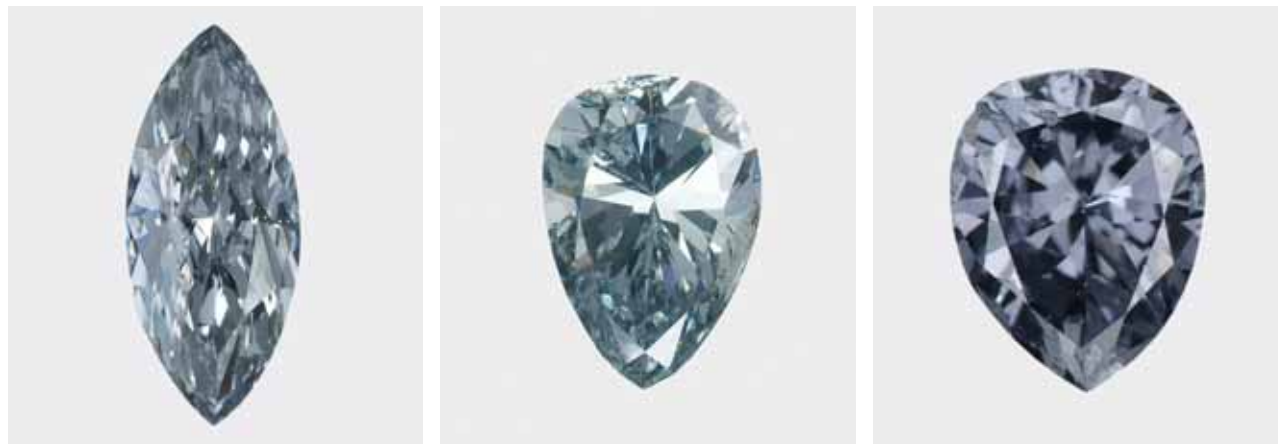


Figure 7. In GIA's color grading system, the 0.24 ct type Ia pear-shaped diamond in the center is described with the same terminology (blue-gray) as the 0.63 ct marquise on the left, but—because it falls at the extreme opposite end of that color range—it has a different appearance. The 0.18 ct pear shape on the right is also a type Ia diamond, but its violet-gray color is more typical of that seen in diamonds with a color related to hydrogen defects.

to-blue diamonds that owe their color to the presence of hydrogen-related defects (see E. Fritsch and K. Scarratt, "Natural-color nonconductive gray-to-blue diamonds," Spring 1992 *Gems & Gemology*, pp. 35–42).

Recently, the East Coast laboratory had an opportunity to examine a nonconductive blue-gray diamond that had other unusual characteristics. The 0.24 ct pear brilliant cut was color graded Fancy blue-gray (figure 7, center). When examined with magnification, it showed a number of moderately sized indented naturals and some feathers breaking the surface. At high magnification using a fiber-optic light, we also saw very fine clouds. The color appeared evenly distributed—unlike type IIb blue diamonds, which commonly show color zoning. Very weak strain, which looked to be associated with some of the surface-reaching inclusions, was visible when the stone was examined with crossed polarizers.

The diamond fluoresced a moderate blue to long-wave UV radiation and a moderate yellow to short-wave UV. In the desk-model spectroscope, absorption bands were present at 415 (N3), 425, and a broad band centered at 550 nm. These features confirmed that the diamond was type Ia. With FTIR

spectroscopy, the diamond showed sharp hydrogen peaks at 4703, 4168, 3236, 3235, 3107, 2811, 2785, 1547, and 1498 cm^{-1} (again, see Fritsch and Scarratt, 1992). The UV-Vis spectrum showed a similar absorption as that seen in the desk-model spectroscope, with the addition of an increase in absorption from about 600 nm toward the infrared region, which can be associated with hydrogen-rich diamonds (see K. Iakoubovskii and G. J. Adriaenssens, "Optical characterization of natural Argyle diamonds," *Diamond and Related Materials*, Vol. 11, No. 1, 2002, pp. 125–131; E. Fritsch et al., "Thermochromic and photochromic behaviour of 'chameleon' diamonds," *Diamond and Related Materials*, Vol. 16, No. 2, 2007, pp. 401–408).

What was so unusual about this diamond was its color appearance, which was closer to the green side of the blue hue range rather than the more typical appearance closer to the violet boundary. This suggests that these nitrogen- and hydrogen-related defects can give rise to colors other than gray-to-blue or violet.

It is important to note that the color differences described here are quite subtle even when observed with standard color-grading conditions. In the GIA system for color grading col-

ored diamonds, fewer terms are used as the color becomes darker in tone and/or weaker in saturation because the human eye makes fewer distinctions (see J. M. King et al., "Color grading of colored diamonds in the GIA Gem Trade Laboratory," Winter 1994 *Gems & Gemology*, pp. 220–242, figure 23). Therefore, even though this diamond was slightly greener in hue, it was still described as *blue-gray* due to its location in color space. While the subtle color difference noted between this diamond and type IIb blue-gray diamonds under controlled conditions is not considered noticeable enough to warrant a change in terminology, it is sufficient to represent a rare appearance for this color description (see, e.g., J. M. King et al., "Characterizing natural-color type IIb blue diamonds" Winter 1998 *Gems & Gemology*, pp. 246–268).

Jason Darley and John M. King

Type IIa Diamond with Intense Green Color Introduced by Ni-Related Defects

Nickel-related defects are common in HPHT-grown synthetic diamonds. They have also been documented in some natural diamonds, though they

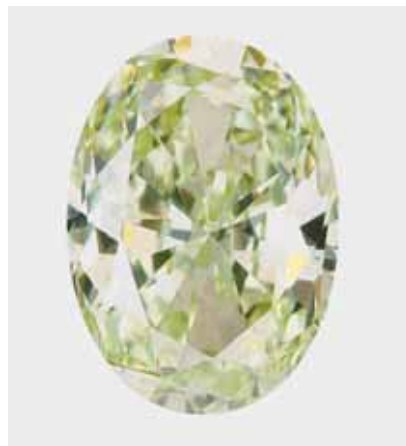
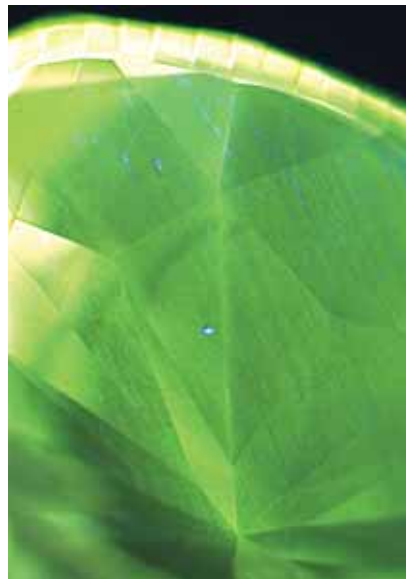


Figure 8. This oval-cut 2.81 ct Fancy Intense yellowish green diamond is colored mainly by Ni-related defects.

are rarely the main contributor to bodycolor in these stones or their function is not clear. However, the East Coast laboratory recently char-

Figure 9. The diamond in figure 8 showed moderately strong green fluorescence in the DiamondView, with narrow dark green bands and a few blue ones. These features ruled out a synthetic origin.

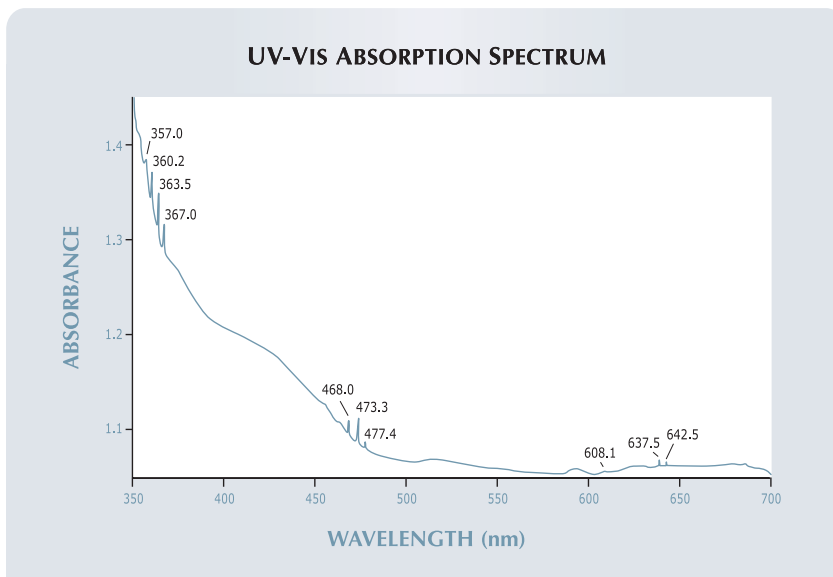


acterized an intensely colored natural yellowish green diamond that proved to be colored by Ni-related defects.

This oval-cut 2.81 ct diamond was color graded Fancy Intense yellowish green (figure 8). Color distribution was even, and the few small pinpoints noted resulted in a clarity grade of VS₁. A small natural with typical etching features was present near the girdle. The diamond displayed strong yellow fluorescence to long-wave UV radiation and very strong greenish yellow fluorescence to short-wave UV, with no phosphorescence seen at these wavelengths. When examined with the DiamondView, the stone showed moderately strong green fluorescence with narrow dark green bands and a few blue ones (figure 9); a weak yellow phosphorescence was also observed. The evenly distributed fluorescence features and the absence of a typical HPHT-synthetic growth pattern ruled out a synthetic origin for this diamond.

The infrared spectrum did not show any absorption in the one-phonon region, nor any boron-related absorption, and established the stone as a type IIa. Only very weak absorptions at 3107 and 1405 cm⁻¹ due to hydrogen and a weak peak at 1332 cm⁻¹ (very likely from N⁺) were observed. The UV-Vis spectrum showed weak but distinct absorptions at 350–370 nm, 460–480 nm, and 600–650 nm (figure 10). All these sharp absorptions, except for the 608.1 and 637.5 nm peaks, are known to originate from Ni-related defects (see, e.g., S. C. Lawson and H. Kanda, "An annealing study of nickel point defects in high-pressure synthetic diamond," *Journal of Applied Physics*, Vol. 73, 1993, pp. 3967–3973). The spectrum also had broad absorption bands with maxima at approximately 310, 520, and 688 nm. The 688 nm band extended to ~600 nm, and limited the transmission of red and orange light. Because of all these selective

Figure 10. Ni-related defects with absorptions at 350–370 nm, 460–480 nm, and 642.5 nm, together with the broad band around 688 nm and additional peaks at 608.1 and 637.5 nm, created a transmission window in the 540–550 nm region, which resulted in the yellowish green bodycolor. The 688 nm band is associated with the 1.40 eV center (zero-phonon line at 883.1 and 884.8 nm), which occurred as predominant emissions in the PL spectra (figure 11).



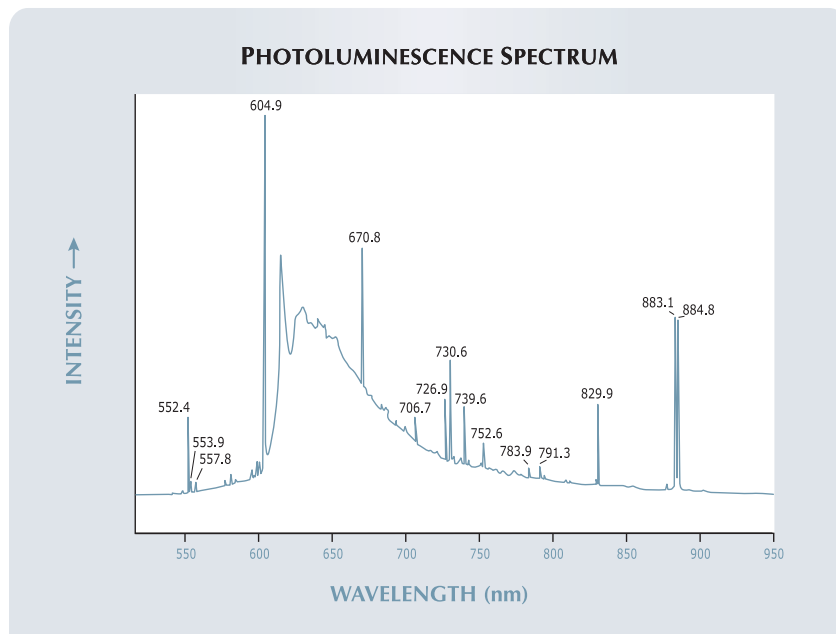


Figure 11. The PL spectra confirm the extremely strong emissions from Ni-related defects (e.g., the 883.1/884.8 nm pair). However, most of these sharp emission peaks remain unclear in assignment.

absorptions, a transparent “window” centered around 540–550 nm is created, leading to the yellowish green body-color. The 688 nm band is associated with the 1.40 eV center (zero-phonon line at 883.1 and 884.8 nm; again, see Lawson and Kanda, 1993), which occurs as predominant emissions in photoluminescence (PL) spectra collected with various laser excitations (e.g., figure 11, spectrum collected using 514 nm laser excitation). Other strong emission peaks were recorded, most of which remain unclear in assignment. In contrast, some common emissions in natural diamonds (e.g., H3, H4, N-V centers) are absent.

Green in natural diamonds can be introduced by a number of known defects or defect combinations. Selective absorptions from the GRI and some hydrogen-related defects, along with fluorescence of the H3 defect, are considered the main causes. Ni-related defects have long been recognized as color contributors in HPHT synthetic diamonds, depending on the concentration of isolated nitrogen, but they have not been reported as a

major color contributor in natural diamond. The absence of these previously mentioned defects and the almost exclusive occurrence of Ni-related defects (in particular the 1.40 eV center) strongly indicate that the intense green hue of this diamond is caused by Ni-related defects. The size, high clarity, and attractive Ni-related intense green color of this diamond make it very unusual.

This rare diamond reveals another cause of green color in naturally colored diamonds. The 1.40 eV center—which is caused by the interstitial charged ion Ni⁺—has been documented in chameleon diamonds (see, e.g., J. E. Shigley et al., “Photoluminescence features of chameleon diamonds,” *Proceedings of the 55th De Beers Diamond Conference*, Coventry, UK, 2004, pp. 4.1–4.2; T. Hainschwang et al., “A gemological study of a collection of chameleon diamonds,” *Spring 2005 Gems & Gemology*, pp. 20–35), as have other Ni-related defects (e.g., the 1.563 eV center with a zero-phonon line at 793.5 nm).

Wuyi Wang and Tom Moses

Diamond with Zigzag Cleavage

In addition to its superior scratch and indentation hardness, the other physical property for which diamond is best known is its four directions of perfect {111} octahedral cleavage. This property has been used to help pre-shape diamond rough through the process of cleaving for as long as diamonds have been fashioned as gems. In a gem diamond, however, a cleavage is also the single most damaging internal feature or clarity characteristic that a stone can possess. Sometimes referred to as a “feather,” a prominent cleavage can significantly affect the structural integrity of its host diamond, particularly if it is exposed to the surface where it can absorb water and other unwanted matter that might alter its visibility. That is where glass filling is particularly useful, because it seals surface-reaching cleavage cracks, preventing the introduction of unwanted and unsightly debris, at the same time that it reduces the apparent visibility of those cracks.

During the course of testing to determine the color origin of a round brilliant-cut diamond, we recently encountered a relatively shallow surface-exposed cleavage system that had a most unusual elongated zigzag pattern, much like a zipper. This system extended into the crown and table of its host and, as shown in figure 12, appeared to result from a combination of at least two directions of cleavage. To the best of our knowledge, this is the first time such a well-developed pattern has been encountered in the GIA Laboratory.

Its presence and clear presentation as a cleavage pattern also make it the ideal subject to once again point out that in the fields of crystallography, gemology, and mineralogy there is a distinct and definable difference between *cleavage* and *fracture*. Essentially, a fracture is a break in a mineral *other* than along a cleavage plane. In fact, very few single-crystal gem-quality diamonds ever actually fracture. Diamond is very tough, and



Figure 12. Extending from the edge of the crown into the table facet of this diamond, this most unusual 3.2-mm-long zigzag crack shows at least two directions of the diamond's perfect cleavage.

when it breaks, it almost always breaks along a cleavage plane or a combination of two or more of its four cleavage directions.

John I. Koivula and
Cheryl Y. Wentzell

HPHT-Grown SYNTHETIC DIAMOND Crystal with Unusual Morphology and Negative Trigons

Recently, the East Coast laboratory examined a 1.56 ct highly saturated red crystal (7.25 × 5.75 × 3.42 mm; figure 13). Gemological and spectroscopic characterization identified it as an HPHT-grown synthetic diamond that apparently was artificially irradiated and annealed. In the past, we have had the opportunity to document similarly color-treated pink to purplish pink synthetic crystals and red synthetic faceted diamonds (T. M. Moses et al., "Two treated-color synthetic red diamonds

seen in the trade," Fall 1993 *Gems & Gemology*, pp. 182–190). However, this specimen differed from samples we had previously seen.

Consistent with other HPHT-grown synthetic diamonds, features such as subtle growth sector-related color zoning and remnants of the seed crystal were apparent when the sample was examined with a gemological microscope. The sample fluoresced bright orange in the DiamondView, and a cross-shaped green fluorescence pattern was observed through the {111} faces. The green pattern suggested the possibility of a higher concentration of H3 centers in this area, while the strong orange color is most likely a result of high concentrations of N-V centers.

Many HPHT-grown synthetic diamond crystals have a distinctive cuboctahedral morphology (J. E. Shigley et al., "Lab-grown colored diamonds from Chatham Created Gems," Summer 2004 *Gems & Gemology*, pp. 128–145), typically with both cubic {100} and octahedral {111} faces having equivalent surface area. In contrast (but similar to natural diamond), this synthetic specimen had well-developed octahedral growth but virtually no cubic faces. The highly developed {111} faces suggest that it may have been grown at higher temperatures than most HPHT-grown synthetics, possibly in excess of ~1800°C (I. Sunagawa, "Morphology of natural and synthetic diamond crystals," in I. Sunagawa, Ed., *Materials Science of the Earth's Interior*, Terra Scientific Publishing Co., Tokyo, 1984, pp. 303–330).

In addition, indented triangular etch regions were present on almost every octahedral surface. Triangular features have been reported on synthetic diamonds in the past (see, e.g., J. E. Shigley et al., "Gemological properties of near-colorless synthetic diamonds," Spring 1997 *Gems & Gemology*, pp. 42–53); however, in those cases, they protruded from the surface, creating small pyramids. On this synthetic diamond, the triangular etch marks were negative (i.e., indented), very similar to trigons observed on natural diamonds.

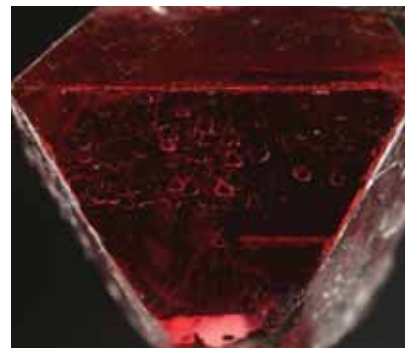


Figure 13. This deeply saturated 1.56 ct red synthetic diamond crystal displays well-developed octahedral faces and the presence of negative trigons. Magnified 15x.

Thus, it appears that the occurrence of negative trigons may not always be a useful criterion for the separation of natural from HPHT-grown synthetic diamonds.

Also with magnification, we observed a few metallic flux particles and graphitized inclusions, both of which are characteristic of HPHT-grown synthetics. A large graphitized fracture was seen breaking the surface on both sides, and both ends of the crystal were heavily etched and pitted, with some deeply pitted areas filled with graphitized material.

The red color of this synthetic diamond was more highly saturated than other color-treated red synthetic diamond crystals submitted to the laboratory, which were more pink. The infrared spectrum showed mostly type Ib nitrogen with some type IaA aggregates, which is consistent with a relatively high growth temperature. The overall nitrogen concentration from the IR absorption spectrum was calculated to be ~100 ppm. This absorption in general is higher than that of other pink HPHT-grown synthetic diamonds we have examined (again, see Shigley et al., 2004). Obvious H1a (1450 cm⁻¹) and H1b (4935 cm⁻¹), as well as H2 (986.3 nm), absorptions indicate that this synthetic diamond underwent irradiation and annealing.

Matthew Hall and Jason Darley

Idocrase in JADEITE: A Heavenly Home

The GIA Laboratory sees a wide variety of jade items for identification. These examinations are usually routine and generally do not offer any surprises. A recent exception was provided by a mottled translucent green-and-white bangle bracelet. The gemological identification as jadeite and the determination that it had not been treated were both straightforward. The surprise came during the microscopic examination, when we were searching for possible dye concentrations in any surface-reaching cracks.

While no dye was observed in the bangle, this inspection did reveal the presence of several small euhedral-to-subhedral translucent white to light brown modified prismatic inclusions (figure 14) that appeared to have crystallized in the tetragonal system. While it is often very difficult to identify inclusions that are completely enclosed in a massive material such as jade, several were exposed on the bracelet's surface, so they made convenient targets for Raman microanalysis. This conclusively identified

Figure 14. During an otherwise routine gem identification, it was a pleasant surprise to find these relatively well-formed translucent crystals of idocrase included in a jadeite bangle bracelet. Field of view is 5.2 mm.

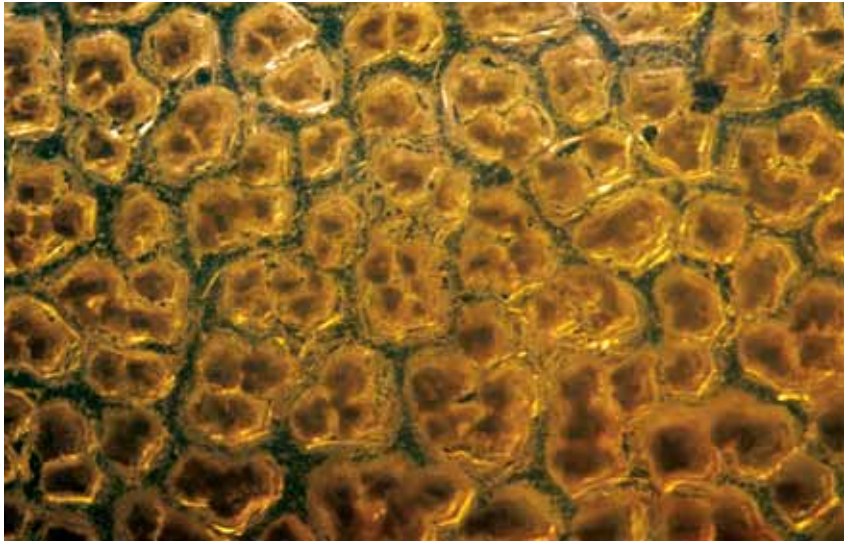


Figure 15. This unusual pattern appears to have been generated when opal was deposited over a surface covered with numerous more-or-less evenly spaced microcrystals of quartz. Field of view is 4.2 mm.

one inclusion as idocrase, a tetragonal mineral known to mineralogists as vesuvianite.

Since jadeite and idocrase are both minerals formed through metamorphism, and since they have common mineral associations as well, it is not completely surprising to find inclu-

sions of idocrase in jadeite. However, this is the first time we have encountered such idocrase inclusions, and mineralogical texts do not list jadeite and idocrase as mineral associates. This discovery adds a bit of new information to the gemological literature and increases our knowledge of gem-quality jadeite jade.

With its long-standing popularity as a gemstone and carving material, and in view of its rich history, jade is often referred to as the "stone of heaven." Now we know it is also a home to idocrase.

*John I. Koivula, Mike Breeding,
and Eric Fritz*

OPAL with Unusual Structure

Opal is one of the most fascinating of the phenomenal gems. Not only is it well known for its myriad play-of-color patterns, but it is also prized as a fossilizing agent and preservative of the structural features of other materials it replaces or envelops. In the past, GIA Laboratory staff members have seen opalized clams and other mollusks, portions of dinosaur bones preserved by opal, and opalized wood and

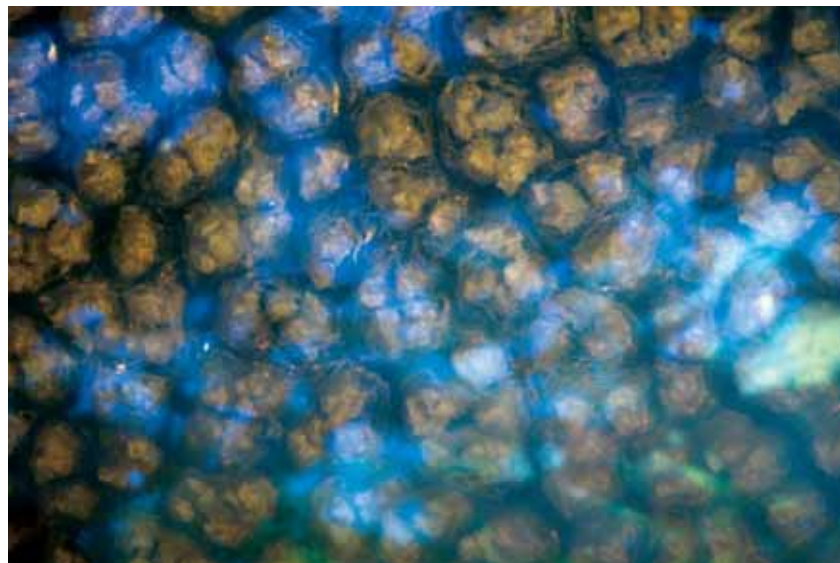


Figure 16. The play-of-color creates a hazy glow over the quartz casts on the base of their opal host. Field of view is 4.2 mm.

bark showing excellent cell detail (see, e.g., Fall 2001 Lab Notes, pp. 218–219).

We recently had the opportunity to examine an opal that appeared to have a columnar structure of relatively evenly spaced cells, so that it resembled synthetic opal without the

aid of magnification. The 1.09 ct translucent light brown cushion-shaped tabular cabochon measured $10.02 \times 7.72 \times 1.98$ mm. Our client was told that it came from an opal field in Queensland, Australia, but the structure had generated a certain

amount of suspicion about its origin.

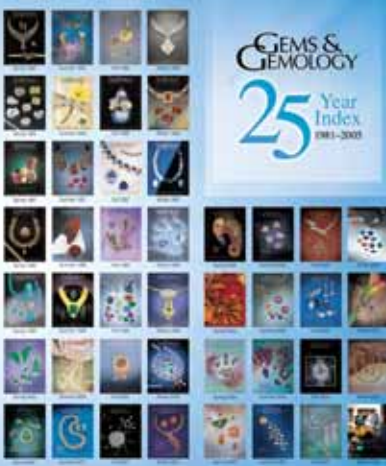
Standard gemological testing easily identified the opal as natural. With magnification, it appeared that the unusual structural pattern was generated when the opalizing solution was deposited over a drusy surface covered with numerous uniformly spaced quartz microcrystals, as shown in figure 15. The blue and green play-of-color displayed by the opal highlighted this structure like a colorful mist, adding a mysterious, alien haziness to the gem (figure 16) that seemed to float over the surface as the stone was moved. Throughout the years in the GIA Laboratory, we have had the opportunity to identify many marvelous opals from a variety of localities worldwide, but this is the first time we have encountered such a structure.

John I. Koivula

PHOTO CREDITS

John I. Koivula—1, 6, 12, and 14–16; Jian Xin (Jae) Liao—2 and 8; Wuyi Wang—3 and 9; Jessica Arditi—7; Jason Darley—13.

SPECIAL OFFER! Buy any 12 back issues, and receive a **FREE 25 Year Index!**




GEMS & GEMOLOGY
25 Year Index
1981–2005

Twenty-Five Years at Your Fingertips

Twenty-five years of GEMS & GEMOLOGY means a lot of valuable research. Fortunately, we've got it all—articles, lab notes, gem news, editorials, and book reviews—indexed in this one handy volume. It's an invaluable tool for the serious gemologist, for the far-from-invaluable price of just \$14.95. (\$19.95 internationally) **FREE shipping!**

Order Yours Today!

To order, visit www.gia.edu/gemsandgemology and click on *Ordering and Renewals*. Call 800-421-7250 ext. 7142 within the U.S., or 760-603-4000 ext. 7142.



GEMS & GEMOLOGY

25 Year Index
1981–2005



EDITOR

Brendan M. Laurs (blaurs@gia.edu)

CONTRIBUTING EDITORS

Emmanuel Fritsch, *IMN, University of Nantes, France* (fritsch@cnrs-immn.fr)

Henry A. Hänni, *SSEF, Basel, Switzerland* (gemlab@ssef.ch)

Franck Notari, *GemTechLab, Geneva, Switzerland* (franck.notari@bluewin.ch)

Kenneth V. G. Scarratt, *GIA Research, Bangkok, Thailand* (ken.scarratt@gia.edu)

DIAMONDS

Bar code technology applied to diamonds. Inscribing diamonds using lasers and other technologies has become a routine method for identifying a stone and personalizing it for individual situations. At the same time, bar coding has evolved from the traditional one-dimensional array of lines to a two-dimensional matrix code that can hold far more information.

Diamond laser inscription technology has now progressed to the point where a miniature matrix code can be inscribed on the girdle of a diamond (see, e.g., figure 1). Instead of just a grading report number, the matrix code can store all of the information in the report itself, such as clarity, cut, and color grades, as well as country of origin (if known), the name of the manufacturer, and other specifics. This has distinct advantages for diamond dealers and manufacturers when managing inventory, security issues, and finances. Unlike traditional laser inscriptions, which can be read with a loupe or a microscope, a matrix code requires a scanner to decode the information. While this does entail investment in additional equipment, it can also provide confidentiality to the owner of the stone.

One manufacturer of the inscription and code-reading equipment, PhotoScribe Technologies of New York, noted that the cost of applying a diamond matrix code is comparable to that of current laser inscriptions.

*Russell Shor (rshor@gia.edu)
GIA, Carlsbad*

U.S. Supreme Court ruling may affect viability of some diamond cut patents. On April 30, 2007, the United States Supreme Court handed down a decision in the case of *KSR International v. Teleflex* (available online at www.supremecourtus.gov/opinions/06pdf/04-1350.pdf). Although this case involved a patent for an automobile gas pedal, the ruling affects the standards by which the

U.S. Patent and Trademark Office (USPTO) awards patents, and consequently it may affect the validity of a number of patents on diamond cut designs.

A general review of U.S. patent law as it applies to diamond cuts can be found in the Winter 2002 *Ge&G* (T. W. Overton, "Legal protection for proprietary diamond cuts," pp. 310–325). One of the factors that the USPTO considers in awarding a patent is whether the claimed invention is a development that would be "obvious" to a person having ordinary skill in the relevant field. An obvious invention is not eligible for a patent. Until the *KSR International* case, the U.S. Court of Appeals for the Federal Circuit (which has jurisdiction over patent disputes) applied a fairly narrow definition of obviousness: whether a specific motivation or suggestion to combine prior inventions or knowledge (referred to as *prior art* in patent law) could be found in the patent literature, the nature of the problem, or the knowledge of a person having ordinary skill in the field. The justification for this narrow test was the straightforward recognition that nearly all inventions involve some synthesis of previous knowledge, and that fact alone does not make an invention obvious.

Editor's note: The initials at the end of each item identify the editor or contributing editor who provided it. Full names and affiliations are given for other contributors.

Interested contributors should send information and illustrations to Brendan Laurs at blaurs@gia.edu or GIA, The Robert Mouawad Campus, 5345 Armada Drive, Carlsbad, CA 92008. Original photos will be returned after consideration or publication.

*GEMS & GEMOLOGY, Vol. 43, No. 2, pp. 162–183
© 2007 Gemological Institute of America*



Figure 1. This simulated data matrix bar code on the girdle facet of a diamond reads “PhotoScribe.” The data matrix measures $80 \times 80 \mu\text{m}$; the same inscription using letters would require about 10 times the space. Courtesy of PhotoScribe Technologies, New York City; magnified $130\times$.

In this case, the invention consisted of an adjustable electronic gas pedal design that was a combination of several previous patents covering the component parts and the method by which they were arranged. Teleflex (the patent holder) sued KSR for infringement. Although KSR argued that the progress of science would have inevitably led to the combination at issue here (and previous patents had addressed the problem in a general sense), the Federal Circuit upheld the patent because, looking strictly at the language in the previous patents, there was no specific suggestion to combine them.

The Supreme Court, however, held that the Federal Circuit was applying this test too rigidly. Instead, the Court held that obviousness should be determined against a general background considering the scope of the prior art, the differences between the prior art and the invention, and the level of ordinary skill—essentially, much more of a holistic, common sense approach. Where a certain combination of elements is something obvious to try—as it was in this case—the invention itself is likely obvious as well.

Although this new standard implicates a broad range of issues, this contributor believes it presents a particular hazard to diamond cut patents, since so many recent cut designs are minor variations of previous cuts (see, e.g., Overton, 2002; Spring 2004 Gem New International, pp. 75–76). As the Supreme Court stated, “If a person of ordinary skill can implement a predictable variation, [the law] likely bars its patentability” (*KSR International*, p. 13). Further, the Court held that when there is market pressure to solve a problem for which there are a finite number of predictable solutions, an invention resulting from the pursuit of known options is likely the product not of innovation but of ordinary skill and common sense. For this reason, it will likely be more difficult to defend those cut patents that are but minor evolutions of previous designs. There is, after all, little question that there has been substantial market pressure in recent years for manufacturers and jewelers to develop in-house

variations of traditional round and square diamond cuts.

This decision (which effectively overturns several decades of established precedent) still needs to be interpreted and applied by the Federal Circuit and the USPTO, so it is premature to say whether any particular diamond cut patent is in danger. It does, however, counsel caution in the enforcement of existing cut patents and in the development of new designs.

Thomas W. Overton (toverton@gia.edu)
GIA, Carlsbad

COLORED STONES AND ORGANIC MATERIALS

First discovery of amazonite in Mexico. Amazonite is a bluish green variety of potassium feldspar that has been found on every continent except Antarctica (see M. Ostrooumov, “L’amazonite,” *Revue de Gemmologie*, Vol. 108, 1991, pp. 8–12). More than 100 large amazonite deposits are known, and there are numerous smaller ones. Recently, blue to bluish green amazonite was discovered for the first time in Mexico (figures 2 and 3). This material is hosted by the Peñoles pegmatite, which is located about 60 km southeast of the village Valle de Allende (Sierra de Peñoles, Allende municipality, Chihuahua State). The pegmatite is genetically related to a Li-F granite of Miocene age (32 million years, according to K-Ar dating); this is younger than all other known amazonite deposits. The pegmatite consists of an outer zone of coarse-grained albite-oligoclase and quartz with a small amount of pale blue amazonite. Toward

Figure 2. Amazonite was recently discovered in Chihuahua State, Mexico. This specimen is 28 cm wide; photo by Juan Manuel Espinosa.





Figure 3. These beads and cabochons (4.82–11.32 ct) of Mexican amazonite were recently cut in the mineralogical laboratory at the University of Michoacán. Photo by Robert Weldon.

the interior, the pegmatite attains >50 vol.% amazonite, which occurs as distinctly blue crystals up to 2–3 cm in longest dimension that are associated with albite, quartz, and micas (biotite and zinnwaldite). The central zone of the pegmatite consists mainly of a quartz core with bluish green crystals of amazonite. Chemical analysis (by EDXRF spectroscopy) of the amazonite from the outer zones to the core of the pegmatite showed increasing K, Rb, Cs, Pb, Tl, Ga, Be, Sr, U, and Th, and decreasing Al, Na, Fe, and Ba. X-ray diffraction analysis and optical microscopy showed that the amazonite is microcline with a high degree of Al-Si order.

Five samples of rough amazonite (measuring 1–2 cm in longest dimension) were gemologically characterized for this report, and the following properties were determined: color—blue and bluish green; pleochroism—weak to moderate; RI— $n_{\alpha}=1.516$ – 1.520 , $n_{\beta}=1.518$ – 1.525 , and $n_{\gamma}=1.525$ – 1.529 ; birefringence— 0.007 – 0.010 ; hydrostatic SG— 2.56 – 2.60 ; and fluorescence—yellow-green to long-wave and inert to short-wave UV radiation. Microscopic examination revealed perthitic and micropertthitic textures with albite.

UV-Vis absorption and electron paramagnetic resonance spectroscopy, UV fluorescence, and heating/irradiation experiments on the Mexican amazonite showed that the various shades of the blue-green color are caused by absorption bands in the red-orange region (at 625 and 740 nm) and in the near-UV region (380 nm) of the spectrum. All of the absorption bands were strongly polarized in the β -direction [i.e., perpendicular to (001)] and weakly polarized in the a -direction [i.e., perpendicular to (010)]. The coloration mechanisms of the Mexican material are the same as for other amazonite (see M. Ostrooumov et al., "On nature of color of amazonite," in M. Ostrooumov, Ed., *Amazonite*, Nedra, Moscow, 1989, pp. 151–161).

Although the economic potential of the Mexican amazonite discovery has not been evaluated, and the material is not yet available commercially (there has been no orga-

nized mining to date), the deposit shows mineralogical, geochemical, and geological characteristics that are analogous to other important amazonite deposits worldwide (Ostrooumov, 1991).

Mikhail Ostrooumov (ostroum@zeus.umich.mx)
University of Michoacán, Mexico

Jacinto Robles Camacho
National Anthropology and History Institute
Mexico City

Astorite—A rhodonite-rich rock from Colorado. *Astorite* is the trade name for a rhodonite-rich gem from Colorado (although this term also has been used as a synonym for richterite, which is an amphibole, and the name *asterite* has been applied to star sapphire; see J. de Fourestier, *Glossary of Mineral Synonyms*, Canadian Mineralogist Special Publication 2, Mineralogical Association of Canada, Ottawa, Ontario, 1999, p. 29). *Astorite* originates from the Toltec mine in the San Juan Mountains of southwestern Colorado, approximately 18 km from Silverton. This historic mine, which was originally opened for gold and other metals, was once the property of Colonel John Jacob Astor IV, who among other accomplishments co-founded the Waldorf-Astoria Hotel in New York City before perishing on the *RMS Titanic* in 1912 (J. C. Zeitner, "Astorite: A new gem material," *Rock & Gem*, Vol. 32, No. 9, 2002, pp. 70–71; J. R. Yakabowski, "Astorite—A distinctive new gem material," *Wire Artist Jeweller*, Vol. 6, No. 6, 2003, pp. 4–5).

Since May 2003, the *Astorite* claim has been held by Keith and Connie McFarland of K&C Traders in Silverton. The material is mined from a vein approximately 0.2–0.4 m wide, and is worked on a small scale by drilling and blasting. There is no road leading to the mine, and it is only accessible for part of the summer season, so the production is limited to less than a ton of mixed-grade rough material per year.

Several samples of *Astorite* have been donated to the GIA Collection by the McFarlands; these consist of seven cabochons (six were between 5.67 and 7.09 ct, while the largest weighed 58.84 ct) and two tumbled pieces (10.96 and 12.41 ct). Since we were not aware of a previous gemological description of this material, we characterized some of these samples for this report. As can be seen in figure 4, the samples displayed an attractive mixture of pink, gray, black, and brown. Although the material superficially resembled rhodonite, a visual inspection established that it was a polymineralic aggregate. Gemological properties were determined on two of the cabochons (6.71 and 58.84 ct): color—predominantly pink with bands of gray and brown and small patches of black (larger cabochon), or black and pink with small patches of gray and brown (smaller sample); spot RI, taken on pink areas—1.71; SG—3.22 and 3.42 for the larger and smaller cabochons, respectively; diaphaneity—translucent to opaque; luster—subvitreous; and no spectrum seen with

the desk-model spectroscope. The samples were mostly inert to long-wave UV radiation, with patches of violet and orange in some areas, and a similar but weaker reaction to short-wave UV. The areas of violet fluorescence corresponded to transparent colorless material, while those with orange fluorescence generally correlated to pale brown/“peachy” colored material. Probably because of the heterogeneous nature of our samples, these results differed somewhat from those for rhodonite, which has the following properties: RI—1.733–1.747 (spot reading usually 1.73); SG— 3.5 ± 0.3 ; absorption spectrum—a broad band centered at around 545 nm and a line at 503 nm; and UV fluorescence—inert (*Gem Reference Guide*, GIA, Santa Monica, CA, 1995, pp. 201–202).

Raman spectroscopy was performed to further characterize both samples. The Raman spectra of some pink areas provided good matches for rhodonite, while other pink areas were identified as rhodochrosite or a mixture of both rhodonite and rhodochrosite. Some of the gray areas were identified as quartz (which probably caused the lower SG value of the larger cabochon, in which it was more abundant). The transparent colorless areas with violet fluorescence matched fluorite (for which this fluorescence color is consistent). Raman spectra from small whitish gray areas matched calcite (which could possibly be responsible for the orange fluorescence, as could rhodochrosite). Various spots analyzed in the black areas gave matches to chalcocite, galena, pyrite, and sphalerite. EDXRF spectroscopy of a pink area on the larger sample was consistent with rhodonite. Hence, these two samples of Astorite were characterized as a rock composed of rhodonite, quartz, and rhodochrosite, with traces of calcite, chalcocite, fluorite, galena, pyrite, and sphalerite. This composition is consistent with the literature, except that calcite and chalcocite were not previously mentioned and additional components were listed by Zeitner (2002) and Yakabowski (2003): chalcopyrite, tennantite, tetrahedrite, native metals, helvite, tephroite, and friedelite.

The McFarlands indicated that the Astorite is polished



Figure 4. This material, sold under the trade name Astorite, proved to be a rock composed of rhodonite, quartz, rhodochrosite, and other minerals. The largest piece in the center weighs 58.84 ct. Gift of Keith and Connie McFarland, GIA Collection no. 37095 (all samples); photo by Maha Tannous.

into cabochons of graduated sizes ranging from 5 mm rounds to 40 × 50 mm ovals. They also produce freeform and inlaid Astorite jewelry.

*Sam Muhlmeister and
Karen Chadwick (karen.chadwick@gia.edu)
GIA Laboratory, Carlsbad*

Color-change bastnäsite-(Ce) from Pakistan. In February 2007, the Asian Institute of Gemological Sciences (AIGS) Laboratory in Bangkok had the opportunity to examine an unusual 2.09 ct bastnäsite (figure 5), which is a rare-earth carbonate mineral. It was submitted for identification and study by gem dealer Scott Davies (American-Thai Trading,



Figure 5. This unusual 2.09 ct bastnäsite shows a distinct color change, from brownish yellow in daylight/fluorescent light (left) to orange in incandescent light (right). Photos © Scott Davies.

Bangkok), due to its distinct color change, he reported that very few of the bastnäsites he has cut have displayed any significant change of color.

Mr. Davies purchased the original piece of rough in Peshawar in 2006. The material was reportedly mined at the Zagi Mountain deposit northwest of Peshawar, which is known for bastnäsite and other rare-earth minerals (H. Obodda and P. Leavens, "Zagi Mountain, Northwest Frontier Province, Pakistan," *Mineralogical Record*, Vol. 35, No. 3, 2004, pp. 205–220). Bastnäsite gemstones up to nearly 20 ct have been faceted from this locality (see Summer 1999 Lab Notes, pp. 136–137; Obodda and Leavens, 2004).

The following gemological properties were determined on this sample: color—brownish yellow in daylight/fluorescent light and orange in incandescent light; diaphaneity—transparent; RI—1.720 and >1.81 (i.e., over the limits of our standard refractometer); optic character—uniaxial positive; SG (measured hydrostatically)—5.09; and inert to both long- and short-wave UV radiation. Except for the color change, these properties are comparable to those reported for bastnäsite in the Summer 1999 Lab Note and by W. L. Roberts et al. (*Encyclopedia of Minerals*, 2nd ed., Van Nostrand Reinhold, New York, 1990, pp. 73–74).

The visible spectrum obtained with a spectrophotometer showed typical rare-earth absorptions at 444, 461, 468, 482, 511, 521, 532, 578 (strong), 625, 676, 688, and 739 nm (strong). X-ray micro-fluorescence (XRMF) analysis, performed at the Central Institute of Forensic Science (CIFS) Laboratory in Bangkok, revealed the presence of cerium as well as minor amounts of lanthanum, praseodymium, and iron. The IR spectrum showed peaks at 6484 (strong), 6320, 5827, 5070, 4464, 4294, ~4000 (strong), 3590, 3494, 3407, and 3154 cm^{-1} . Raman spectroscopy revealed peaks at 1736, 1435, 1095 (strong), 735, 397, 350, and 260 cm^{-1} . The visible, IR, and Raman spectra—available in the *GeG* Data Depository at www.gia.edu/gemsandgemology—are in agreement with the bastnäsite-(Ce) data we have in our library, and are also comparable to previous reports (e.g., the Summer 1999 Lab Note).

The origin of the unusual color-change behavior in this bastnäsite is unknown. There are a number of gem materials, both natural and synthetic, in which color change is linked to the presence of rare-earth elements. Examples include color-change monazite, fluorite, zircon, and some types of manufactured glass. The process responsible for this color behavior is complex. It is known, however, that light-induced electronic transitions of the rare-earth elements (i.e., f-f transitions) are responsible for most of the sharp absorptions seen in the visible spectrum of these minerals (e.g., L. R. Bernstein, "Monazite from North Carolina having the alexandrite effect," *American Mineralogist*, Vol. 67, 1982, pp. 356–359), and it is these sharp absorptions that are responsible for any change of color. Therefore, the color change in the present bastnäsite may be due to the specific proportions of its constituent rare-earth elements. The rare earth-induced color behavior is



Figure 6. This 30.32 ct citrine from Minas Gerais, Brazil, contains abundant inclusions of pyrite. GIA Collection no. 36747; photo by Robert Weldon.

in contrast to the "alexandrite effect" exhibited by alexandrite and color-change garnet, among other minerals, which is due to a small number of broad bands linked to chromium and/or vanadium absorption.

To the best of our knowledge, color change has not been reported previously in bastnäsite, and this was the first example of color-change bastnäsite seen in the AIGS Laboratory.

Acknowledgments: This contributor wishes to acknowledge K. Plagbunchong, S. Arepornrat, and T. Thongtawee of the CIFS Laboratory for assistance with the XRMF analysis.

Laurent Massi (info@aigslaboratory.com)
AIGS Gem Laboratory, Bangkok

Citrine with pyrite inclusions. At the 2007 Tucson gem shows, these contributors were shown some unusual faceted stones and cabochons of citrine that contained conspicuous inclusions of pyrite. The material was offered by Michele Macri (Laboratorio di Gemmologia Geo-Land, Rome, Italy), who indicated that it was mined in approximately 2002 in Minas Gerais, Brazil. Until recently, only clean citrine gemstones had been cut from the rough, while all the material containing inclusions had been stockpiled. Mr. Macri obtained ~1 kg of the rough material containing pyrite inclusions from the mine owner, which yielded about 400 carats of faceted stones and cabochons. The color of the citrine reportedly is natural, and the material has not been treated in any way. According to the mine owner, the property was closed in 2005, but the deposit still contains additional reserves of the material.

A 30.32 ct dark brownish orange oval buff-top citrine was donated to GIA by Mr. Macri and examined for this report (figure 6). Standard gemological testing verified that this gem was quartz, while the condition of the pyrite (figure 7) and intact fluid inclusions provided evidence that the citrine was natural and untreated. Although beautifully

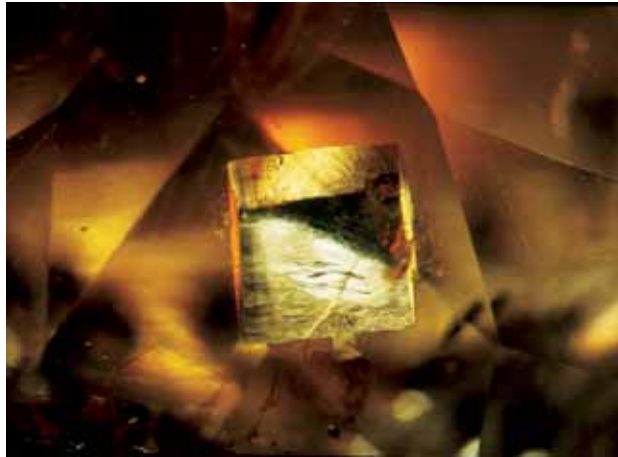


Figure 7. Measuring approximately 1.6 mm across, this well-formed cubic pyrite inclusion in the citrine illustrated in figure 6 shows a metallic luster, brassy color, and surface details that are characteristic of this sulfide mineral. Photomicrograph by J. I. Koivula.

formed pyrite crystals are known to occur in colorless rock crystal, such inclusions are very unusual in both amethyst and citrine. The inclusions of pyrite examined for this report are the best we have seen to date in any citrine.

John I. Koivula (jkoivula@gia.edu)
GIA Laboratory, Carlsbad

BML

Unusual danburite pair. At the 2007 Tucson gem shows, this contributor saw an unusual matched pair of yellow danburites set as earrings (figure 8) at the booth of Pillar & Stone International (San Francisco, California). The stones had a total weight of 34.60 ct and displayed a strikingly saturated yellow hue. According to the owners, Roland

Figure 9. The danburites contained multiple overlapping “fingerprint” inclusions. Photomicrograph by Hpone Phy Kan-Nyunt; magnified 20×.

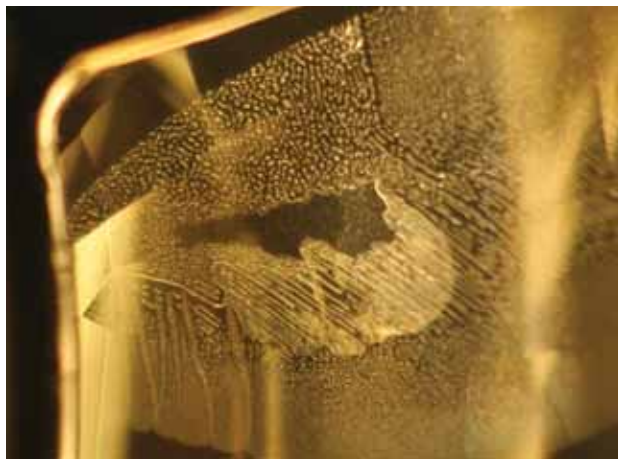


Figure 8. This matched pair of bright yellow danburites weighs a total of 34.60 ct. Courtesy of Pillar & Stone International, San Francisco; photo by Judy Chia.

and Nata Schlüssel, they were mined west of the town of Kyatpyin, in Myanmar’s Mogok region.

The refractive indices of the yellow danburites were $n_o=1.630$ and $n_e=1.634$, yielding a birefringence of 0.004, and they fluoresced blue to both long- and short-wave UV radiation. These properties matched those described in the *Gem Reference Guide* (Gemological Institute of America, Santa Monica, CA, 1995, pp. 84–85), except that reference did not mention the saturated yellow color, and the birefringence we obtained was lower than the reported value of 0.006 (probably because the mountings prevented us from measuring the maximum birefringence). Danburite has a Mohs hardness of 7–7.5.

With magnification, both samples showed overlapping “fingerprints” (figure 9). One had elongate growth tubes that sometimes ended in a curled shape (figure 10). No growth

Figure 10. One of the danburites also contained elongate growth tubes. Photomicrograph by Hpone Phy Kan-Nyunt; magnified 20×.





Figure 11. These crystals of gem-quality fluorite (8.6 g total weight) were selected to show the range of color of material from a new source in southern Ethiopia.

Photo by M. Macri.

banding was observed; however, one of the danburites showed variable color concentration between the center of the stone and the rim. No other inclusions or growth features were present.

EDXRF chemical analysis revealed Ca and Si as major elements; this is consistent with the chemical formula of $\text{CaB}_2(\text{SiO}_4)_2$ for danburite (boron cannot be detected with EDXRF). In addition, a minor amount of Sr was detected. The Raman spectrum matched that of our danburite reference, confirming the identification.

According to Mark Smith (Thai Lanka Trading Ltd., Bangkok), yellow danburite is known from several alluvial and primary deposits in the Mogok region. Recently, it has been recovered from pegmatites near Molo in the Momeik area; a pegmatite in this same region has also produced pezzottaite (see Spring 2006 Gem News International, pp. 70–72). Other *in-situ* deposits are known at Dat Taw, Sakangyi, and an important new locality called Lay Gyi. Mr. Smith also noted that the local miners are adept at identifying danburite (due to its distinctive etched surface and characteristic growth-tube inclusions), and they value it highly as a jewelry stone.

Lore Kiefert (lkiefert@agta-gtc.org)
AGTA Gemological Testing Center
New York

Fluorite from Ethiopia. Ethiopia has grown rapidly in gemological importance during the past several years. Among other developments, it has become a significant source of gem-quality opal (see, e.g., M. L. Johnson et al., "Opal from Shewa Province, Ethiopia," Summer 1996 *Gems & Gemology*, pp. 112–120). As a result of this growing interest, there has been much recent exploration for gem materials and efforts to open new mines.

In March 2007, one these contributors (MM) encountered a new gem material at the Bologna mineral show in Italy. Mr. Tesfay Desta, an Ethiopian dealer, had an interesting 500 g parcel of some unidentified gem-quality rough. The material was reportedly from a mine in the Guji zone, southern Ethiopia. Five samples (figure 11) were purchased for testing.

The crystals weighed approximately 1–2 g each, and were crystallized as pentagonal icositetrahedra with slightly concave faces. They were colorless, reddish brown to brownish red/pink, and pale blue-violet. The following gemological properties were determined from two of the samples using standard techniques: RI—1.434; SG—3.16; fluorescence—inert to moderate green to long-wave UV, inert to strong green to short-wave; and phosphorescence—moderate green. Internal features consisted of fluid inclusions, and straight parallel growth features and color zoning. These properties are consistent with those for fluorite (see M. O'Donoghue, *Gems*, 6th ed., Butterworth-Heinemann, Oxford, UK, p. 411), although the crystal habit is unusual for this mineral.

X-ray powder diffraction data collected for three samples on a parallel-beam Bruker AXS D8 Advance automated diffractometer confirmed the identification as fluorite. The lattice parameter a extracted via Rietveld refinement is $a = 5.46378(1) \text{ \AA}$, in agreement with V. A. Streltsov et al. ("Electronic and thermal parameters of ions in CaF_2 : Regularized least squares treatment," *Kristallografiya*, Vol. 33, 1987, pp. 90–97).

At the Verona mineral show in late May 2007, Mr. Desta had a 25 kg parcel of rough Ethiopian fluorite that included some color-change material. The color appeared



Figure 12. Some of the fluorite from Ethiopia (here, 21.0 g total weight) shows a color change from blue or grayish blue in sunlight to purple or reddish purple in incandescent light. Photos by M. Macri.

blue to grayish blue (similar to iolite) in sunlight and in daylight-equivalent fluorescent light, and purple (like amethyst) to reddish purple in incandescent light (figure 12). In addition, some of the deep reddish brown fluorite crystals appeared deep red (like rhodolite) in incandescent light. The other colors did not show the color-change effect, so it was estimated that only 3–5% of the stones show this behavior.

Ethiopian fluorite has the potential to be an interesting collector's gem. According to Mr. Desta, the total weight of rough material available on the market as of May 2007 was approximately 200 kg.

Michele Macri (michele@minerali.it),
Adriana Maras, Elisa Melis, and Paolo Ballirano
Department of Earth Sciences
University of Rome "La Sapienza"
Rome, Italy

Heliodor and other beryls from Connecticut. For more than a century, granitic pegmatites of the Middletown District in Connecticut have been known for producing small amounts of gem beryl and tourmaline, although they have been principally mined for industrial feldspar, mica, beryl, and other minerals (see E. N. Cameron et al., *Pegmatite Investigations, 1942–1945, in New England*, U.S. Geological Survey Professional Paper 255, 1954, 347 pp.; J. A. Scovil, "The Gillette Quarry, Haddam Neck, Connecticut," *Mineralogical Record*, Vol. 23, No. 1, 1992, pp. 19–28). A variety of beryl colors have been reported from these pegmatites, including colorless, "golden" yellow, blue to green, and pink (e.g., Scovil, 1992).

At the 2007 Tucson gem shows, Jim Clanin (JC Mining, Hebron, Maine) obtained two faceted heliodors from Connecticut that were notable for their saturated "golden" yellow color (figure 13). The stones were purchased from Jan Brownstein (Songo Pond Gems, Bethel, Maine), who had cut them from a collection of gem rough that he recently obtained from the Howard Hewitt estate. This beryl collection consisted mostly of rough pieces, polished rough, and preforms of various colors (e.g., figure 14) that were mined by Mr. Hewitt over the past several decades from three quarries in Connecticut: Merryall (or Roebling) in Litchfield County ("golden" yellow), Slocum near East Hampton ("lemon" yellow), and Turkey Hill near Haddam (pale blue, with inclusions; John Betts, pers. comm., 2007). In total, Mr. Brownstein obtained a few kilograms of the Connecticut beryl, and he has faceted about 250 stones so far with a maximum weight of ~13 ct. All of the rough material consisted of broken pieces that most likely were derived from beryl crystals that were "frozen" in the pegmatite matrix; there was no evidence of any crystal faces indicative of growth in gem pockets.

Examination of the two cut heliodors (1.54 and 2.36 ct) by one of us (EAF) showed the following properties: color—orange yellow to orange-yellow, with no pleochroism; RI—1.575–1.581; birefringence—0.006; hydrostatic SG—2.73 and 2.75; Chelsea filter reaction—none; and fluorescence—inert to long- and short-wave UV radiation. These proper-



Figure 13. Strong "golden" yellow coloration is shown by these attractive beryls (2.36 and 1.54 ct) from Connecticut. Courtesy of Jim Clanin; photo by Robert Weldon.

ties are consistent with those reported by M. O'Donoghue (*Gems*, 6th ed., Butterworth-Heinemann, Oxford, UK, 2006, pp. 124–129) for aquamarine, which O'Donoghue indicates has properties equivalent to yellow beryl. Microscopic examination revealed numerous fine growth tubes and clouds of pinpoint-sized particles. The stones displayed a weak absorption band around 500 nm when observed with the desk-model spectroscope, as mentioned for strongly colored yellow beryl by O'Donoghue (2006). This reference also indicated that the Merryall mine has been the only important source of yellow beryl in the United States.

BML

Eric Fritz
GIA Laboratory, Carlsbad

Figure 14. Beryl from Connecticut comes in a variety of colors, as shown by these gemstones (1.87–3.18 ct) and preforms (1.3–2.5 g). Courtesy of Jan Brownstein; photo by Robert Weldon.





Figure 15. All of these chatoyant gems (6.45–19.32 ct) are currently available from Tanzania. From left to right, they are scapolite, K-feldspar, opal, and apatite. Courtesy of Anil B. Dholakia Inc.; photo by Robert Weldon.

Cat's-eye K-feldspar and other chatoyant gems from Tanzania. A wide variety of cat's-eye and star gems have been reported from Tanzania and Kenya, including apatite, beryl, corundum (ruby and sapphire), garnet (almandine, grossular, and rhodolite), kyanite, kornerupine, scapolite, tourmaline, and zoisite (N. R. Barot et al., "Cat's-eye and asteriated gemstones from East Africa," *Journal of Gemmology*, Vol. 24, No. 8, 1995, pp. 569–580). During the 2007 Tucson gem shows, Anil Dholakia (Anil B. Dholakia Inc., Franklin, North Carolina) showed one of these contributors (BML) some cabochons that he was selling as cat's-eye feldspar from Tanzania. He indicated that such material has been identified as labradorite by some gemologists, and also shows a close resemblance to Tanzanian cat's-eye scapolite. The feldspar/scapolite confusion was reinforced by gem dealer Scott Davies, who purchased some Tanzanian rough sold as "red moonstone" in 2004 that proved to be scapolite. He indicated that both gems show good chatoyancy and

have a similar color range (light brownish red to very dark reddish brown).

Mr. Dholakia loaned some cabochons of each gem to GIA for examination, as well as chatoyant opal and apatite from Tanzania for comparison. A representative sample of each gem (6.45–19.32 ct; figure 15) was selected for characterization by one of us (EAF), and the results are given in table 1.

The properties of the cat's-eye feldspar were consistent with alkali feldspar, rather than labradorite (a calcic plagioclase). This was confirmed by EDXRF analysis, which detected major amounts of Al, Si, and K, and traces of Ca and Ba. Similar alkali feldspars were documented by U. Henn et al. ("Chatoyancy and asterism in feldspars from Tanzania," *Gemmologie: Zeitschrift der Deutschen Gemmologischen Gesellschaft*, Vol. 54, No. 1, 2005, pp. 43–46), although only faint asterism was seen when our sample was rotated in front of a fiber-optic light source. Henn et al. (2005) attributed the optical phenomena to ori-

TABLE 1. Properties of some chatoyant gems from Tanzania.^a

Property	K-feldspar	Scapolite	Opal	Apatite
Weight (ct)	19.32	13.70	6.45	15.13
Color	Orangy brown	Brown-red	Orange-brown	Yellowish green
RI (spot)	1.53	1.55	1.45	1.63
SG (hydrostatic)	2.59	2.75	2.09	3.23
Fluorescence				
Long-wave	Inert	Inert	Inert	Inert
Short-wave	Very weak red	Very weak red	Inert	Inert
Spectroscope spectrum	General absorption to 510 nm	No features seen	General absorption to 550 nm	Line at 530 nm and doublet at 580 nm
Inclusions	Fine black needles, small reddish trigonal platelets, and long orangy rectangular platelets	Small red angular platelets, fine red needles, and small black dendritic platelets	Long needles with an almost fibrous appearance	Fine iridescent needles or growth tubes

^aNo pleochroism or reaction to the Chelsea filter was seen in any of the samples.

ented lath-shaped inclusions of hematite. A similar K-feldspar (from an undisclosed source) was described in a Summer 1997 Lab Note (p. 137), but in that cabochon the platy inclusions were too large and poorly oriented to account for the chatoyancy or asterism.

The properties obtained for the chatoyant scapolite are consistent with those previously reported for this gem variety (e.g., Summer 2003 Gem News International, pp. 158–159; Spring 1984 Lab Notes, pp. 49–50) except that the RI we measured was slightly lower. Since the refractive indices (and specific gravity) of scapolite increase with greater Ca content, our results indicate a composition that is closer to the marialite end member ($3\text{NaAlSi}_3\text{O}_8 \cdot \text{NaCl}$) of the solid-solution series with meionite ($2\text{CaAl}_2\text{Si}_2\text{O}_8 \cdot \text{CaCO}_3$). A further decrease in Ca content would be expected to cause a spot-RI value that is at or slightly below 1.54 (e.g., P. C. Zwaan and C. E. S. Arps, "Properties of gemscapolites [sic] from different localities," *Zeitschrift der Deutschen Gemmologischen Gesellschaft*, Vol. 29, No. 1–2, 1980, pp. 82–85), which is quite similar to that of K-feldspar.

The properties of the other chatoyant gems documented in this study are consistent with those described in the literature for Tanzanian opal (Summer 1998 Gem News, pp. 138–140) and apatite (E. Gübelin and K. Schmetzer, "Eine neue Edelstein-Varietät aus Tansania: Gelbe, grüne und rötlich-braune Apatit-Katzenaugen," *Zeitschrift der Deutschen Gemmologischen Gesellschaft*, Vol. 31, No. 4, 1982, pp. 261–263).

The cat's-eye K-feldspar can be readily separated from chatoyant opal and apatite by its standard gemological properties. However, distinguishing it from scapolite might be difficult in cases where a stone cannot be unmounted for SG measurement. In such situations, a careful RI reading can separate the two minerals, but an accurate identification may depend on performing more advanced (spectroscopic) testing.

Eric Fritz (eric.fritz@gia.edu)
GIA Laboratory, Carlsbad

BML

Green opal. During the 2007 Tucson gem shows, one of these contributors (BML) was shown some cabochons of bright green opal by Hussain Rezayee (Pearl Gem Co., Beverly Hills, California). Mr. Rezayee obtained the rough in December 2004 while in Turkey, but he was not able to confirm its source. From several tons of mostly low-quality material, he selected 100 kg of usable pieces that ranged from 20 g to 1 kg. He subsequently cut about 5,000 carats of cabochons, which weighed up to 70–80 ct each. He reported that none of the cabochons were treated in any way.

Five of the opal cabochons (5.36–17.74 ct; e.g., figure 16) were loaned to GIA by Mr. Rezayee for examination, and the following gemological properties were determined by one of us (KMR): color—semitranslucent-to-translucent light green; spot RI—1.46–1.47; hydrostatic SG—



Figure 16. Although the rough material was purchased in Turkey, these green opal cabochons (5.36–17.74 ct) have properties comparable to those recorded for Serbian material. Courtesy of Hussain Rezayee; photo by Robert Weldon.

2.10–2.13; fluorescence—weak green to long-wave and very weak green to short-wave UV radiation, with no observable phosphorescence; and general absorption below 450 nm and above 620 nm seen with the desk-model spectroscope. These properties are consistent with those reported for green opal from Serbia in the Fall 1995 Gem News section (p. 208), except that the sample documented in that report was opaque and also inert to short-wave UV. Microscopic examination of Mr. Rezayee's samples revealed fine veins and cavities lined with small spheroids of botryoidal opal (identified by JIK). EDXRF chemical analysis (performed by EAF) detected minor amounts of Ni, as well as traces of Ca and V.

The Fall 1995 Gem News entry indicated that the properties of the Serbian material are comparable to those of green opal from Tanzania (see J. I. Koivula and C. W. Fryer, "Green opal from East Africa," Winter 1984 *Gems & Gemology*, pp. 226–227), and that green Ni-bearing opal has also been found in Poland, Australia, and Peru. The opal described in the present report is most likely from Serbia, given its similarity to the material described previously and information provided to Mr. Rezayee at the 2007 Tucson shows by a German opal dealer, who indicated that the opal was very similar to material from the province of Kosovo.

Kimberly M. Rockwell (krockwell@gia.edu),
John I. Koivula, and Eric A. Fritz
GIA Laboratory, Carlsbad

BML

Chinese akoya cultured pearls. In 2006, Chinese farmers produced about 20 tonnes of akoya cultured pearls along the southern coasts of Guangdong and Guangxi provinces (You Hong Qing, Xuwen Jinhui Pearl Co., pers. comm.,



Figure 17. These Chinese akoya cultured pearl strands are composed of natural-color, silver-blue baroques (7.5–11.3 mm) and bleached white rounds that show a rosé overtone produced by “pinking” (7.5–8 mm). Courtesy of J. Shepherd; photo by Kevin Schumacher.

2007). The production region extends east from the Vietnam border past Beihai, around the Leizhou Peninsula and Hainan Island, and continues east toward Hong Kong. Beihai in the west and Xuwen on the peninsula are two processing centers. Between the Beihai area and the Leizhou Peninsula’s east side, there are more than 2,000 akoya pearl farms. About 100 farms maintain more than 500,000 nucleated mollusks, about 200 culture 200,000–500,000 mollusks, and about 1,700 maintain fewer than 200,000.

Chinese akoya farmers identify the mollusk they use as *Pinctada fucata martensii*. This is the same species that farmers in Japan identify as the akoya mollusk. However, there has been so much hybridization with closely related species that *P. fucata martensii*’s purity as a cultured pearl producer in China and Japan is questionable (Shigeru Akamatsu, Mikimoto Co., pers. comm., 2006; You H. Q., pers. comm., 2007). On Chinese akoya farms, all the mollusks are hatchery bred, although hatcheries do introduce wild mollusks to ensure genetic diversity. There are at least 12 hatcheries in the pearl-culturing region, two of which are government-run facilities on Hainan Island.

In April 2007, the present authors visited several pearl farms and nucleation facilities on Longye Bay near Xuwen. Nucleators there implanted one or two spherical shell-bead nuclei ranging from 5 to 7.75 mm, each with a tissue

piece from a donor mollusk, in host mollusks that measured 6.4–7 cm in diameter. At that size, the mollusks are about 18 months old. We were told that the pearl-growth period ranges from six months to two years, but 10–12 months is most common. Nacre thickness (per radius) ranges from 0.1 to 1.2 mm, while 0.4–0.6 mm is most common. Cultured pearl sizes range from 2 to 11 mm. Shapes are round, near-round, semibaroque, baroque, drop, pear, and oval. Colors include bleached white with a rosé overtone produced by “pinking” (immersing the cultured pearls in an extremely dilute red pigment) and natural silver-blue (figure 17). Quality ranges from commercial to gem grade.

According to Mr. You, processors in the Xuwen area bleach about 98% of the akoya cultured pearls they handle. Many are also heavily dyed, with black being the most common color. A medium-volume processing factory produces about 10,000 temporary strands (16–16.5 inch [40–42 cm]) per year, while a large factory produces about 42,000 such strands annually.

About 50% of the Chinese akoya cultured pearls are sold in Hong Kong, either at trade fairs or by direct sale through five Hong Kong wholesalers. Local wholesalers in the culturing region sell the balance by direct sale. In 2006, the top wholesale markets were Japan, the U.S., and Europe.

The 2006 volume was down from the 27 metric tons produced in 2005, and production is expected to dip again in 2007 (You H. Q. and Cissy Wong, pers. comms., 2007). The decline is partly due to falling demand, but the motives of hundreds of independent Chinese akoya pearl farmers also contribute. For akoya farmers in China, pearl culturing is very much a dollars-and-cents business. When the short-term gain looks better in shrimp farming or another type of aquaculture, many farmers switch products. The akoya volume we see now can be determined by how the farmers’ economic picture looked about a year ago.

Doug Fiske (dfiske@gia.edu)

GIA Course Development, Carlsbad

Jeremy Shepherd

PearlParadise.com Inc., Los Angeles

Pyrope-almandine from Tanzania. John D. Dyer (Precious Gemstones Co., Edina, Minnesota) had some attractive orange-red to orangy red garnets that he marketed as “rose malaya” at the 2007 Tucson gem shows. This trade name was based on the identification of the material as pyrope-spessartine by independent gemologists. The garnets reportedly have been produced since mid-2005 from Tanzania’s Umba Valley.

Mr. Dyer loaned three samples and donated an additional 1.35 ct garnet to GIA for examination (figure 18). The following properties were determined on all four stones by one of us (EAF): color—orange-red; RI—1.742; no birefringence; hydrostatic SG—3.80; Chelsea filter reaction—none; fluorescence—inert to long- and short-wave UV radiation; and absorption lines at 504, 520, and 573 nm



Figure 18. These attractive orange-red garnets (1.35–6.92 ct) from Tanzania's Umba Valley proved to be pyrope-almandine. The trilliant is a gift of Precious Gemstones Co.; GIA Collection no. 36746. Photo by Robert Weldon.

visible with the desk-model spectroscope. There was no observable shift in color between daylight-equivalent and incandescent light sources. These properties are similar to those reported for pyrope-spessartine, but they are more consistent with pyrope-almandine, according to C. M. Stockton and D. V. Manson ("A proposed new classification for gem-quality garnets," Winter 1985 *Gems & Gemology*, pp. 205–218). Microscopic examination revealed no inclusions and only minor surface abrasions on the stones.

EDXRF spectroscopy of the 1.35 ct garnet showed major amounts of Si, Al, Mg, and Fe, as well as minor Ca and Mn. Electron-microprobe analysis of the other three samples at the University of New Orleans confirmed the identification as pyrope-almandine, yielding the following components: 71.1–73.1% pyrope, 18.9–21.7% almandine, 7.0–8.5% grossular, and 0.2–0.4% spessartine, along with traces of the andradite component.

East Africa is a common source for pyrope-almandine that typically ranges from reddish orange to red-purple, with the latter color referred to as *rhodolite* by the gem trade. The red-purple coloration of rhodolite is very different from the orange-red color of the pyrope-almandine examined for this report. Rhodolite also commonly contains abundant oriented needle-like rutile crystals (e.g., P. C. Zwaan, "Garnet, corundum, and other gem minerals from Umba, Tanzania," *Scripta Geologica*, Vol. 20, 1974, pp. 1–41), which were not seen in the pyrope-almandine garnets we studied.

East Africa is also known for producing pyrope-spessartine in the pink to red to orange to yellow-orange range, which has been marketed as *malaya* garnet (see Stockton and Manson, 1985; K. Schmetzer and H. Bank, "Garnets from Umba Valley, Tanzania—Members of the solid solu-

tion series pyrope-spessartine," *Neues Jahrbuch für Mineralogie, Monatshefte*, Vol. 8, 1981, pp. 349–354). A wide range of compositions have been reported for malaya garnets from East Africa, with most having a 30–55% spessartine component, but some having as low as 10–30% spessartine (Stockton and Manson, 1985).

The garnets examined for this report did not contain enough spessartine component to be called malaya garnets, and they are best referred to as pyrope-almandine since they lack the purple hue of rhodolite.

Troy Blodgett (tblodgett@gia.edu) and Eric Fritz
GIA Laboratory Carlsbad

William B. Simmons and Alexander U. Falster
University of New Orleans
New Orleans, Louisiana

Pink-to-red tourmaline from Myanmar. Rubellite tourmaline from Myanmar is well known as fibrous mushroom-like crystals from the Mogok area (see T. Hlaing and A. K. Win, "Rubellite and other gemstones from Momeik Township, northern Shan State, Myanmar," *Australian Gemmologist*, Vol. 22, 2005, pp. 215–218). From late 2006 to February 2007, well-formed prisms of pink-to-red tourmaline were mined from a pegmatite located about 80 km northeast of Mandalay, at Letpanhla in Singu Township. The pegmatite is hosted by rocks of the Mogok metamorphic belt that strike in a north-south direction.

The tourmaline crystals had typical striated prism faces and were terminated by rhombohedral faces (e.g., figure 19). This contributor estimates that ~5 kg of fine-quality crystals were produced, as well as >100 kg

Figure 19. A new source of Burmese tourmaline was found in late 2006 at Letpanhla, located between Mogok and Mandalay. The Letpanhla crystals shown here range from 3.5 to 7.1 cm tall. Courtesy of Pala International, Fallbrook, California; photo by Robert Weldon.





Figure 20. This 31.5 ct cabochon of Letpanhla tourmaline shows a saturated pink color that is considerably more intense than is typically seen in tourmaline from this locality. Courtesy of U Tin Hlaing.



Figure 21. Chatoyant tourmaline has also been cut from the Letpanhla material (here, 6.24 and 7.21 ct). Photo by Mark Smith, Thai Lanka Trading Ltd., Bangkok.

of lower-quality pink material. The tourmaline typically contains fine tubes parallel to the c-axis and abundant fluid inclusions (trichites). Several hundred cabochons have been cut, ranging from 5 to 50 ct each (e.g., figure 20). Rare cat's-eye cabochons also have been produced from the Letpanhla material (figure 21).

There appears to be good potential for additional finds of tourmaline and other pegmatite minerals from the Mogok metamorphic belt in the area between Thabeikyin and Sagyin.

U Tin Hlaing
Dept. of Geology (retired)
Panglong University, Myanmar

SYNTHETICS AND SIMULANTS

Glass object with circular bands. Rock crystal quartz is often used as a carving material for various symbolic objects in India, but these items are commonly imitated by colorless glass, so they are routinely sent to gemological laboratories for identification. Recently, at the Gem Testing Laboratory in Jaipur, India, we received an approximately 188 ct colorless specimen (figure 22) in the shape of a "Shivling," which is the symbol representing Lord Shiva in Hindu theology.

Our initial observation included the use of fiber-optic lighting to look for tell-tale signs of glass, such as gas bubbles or swirls. The most conspicuous feature was a curved zone of whitish bands visible through the base of the object (figure 23, left); these bands resembled the curved striae seen in flame-fusion synthetic sapphire. However, the specimen had a lighter heft than would be expected for that material. When viewed from the side (in a direction perpendicular to the axis of curvature of the whitish bands), straight parallel lines were seen (figure 23, center).

At higher magnification, the curved bands appeared to

be composed of planes of white pinpoint inclusions (figure 23, right) that created a hazy effect in some areas of the specimen. Also present were scattered whitish crystallites and gas bubbles.

The combination of the white crystallites, gas bubbles, and swirls identified the material as glass; a spot RI value of 1.52 was consistent with this identification. Still, further tests were performed for our records. Examination between crossed polarizers revealed a strain pattern (as is typically seen in glass) along the edges of the curved whitish zone. When exposed to short-wave UV radiation, a strong pinkish purple fluorescence was confined to this zone, which was bordered by a narrow fringe of blue fluorescence (figure 24); the sample was inert to long-wave UV. We have noted

Figure 22. This 188 ct "Shivling," approximately 4.0 cm tall, was represented as rock crystal quartz, but proved to be manufactured glass. Photo by G. Choudhary.



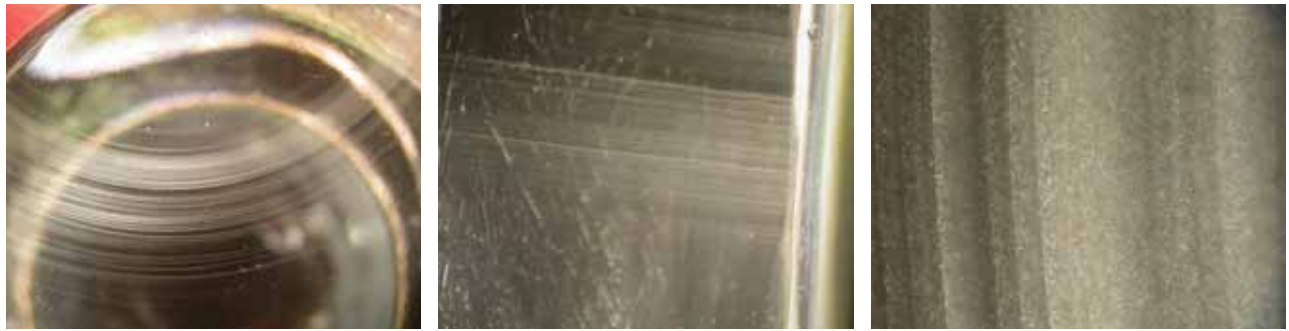


Figure 23. A zone of concentric whitish bands, similar to those seen in flame-fusion synthetic sapphire, was visible through the base of the glass object (left); note the white crystallites along the inner edge of the zone. When the glass object was viewed from the side (center), the curved whitish bands appeared as straight parallel planes, as would be expected for a cross-section through concentric cylindrical tubes. At higher magnification (right), the circular bands were seen to be composed of planes of white pinpoint inclusions. Photomicrographs by G. Choudhary; magnified 10× (left and center) and 65× (right).

similar fluorescence behavior in many colorless glasses.

In the past we have encountered some unusual features in glass, but this was the first time we had seen these circular features.

Gagan Choudhary (gtl@gjepcindia.com)
Gem Testing Laboratory, Jaipur, India

Heat-treated Kashan flux-grown synthetic ruby. In March 2006, a 10.12 ct transparent purplish red oval mixed cut (figure 25) was submitted for identification to the Dubai Gemstone Laboratory. The client indicated that it had been purchased in and originated from Myanmar.

Standard gemological testing established the following properties: RI—1.762–1.770; birefringence—0.008; optic sign—uniaxial negative; pleochroism—moderate orangy red to purplish red; SG (determined hydrostatically)—3.98; fluorescence—strong red to long-wave and moderate red to

short-wave UV radiation, with a strong chalky blue luminescence on the surface; and “chrome” lines seen in the absorption spectrum with a desk-model spectroscope. These properties were consistent with ruby, while the strong chalky blue surface fluorescence to short-wave UV radiation suggested heat treatment.

When examined with magnification, this sample at first showed internal features that looked very much like those seen in flux-assisted heated natural rubies (figure 26). However, when examined carefully, these inclusions proved to be various forms of flux residue, such as are found in flux-grown synthetics. Also apparent were white, high-relief, parallel rods; feather-like structures or “fingerprints”; rain-like structures resembling comets; and discoid features with so-called paint splash inclusions (figure 27). These inclusions are typical of Kashan flux-grown synthetic ruby. Also present were dissolved white flux-filled negative crystals with associated discoid fis-

Figure 24. The zone containing the whitish bands exhibited strong pinkish purple fluorescence to short-wave UV radiation (upper left in this photo), and the edge of this zone fluoresced blue. Photo by G. Choudhary.



Figure 25. This 10.12 ct sample proved to be a heat-treated Kashan flux-grown synthetic ruby. Photo by S. Singbamroong, © Dubai Gemstone Laboratory.



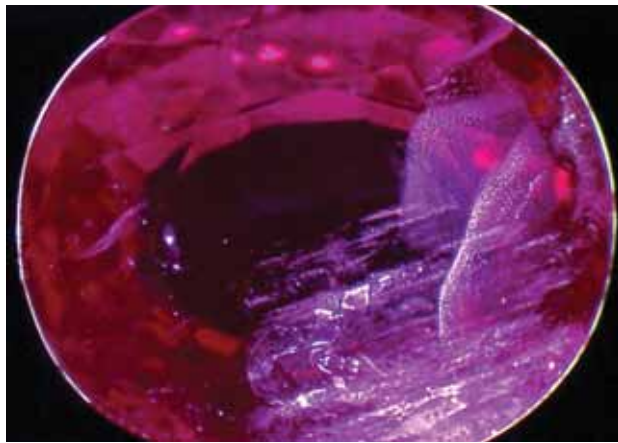


Figure 26. The synthetic ruby contained internal features that resemble those seen in flux-assisted heated natural rubies. Photomicrograph by S. Singbamroong, © Dubai Gemstone Laboratory; magnified 6 \times .

ures, which are indicative of heat treatment (figure 28).

UV-Vis absorption spectroscopy showed broad bands centered at 410 and 560 nm, and a small peak at 694 nm; these are typically responsible for ruby color. However, the spectrum also showed UV transmission at 305 nm that was stronger than the visible-region transmission at ~475 nm (blue region), which is suggestive of synthetic ruby (G. Bosshart, "Distinction of natural and synthetic rubies by ultraviolet spectrophotometry," *Journal of Gemmology*, Vol. 18, No. 2, 1982, pp. 145–160). Note that the opposite trend in the 305 and ~475 nm transmission windows was recently documented in polarized spectra of a heat-treated Kashan synthetic ruby by K. Schmetzer and D. Schwarz

("The causes of colour variation in Kashan synthetic rubies and pink sapphires," *Journal of Gemmology*, Vol. 30, No. 5/6, 2007, pp. 331–337); this is probably due to the higher Ti content of the sample that they heated. Infrared spectroscopy revealed no peaks related to the OH-group (hydroxyl), as expected for flux-grown synthetic ruby. EDXRF analysis revealed traces of Ca, Ti, V, Cr, Mn, Fe, and Ga; no Ni, Cu, La, W, Pt, Pb, Bi, or Mo was detected. The low amounts of Fe, V, and Ga, combined with slightly higher amounts of Ti, are distinctive of Kashan flux-grown synthetic ruby (see S. Muhlmeister et al., "Separating natural and synthetic rubies on the basis of trace-element chemistry," Summer 1998 *Gems & Gemology*, pp. 80–101). We also compared the EDXRF results to those for our reference collection of flux-grown synthetic rubies, and these matched very well the spectrum of the Kashan specimen in our collection. Our EDXRF data also fell within the values listed by Schmetzer and Schwarz (2007), except for slightly higher V and the presence of a trace of Ga.

Since the 1990s, a variety of heat-treated synthetic rubies have been reported (see, e.g., H. Kitawaki, "Heat treated synthetic ruby," Research Lab Report, GAAJ Research Laboratory, May 23, 2005, www.gaaj-zenhokyo.co.jp/researchroom/kanbetu/2005/kan_2005_06en.html). Heat treatment of synthetic ruby makes identification more difficult and complicated. Thus, more careful examination and sophisticated testing were necessary to complete this identification.

Sutas Singbamroong (sssutas@dm.gov.ae)
and Nazar Ahmed
Dubai Gemstone Laboratory
Dubai, United Arab Emirates

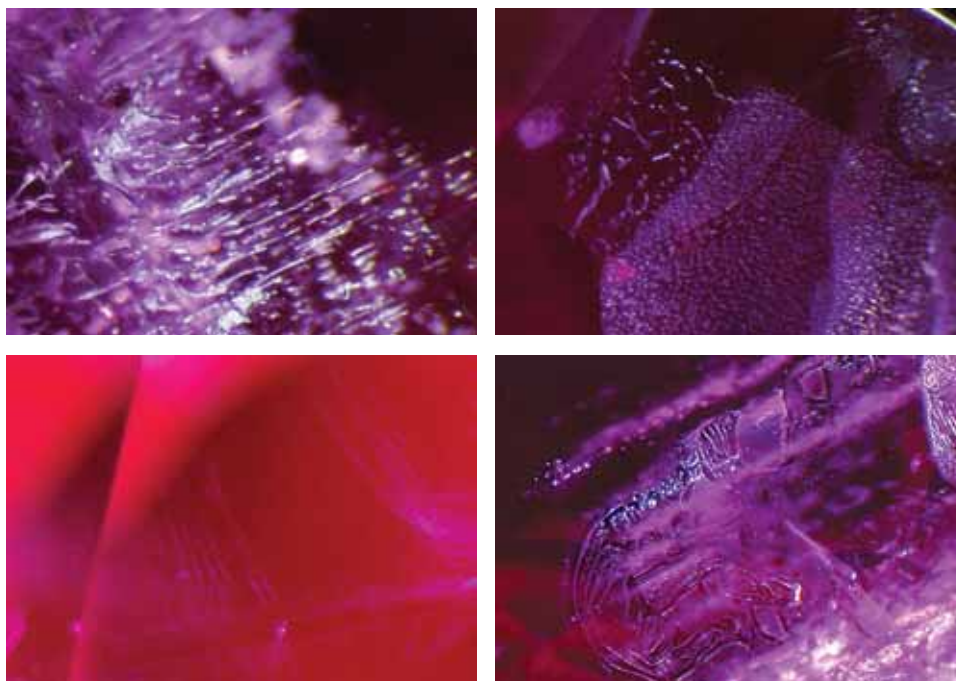


Figure 27. Various forms of flux residue were found in the synthetic ruby: white, high-relief, parallel rods (top left, magnified 40 \times); feather-like structures or "fingerprints" (top right, 20 \times); rain-like structures resembling comets (bottom left, 32 \times); and discoid features with "paint splash" inclusions (bottom right, 16 \times). Photomicrographs by S. Singbamroong and N. Ahmed, © Dubai Gemstone Laboratory.

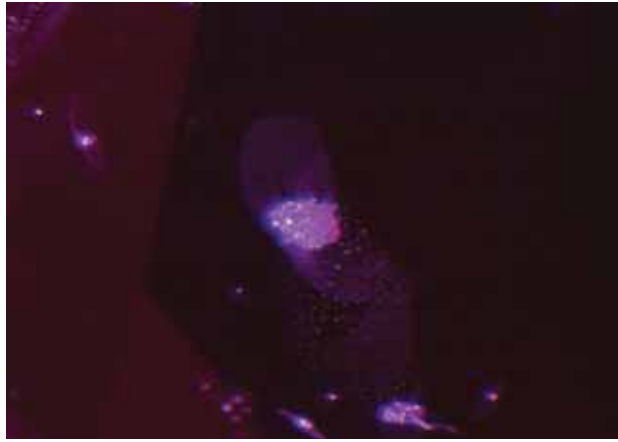


Figure 28. Dissolved white flux-filled negative crystals with discoid fissures, indicative of heat treatment, were also observed in the synthetic ruby. Photomicrograph by S. Singbamroong, © Dubai Gemstone Laboratory; magnified 50x.



Figure 29. This 4.63 ct cabochon proved to be a synthetic star sapphire with hexagonal zoning in its core, which initially suggested natural origin. Photo by G. Choudhary.

Synthetic star sapphire with hexagonal features.

Hexagonal color/growth zoning is a classic identifying feature for natural corundum. Recently, however, at the Gem Testing Laboratory in Jaipur, India, we encountered a synthetic star sapphire (figure 29) with hexagonal zoning. Our initial examination indicated that the sample was a natural sapphire with a diffusion-induced star, as suggested by the wavy appearance of the rays and the presence of “silk” inclusions. The 4.63 ct cabochon fluoresced chalky blue to short-wave UV radiation and showed chromium lines when observed with the desk-model spectroscope.

With magnification and immersion, a hexagonal zone was evident in the core of the cabochon when it was viewed from above (figure 30, left). This zone was surrounded by a wavy stress pattern (see figure 30, left and right). Also present were fine needles oriented in three directions, which were responsible for the star effect.

When the cabochon was viewed from the back, however, we were surprised to discover numerous tiny whitish

pinpoints (likely gas bubbles) arranged in curved clouds (figure 31, left). When the stone was viewed in immersion with diffused illumination, curved color bands also became apparent (figure 31, right). These features are diagnostic of a flame-fusion synthetic origin.

The cause of the hexagonal zone is not clear. We speculate that it may have been the result of a crystallographically oriented concentration of silk in the core. Using higher magnification and a strong fiber-optic light, we noted a concentration of needles in the core as compared to the surrounding area. This was the first time we observed both hexagonal zoning and curved color bands in a single sample. It provides an important reminder that a gemologist should avoid making an identification without considering all of the evidence presented by a sample. If this stone had been mounted in a closed-back setting, it would have been very difficult to make a correct identification.

Gagan Choudhary and Chaman Golecha
Gem Testing Laboratory, Jaipur, India
(gtl@gjpcindia.com)



Figure 30. The central hexagonal core was visible when the synthetic star sapphire was observed with magnification and immersion (left). A wavy stress pattern was present in the area surrounding the core (left and right). Photos by G. Choudhary; magnified 30x (right).

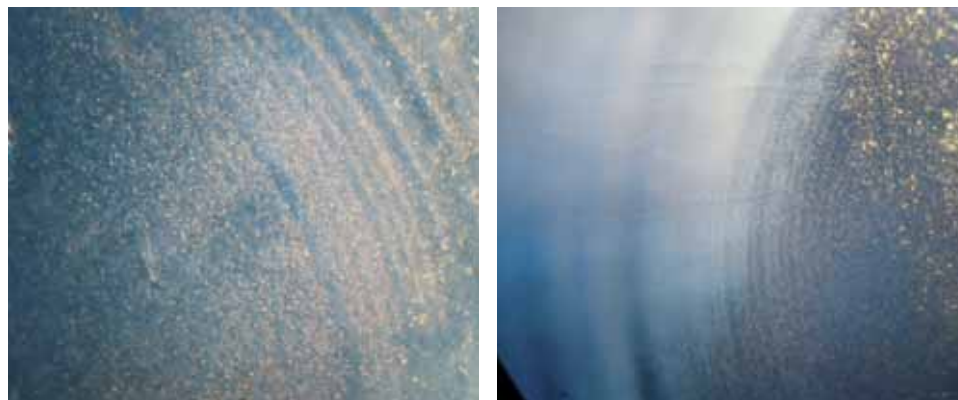


Figure 31. Curved clouds of whitish pinpoints (apparently gas bubbles) were evident on the base of the cabochon (left). With immersion and diffused illumination, curved color bands were also seen (right); these are conclusive of synthetic origin. Photomicrographs by G. Choudhary; magnified 25× (left) and 20× (right).

Pink synthetic spinel colored by iron. Recently, the SSEF Swiss Gemmological Institute was asked to test a parcel of stones represented as pink sapphires. Among them was a 15 ct antique cushion shape (figure 32) with inclusions that were very different from those seen elsewhere in the parcel. In addition to slightly curved dotted lines, there were many stretched and irregular hollow tubes (figure 33). These were similar to the features described by E. J. Gübelin and J. I. Koivula (*Photoatlas of Inclusions in Gemstones*, ABC Edition, Zurich, 1986, p. 514) and L. Kiefert (Fall 2003 Gem News International, pp. 239–240) in flame-fusion synthetic spinel.

Gemmological testing revealed that the specimen was singly refractive with an RI of 1.728; the hydrostatic SG was 3.64. With crossed polarizing filters, the sample showed prominent anomalous birefringence. However, in contrast to chromium-bearing pink and red spinel, it showed no reaction to long- or short-wave UV radiation. EDXRF spectroscopy revealed a preponderance of Al over Mg, which is characteristic for flame-fusion synthetic spinel. Iron was the only trace element present. Cr, V, Co, Zn, and Ga were all at or below the detection limit (0.001–0.002 wt. % oxide).

Figure 32. This unusual 15 ct flame-fusion synthetic spinel proved to be colored by iron. Photo by M. S. Krzemnicki, © SSEF.



The identification of the stone as a flame-fusion synthetic spinel was further confirmed by Raman spectroscopy, which showed relatively wide Raman peaks at 866, 786, 693, and 413 cm^{-1} , compared to the characteristic narrow peaks at 764, 662, and 406 cm^{-1} in natural and flux-grown synthetic spinel. The broadening and shift in these peaks is due to structural disorder in Verneuil-synthetic nonstoichiometric spinel resulting from excess Al (P. Schaub, "Spectroskopische Untersuchungen an Al-Spinell," unpublished diploma thesis, University of Basel, Switzerland, 2004). The absence of Cr was further confirmed by a Raman photoluminescence spectrum (514 nm laser), which showed no characteristic chromium emission bands.

Pink flame-fusion synthetic spinel is very rare, because chromium is not readily introduced as a chromophore during the Verneuil process. The UV-Vis absorption spectrum showed a predominant broad absorption band at 553 nm, a smaller absorption centered at 630 nm, a series of smaller absorption shoulders at 442, 472, and 530 nm, and an absorption cut-off at 400 nm (figure 34). Light violet-pink spinels colored by iron (attributed to

Figure 33. These curved particle trails and straight/kinked hollow tubes identified the sample in figure 32 as a flame-fusion synthetic. Photomicrograph by M. S. Krzemnicki, © SSEF; magnified 30×.



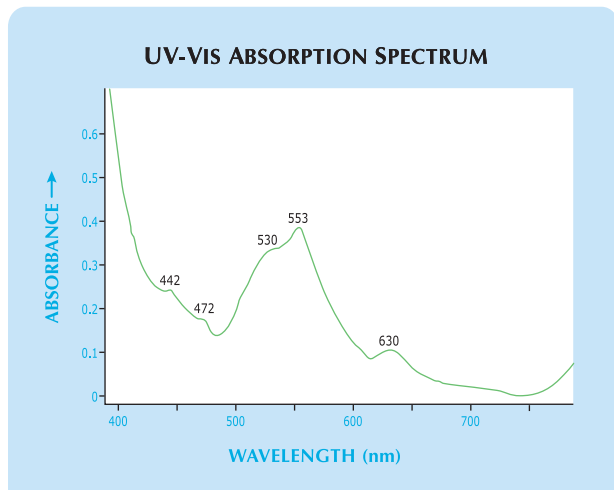


Figure 34. The UV-Vis absorption spectrum of the synthetic pink spinel in figure 32 shows absorption bands that are attributable to iron.

spin-forbidden electronic transitions of tetrahedrally coordinated Fe^{2+}) have shown similar absorption bands (see V. T. Gritsyna et al., "Spectroscopic features of iron-doped magnesium-aluminum spinel crystals," *Journal of Applied Spectroscopy*, Vol. 45, No. 2, 1985, pp. 837–840; M. N. Taran et al., "Electronic absorption spectroscopy of natural $(\text{Fe}^{2+}, \text{Fe}^{3+})$ -bearing spinels of spinel s.s.-hercynite and gahnite-hercynite solid solutions at different temperatures and high-pressures," *Physics and Chemistry of Minerals*, Vol. 32, No. 3, 2005, pp. 175–188). It is possible that very low concentrations of cobalt also contribute to the pink color of this sample.

Although flame-fusion synthetic spinel is typically an easy identification, this specimen was unusual in terms of its pink color, the abundance of inclusions, and the absence of any reaction to UV radiation. Most flame-fusion synthetic spinels are colorless, yellowish green to dark green, or light blue to blue. They often show a reddish fluorescence to long-wave UV radiation (due to cobalt) and a chalky white fluorescence to short-wave UV. Nevertheless, the RI and SG values, and the absence of naturally occurring inclusions, provide identification criteria for an experienced gemologist.

Michael S. Krzemnicki (gemlab@ssef.ch)
and Pierre Lefèvre
SSEF Swiss Gemmological Institute
Basel, Switzerland

A new imitation of Imperial topaz. Topaz is a popular gem due to its attractive appearance, ready availability, and generally low price. The one exception—which is both rare and costly—is the deep yellow-orange-pink variety known as Imperial topaz. By far the most important source of this gem is the Ouro Preto area in Minas Gerais, Brazil. Unlike many other gem materials, synthetic Imperial topaz is not commercially available, and common imitations such as citrine, synthetic spinel, and glass are easily detectable.

While in Minas Gerais in August 2006, one of these contributors (MM) was offered two loupe-clean rough samples that were represented as Imperial topaz, which he subsequently had cut (figure 35). The two pieces had an irregular triangular shape, which the dealer indicated would maximize the yield from the rough. The color and the vitreous-to-subadamantine luster resembled Imperial topaz.

The two pieces (1.18 and 2.03 ct) were analyzed in the Department of Earth Science of the University of Rome "La Sapienza," and the following gemological data were obtained: color—orange-yellow-"rose"; diaphaneity—transparent; RI— $n_o=1.770$ and $n_e=1.761$; birefringence—0.009; optic character—uniaxial negative; SG—4.05; fluorescence—inert to long- and short-wave UV radiation; and no inclusions were seen with a gemological microscope. These properties identified the pieces as corundum; their synthetic origin was strongly suggested by the lack of any natural-appearing inclusions (typical of flame-fusion material) and the relatively inexpensive price. The synthetic origin was confirmed by LA-ICP-MS analysis at GIA of the 2.03 ct sample (donated to GIA by Mr. Macrì); the lack of Ga was characteristic of flame-fusion synthetic corundum. The instrument did find traces of Cr, Ni, Ti, and Mg, but no Be, which indicates that the color of the synthetic corundum was not influenced by Be-diffusion treatment.

Although the color and luster of this synthetic corundum are strikingly similar to Imperial topaz, the two materials can be easily separated by their standard gemological properties. Still, this imitation could present a problem for the unsuspecting buyer. Interestingly, similar-colored synthetic corundum was recently sold as spessartine in the Tanzanian market (see Winter 2006 Gem News International, p. 282).

Michele Macrì (michele@minerali.it)
and Adriana Maras
University of Rome "La Sapienza"
Rome, Italy

Andy H. Shen
GIA Laboratory, Carlsbad

Figure 35. These two samples of synthetic corundum (2.03 and 1.18 ct) were sold in Minas Gerais, Brazil, as Imperial topaz. Photo by M. Macrì.



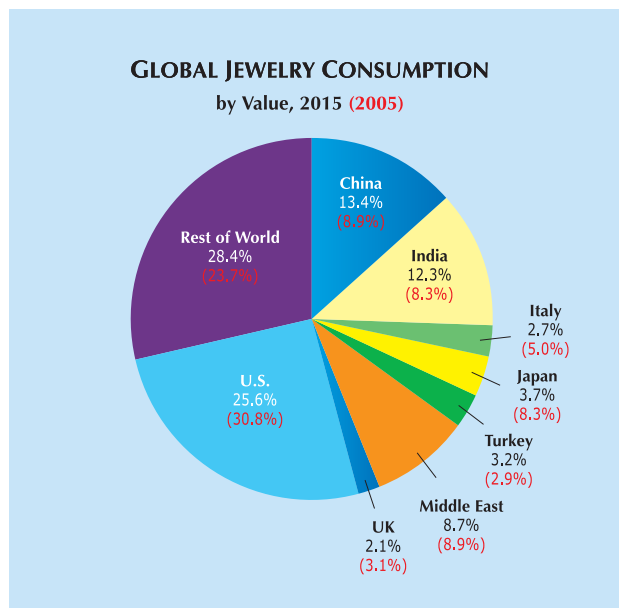


Figure 36. This chart shows the estimated global jewelry consumption by value for the eight key world markets, projected to 2015 (total US\$230 billion). Shown in parentheses are values for 2005 (total \$146 billion). Modified from *The Global Gems and Jewellery Industry—Vision 2015: Transforming for Growth*, by KPMG India.

MISCELLANEOUS

KPMG report predicts growth for the global jewelry industry. KPMG is a global network of professional firms that provide audit, tax, and advisory services. In December 2006, KPMG India released a comprehensive study of the diamond and jewelry industry worldwide, *The Global Gems and Jewellery Industry—Vision 2015: Transforming for Growth* (see www.in.kpmg.com/pdf/Gems_Jewelry_report_06.zip). The report predicts that global jewelry sales will grow by a combined 4.3% annually, from about US \$146 billion in 2005 to \$230 billion in 2015 (figure 36). The study also indicates that 2015 sales have the potential to reach \$280 billion, if the industry were to reform its marketing practices, adopt more transparent and professional business methods, and invest more in product research.

Diamond jewelry accounted for 47.2% of world jewelry sales in 2005, according to the report, followed by plain gold at 41.6%. Platinum was 6.2% (mainly in Japan and China), with colored stones and cultured pearls at 5%. The U.S. accounted for 30.8% of world jewelry sales, with China second at 8.9%, and Japan and India tied for third at 8.3% each (again, see figure 36). Italy was the largest European consumer, with a 5% world market share, while the UK accounted for 3.1%.

Within the 2005 value chain that comprised the total sales of \$146 billion, retail margins accounted for nearly half (\$67.2 billion), while rough diamond production was \$12.7 billion and polished wholesale diamond sales were \$17.6 billion. Precious metals accounted for \$40.6 billion,

and jewelry manufacturing costs were pegged at \$20.6 billion. (The sales figures of the individual categories total \$158.7 billion, rather than \$146 billion, due to some overlap between them.) However, the report offered few details about colored stone and cultured pearl sales, citing the lack of transparency and available statistics. (Note, though, that the Jewelers of America's *Cost of Doing Business Survey* for 2006 reported that colored stone jewelry accounted for 9% of U.S. retail jewelry sales.)

In 2015, diamond jewelry is projected to decline to 41% of worldwide sales, with plain gold remaining steady at ~41%. Platinum will rise slightly to 7% (with another 6% added for palladium jewelry). Synthetic diamonds will likely grab some market share from natural diamonds. KPMG also sees a decline in U.S. retail share of global demand to 25.6%, losing ground to China (13.4%) and India (12.3%). Japan will see its market share halved to 3.7%. Between 2005 and 2015, KPMG predicts, the industry will see further fragmentation of diamond sources and heavy consolidation in the wholesale and retail sectors.

The De Beers Diamond Trading Company's share of rough diamond production is expected to fall to less than 40% (from about 55% in 2005), as more small mining companies market their goods through rough diamond traders. Additionally, more rough will be sold on the open market through invitational auctions, or through "partner" players upstream in the manufacturing and retailing sectors. The polished diamond and finished jewelry markets will see the rise of large, fully integrated mine-to-retail players. Manufacturers will concentrate in low-wage countries, although there will be an increase in smaller niche manufacturing. The industry will undergo consolidation, as difficult cash flow, financing problems, and unsustainable inventory positions force a number of mergers and cause others to go out of business.

The KPMG report offered recommendations for improving marketing and business practices that could, purportedly, result in an additional 15% growth over the 10-year period:

- Promote jewelry as a category, combining separate (and often competing) campaigns by the diamond, gold, and colored stone/cultured pearl sectors into a unified effort that enhances the value proposition of jewelry.
- Identify and serve new consumer needs and segments, create new occasions to sell jewelry, and make jewelry more accessible to consumers.
- Create more innovative designs and products in established markets, while generating demand in emerging markets.
- Improve the industry's public image. Lack of transparency and concerns over quality and treatments dampen consumer demand and discourage involvement by the financial industry.
- Attract talent from outside the industry—particularly the luxury goods sector—and professionalize family-owned businesses.

The report noted that reducing finance costs by adopting these reforms (i.e., making the industry more attractive to lenders) and improving credit practices could increase cash flow. Adoption of these measures could generate an additional \$50 billion in annual sales by 2015.

*Russell Shor (rshor@gia.edu)
GIA, Carlsbad*

CONFERENCE REPORTS

Sinkankas Symposium: The Jades. This fifth annual symposium in honor of John Sinkankas took place April 21 at GIA in Carlsbad. Approximately 140 people attended the sold-out event, which was co-hosted by GIA and the San Diego Mineral and Gem Society. As in previous years, the Symposium was organized by Roger Merk (Merk's Jade, San Diego) and the participants were treated to displays of items from various collections (see, e.g., figure 37).

Fred Ward (Gem Book Publishers and Friends of Jade, Malibu, California) surveyed the various uses for jade (i.e., jewelry, decorative objects, utensils, and ritual items) and described several important localities for jadeite and nephrite. In particular, he indicated that Myanmar is the world's leading source of jadeite jade, whereas most nephrite jade comes from British Columbia, Canada. **Si Frazier** (El Cerrito, California) surveyed various types of jade, including an interesting slab of white to pale blue jadeite from Myanmar that showed distinct patches of a brighter blue in transmitted light (figure 38). **Mary Lou Ridinger** (Jades S.A., Antigua, Guatemala) described several varieties of Guatemalan jadeite that have been mined from seven quarries discovered near the Motagua fault zone from 1974 to 2004. She indicated that her company's manufacture of realistic replicas of jade artifacts has drastically reduced the demand for illegally recovered antique jades from Guatemala.

Don Kay (Mason-Kay Inc., Denver, Colorado) outlined value factors for fine jadeite according to its color and form (i.e., beads, bangles, and carvings). Pure green colors are much more valuable than lavender, yellow, red, and black varieties. In recent years, semitransparent colorless "ice" jadeite (from Myanmar) has commanded high prices, but it



Figure 37. This peacock and lotus flower carving of Burmese jadeite (12 cm tall, without the wooden stand) was on display during the 2007 Sinkankas Symposium. Courtesy of William Larson; photo by Wimon Manrotkul.

is seldom seen on the market. Mr. Kay demonstrated how high-quality jadeite bangles give a distinct "chime" when tapped together; the sound is not as distinct in jadeite with an inferior structure or that has been polymer impregnated (or both). **Richard Hughes** (AGTA Gemological Testing Center, Carlsbad) described some of the challenges he faced during his three visits to the Burmese jade mines near Hpakan, most recently in 2004: obtaining permission from the government, dealing with the politics of the area, and enduring the rugged travel conditions that required several types of transportation and negotiating roads that were impassable due to deep mud.



Figure 38. This unusual slab of Burmese jadeite (7.4 cm long) appeared white to pale blue in reflected light (left), but showed distinct patches of a brighter blue in transmitted light (right). Courtesy of Si Frazier; photos by George Rossman.

Dale Blankenship (San Diego) outlined several steps—and the corresponding equipment—that he uses for carving jade: trimming with a saw, coring with a drill press, grinding with a rotating wheel and a flex-shaft tool, sanding with a flex-shaft tool using resin rods dipped in a diamond compound, and polishing with Linde A and Linde B media. **John Koivula** (GIA, Carlsbad) described the inclusions that have been found in jade: zircon, chromite, vesuvianite, native copper, aegirine, lawsonite, albite, pyrite, and muscovite. **Dr. George Rossman** (California Institute of Technology, Pasadena) differentiated the origins of color in jadeite and nephrite. In jadeite, green is caused by Cr³⁺ substituting for Al³⁺, while a lavender hue is produced by Mn³⁺; red-orange is due to microscopic grains of hematite, while yellow is probably caused by grains of an iron hydroxide such as lepidocrocite. Green in nephrite is mainly due to Cr³⁺ with some contribution from Fe³⁺.

BML

ANNOUNCEMENTS

New CIBJO Blue Book available. CIBJO—The World Jewellery Confederation has released an updated version (2006-1) of its *Blue Book*, which provides standardized guidelines pertaining to the nomenclature, treatments, and/or care requirements for diamonds, colored stones, and pearls. The updated *Blue Book* was ratified at the March 2007 CIBJO Congress in Cape Town, South Africa. PDF files for each of the three sections are available for free download at www.cibjo.org.

AGTA Spectrum Awards competition. The 2008 AGTA Spectrum Awards will recognize outstanding colored gemstone and cultured pearl jewelry designs from North America, as well as achievements in the lapidary arts. Winning entries will be displayed and award recipients honored at the 2008 AGTA GemFairs in Tucson and Las Vegas. The entry deadline is September 25; the competition will be held in New York City during October. For entry forms and more information, visit www.agta.org or call 800-972-1162.

Conferences

PegCamp 2007—East. This one-week course, held August 6–13 in Poland, Maine, will cover the mineralogy, internal structure, and evolution of granitic pegmatites through the field examination of pegmatites and related granites. Visit www.pegmatology.com/pegcamp.htm.

NAJA 28th Annual Mid-Year Education Conference. The National Association of Jewelry Appraisers will hold this conference August 11–14 at the Cobb Galleria Convention Center in Atlanta, Georgia. Topics will include financial tips for appraisers, appraising antique jewelry, and expanding appraisal skill sets. Visit www.najaappraisers.com.

Goldschmidt 2007. The 17th Annual V. M. Goldschmidt Conference will take place August 19–24 in Cologne, Germany, and will feature a session titled “Applied geochemistry—from brines and rare-earth elements to diamonds” in honor of longtime *GeG* contributor Dr. Alfred A. Levinson. The session will consist of two parts: “Exploration Geochemistry” and “Gem Mineralogy, Diamonds and Gemstones.” Visit www.goldschmidt2007.org.

24th European Crystallographic Meeting. Held August 22–27 in Marrakech, Morocco, this conference will include a session titled “Crystallography in Art and Archeology.” Visit www.ecm24.org.

Diamond Symposium in Kimberley. The Geological Society of South Africa’s Directorate of Professional Programmes will host this colloquium August 23–24 in Kimberley, South Africa. The conference program will include field trips on August 25 to diamond deposits in the Kimberley area. Visit www.gssa.org.za and www.rca.co.za.

IV International Conference on the Application of Raman Spectroscopy in Art and Archaeology. This meeting, held September 5–8 in Modena, Italy, will explore current trends and advanced techniques in the application of Raman spectroscopy to art and cultural heritage research. Visit www.chimica.unimore.it/RAA2007/raa2007.htm.

Diamond 2007. The 18th European Conference on Diamond, Diamond-like Materials, Carbon Nanotubes, and Nitrides will be held in Berlin, Germany, September 9–14. Presentations on the growth, processing, and characterization of diamond will be given. Visit www.diamond-conference.elsevier.com.

GIA GemFest Hong Kong. This free educational seminar will be held during the Hong Kong Jewellery and Watch Fair September 27, 8:30–10:30 a.m., in Room 210B of the Hong Kong Convention and Exhibition Centre. Dr. Mink Stavenga, dean of GIA’s School of Business, will speak on the state of the global jewelry industry, and senior vice president of Laboratory & Research Tom Moses and director of GIA Research (Thailand) Ken Scarratt will provide an update on the GIA Laboratory’s current activities. To RSVP by September 14, visit the GIA Alumni Association web site at www.gia.edu, e-mail: events@gia.edu or giahk@netvigator.com, or phone 760-603-4205 (in the U.S.) or +852-2303-0075 (in Hong Kong).

II International Conference “Crystallogenesi and Mineralogy.” Held October 1–5 in St. Petersburg, Russia, this conference will explore mineral formation, crystal growth in nature and the laboratory, and crystal morphology. Visit www.minsoc.ru/KM2007.

CGA Gem Conference 2007. The Canadian Gem-mological Association's annual gemological conference will take place October 19–21 in Vancouver, British Columbia. Visit www.gemconference2007.com.

GSA Annual Meeting. The Geological Society of America will be holding its annual meeting October 28–31, 2007, in Denver, Colorado. The program will include a short course (on Oct. 28) covering the fundamentals and applications of laser ablation–inductively coupled plasma–mass spectrometry (LA-ICP-MS) to the geological sciences and other fields. Visit www.geosociety.org/meetings/2007.

Mineralientage München. The 44th Munich mineral show in Germany will take place November 2–4 and feature a special exhibit on gem crystals from Pakistan. Visit www.mineralientage.com.

Art2008. Held May 25–30, 2008, in Jerusalem, Israel, the *9th International Art Conference on Non-destructive Investigation and Analysis* will focus on items of cultural heritage, but will have implications for gem testing. Visit www.isas.co.il/art2008.

Quebec 2008: GAC-MAC-SEG-SGA. Held May 26–28 in Quebec City, Canada, this joint conference organized by the Geological Association of Canada, Mineralogical Association of Canada, Society of Economic Geologists, and the Society for Geology Applied to Mineral Deposits will include a symposium titled "Challenges to a Genetic Model for Pegmatites." Visit www.quebec2008.net.

SEG-GSSA2008: Africa Uncovered—Mineral Resources for the Future. Diamond presentations will be covered at this conference, hosted by the Society of Economic Geologists and the Geological Society of South Africa in Muldersdrift, South Africa, on July 6–9. Visit www.seg-gssa2008.org.

Goldschmidt 2008. Held July 13–18 in Vancouver, British Columbia, Canada, this geochemistry conference will include a session titled "Diamonds and Fluids in the Mantle." Visit www.goldschmidt2008.org.

Exhibits

Exhibits at the GIA Museum in Carlsbad. From now through March 2008, "Reflections in Stone" will showcase

famed gem carver Bernd Munsteiner's work during the period 1966–2003. On display in the Mikimoto Rotunda, the exhibit includes carved quartz, tourmaline, and beryl, ranging from pieces set in jewelry to large table-top sculptures. Also currently on display in the S. Tasaki Student Lecture Hall is "Celebration of Life," an exhibit of 21 award-winning tanzanite jewelry designs from the Tanzanite Foundation's Celebration of Life Awards held in New York in January. The exhibit will only be on display at GIA during July and August; this is also the final U.S. visit for this collection. Advance reservations for both exhibits are required, to schedule a tour, call 760-603-4116 or e-mail museum@gia.edu.

Gold at AMNH. "Gold," an exhibition exploring the historical fascination with this precious metal, is on display at the American Museum of Natural History in New York through August 19, 2007. The exhibit includes both rare natural specimens and significant cultural artifacts. Visit www.amnh.org/exhibitions/gold.

Wine and Gems in Dijon. "Colour Sparkles: Legendary Wines and Gemstones," a unique exhibition of fine gems and fine wines, is being held in the Sciences Garden at the Parc de l'Arquebuse, Dijon, France, through December 9, 2007. Items from the French National Museum of Natural History are on display with wines from the great vintners of Burgundy and beyond. The exhibit includes both wine tasting and hands-on experiments in light and color. Visit www.dijon.fr/fiche/eclats-de-couleurspierres-et-vins-de-legende.evt.5604.php.

Jewelry of Ben Nighthorse. Ben Nighthorse Campbell, who represented Colorado in the U.S. Senate from 1992–2004, has enjoyed a successful second career as an innovative jewelry designer. This collection of his work, which debuted at the Smithsonian Institution's National Museum of the American Indian in 2004, is on display at the Colorado History Museum in Denver through December 31, 2007. Visit www.coloradohistory.org.

Gems! Colors of Light and Stone at the Bowers Museum. The Michael Scott collection has returned to the Bowers Museum in Santa Ana, California, with an expanded display of rare colored stones, carvings, and sculptures. The exhibit will run until June 16, 2008. Visit www.bowers.org.

For regular updates from the world of **GEMS & GEMOLOGY**, visit our website at:

www.gia.edu/gemsandgemology

Thank You Donors



GIA appreciates gifts to its permanent collection, as well as gemstones, library materials, and other non-cash assets to be used in the Institute's educational and research activities. These contributions help GIA further its public service mission while offering donors philanthropic benefits. We extend sincere thanks to all 2006 contributors.



CIRCLE OF HONOR

\$100,000 AND HIGHER, CUMULATIVE

The Aaron Group
 Dr. Suman Agrawal
 Almaza Jewelers
 (Ziad H. Noshie)
 American Pearl Company
 Amsterdam Sauer
 Aurafin Oro America
 Banks International Gemology, Inc.
 (Daniel & Bo Banks)
 The Bell Group/Rio Grande
 Allan Caplan
 Chatham Created Gems, Inc.
 (Thomas H. Chatham)
 PierLuigi Dalla Rovere
 The De Beers Group
 Fabricjewelry
 Dallas R. Hales

2006 DONORS

\$50,000 to \$99,999

Robert & Marlene Anderson
 Debbie and Mark Ebert

\$10,000 to \$49,999

ALgems
 (Anita Tan)
 Cos Altobelli
 Pamela B. Bankert
 Jerry Bearman
 Dudley Blauwet
 George Brooks
 Jorge Brusa
 Carl Rickly Frudden
 Estet, Russia
 (Gagik Gevorkyan)

Dr. H. Tracy Hall
 Dr. Gary R. and Barbara E. Hansen
 James Y. Hung, M.D.
 Inta Gems Inc.
 J.O. Crystal Company, Inc.
 (Judith Osmer)
 JewelAmerica, Inc.
 (Zvi & Rachel Wertheimer)
 Kazanjian Bros, Inc.
 KCB Natural Pearls
 (K.C. Bell)
 William F. and Jeanne H. Larson
 Honoring Betty H. Llewellyn
 Stephen Lentz
 Sophie Leu
 Marshall and Janella Martin
 Roz & Gene Meieran
 Nancy B & Company
 Kurt Nassau, Ph.D.
 John & Laura Ramsey
 R. Ed Romack
 Art Sexauer
 Shades of the Earth
 (Laura and Wayne Thompson)
 Ambaji Shinde
 S. H. Silver Company
 (Stephen and Eileen Silver)
 Dr. Geoffrey A. Smith
 D. Swarovski & Co
 Touraine Family Trust
 United States Pearl Co.
 (James & Venetia Peach)
 Robert H. Vanderkay
 Vicenza Fair

Jack Hasson
 Jeweler
 Chris & Karen Johnston
 Robert E. Kane
 Lithos Africa
 Herb & Monika Obodda
 Pala International
 Mark Schneider
 Tairus (Thailand) Co. Ltd.
 (Walter Barshai)
 Paul Wild
 Tommy T. Wu
 Timothy Zielinski
 Zultanite Gems LLC

\$5,000 to \$9,999

Jacob Aminoff
 Marya Dabrowski
 JCK Magazine
 Keiko Suehiro

\$2,500 to \$4,999

Alexander's Jewelers
 Barker & Co.
 Blue Fire
 (Gordon Bleck)
 Brumani
 Charles I. Carmona, G.G.
 Eric & Jean Carstensen
 Colgem EL 97, Ltd.
 Scott Davies
 Dalan Hargrave
 Syed Ifikhar Hussain
 La Peregrina Ltd.
 Sidney Schlusberg Company, Inc.
 (Mr. & Mrs. Sidney Schlusberg)
 Nicolai Slomovits
 Thomas M. Schneider Gems

\$1,000 to \$2,499

Corby Ltd.
 Excalibur
 Jewelry Judge
 (Ben Gordon)
 Joseph DuMouchelle International
 Jewelry Auctioneers
 Intimate Gems
 Family of Albert J. Lilly
 Manoel Bernardes
 Mark Mauthner
 Nature's Geometry
 (Brian Cook)
 Terri Ottaway

\$500 to \$999

JC Mining Inc.
 (Jim Clanin)
 Alice S. Keller
 Mary Johnson Consulting
 Raymond Naftule S.A.
 Rühle - Diebener - Verlag
 Publishing House
 J. Blue Sheppard
 Martin P. Steinbach

Under \$500

Dr. Ahmadjan Abduriyim
 Björn Anckar
 Gordon & Cheryl Austin
 Beija Flor Gems
 Bob Berdan
 Pangolin Trading
 (Jo-Hannes Brunner)
 Chase Plastics Services, Inc.
 Rui Galopim de Carvalho
 Crystal Universe Pty. Ltd./Ausrox
 Makhmout Douman
 Gabriel J. Guerra, A.J.P., G.G.
 Brian House
 J. Hyrsl
 Cesar Jacinto Icasiano
 J. Paul Getty Museum
 Jaikishan Joshi
 Dr. Arunas Kleisimantas
 Jackie Li
 John Lucking
 Kelli Ann Marcou
 Neff Jewelers
 David Olson
 David L. Penney
 Pinkstone International
 Sara Olsen Ritchie
 M. F. Ameen Sadik
 M. Sarin
 Siber & Siber
 Robert A. Silverman
 Lawrence W. Snee
 Timothy Stevens
 Reg Thompson
 Tsavo Gem Imports
 Marta Van Zandt
 Vasconcelos LTDA
 John S. White

Thank You

If you are interested in making a donation and receiving tax benefit information, please contact Kimberly Vagner at (800) 421-7250, ext. 4150. From outside the U.S., call (760) 603-4150, fax (760) 603-4199. Or e-mail kimberly.vagner@gia.edu.

BOOK REVIEWS

EDITORS

Susan B. Johnson
Jana E. Miyahira-Smith
Thomas W. Overton

Gemmology, 3rd Ed.

By Peter G. Read, 324 pp., illus., publ. by Elsevier Butterworth-Heinemann, Burlington, MA, 2005. US\$39.95

Peter Read's third edition of *Gemmology* is a comprehensive work covering the fundamentals of gemology and mineralogy. This book was developed to assist students of the British gemmological association (Gem-A), but the scope goes well beyond that of a simple textbook. This revised edition has been updated to include new treatments such as HPHT processing of diamonds and beryllium diffusion of sapphires, new synthetics such as CVD diamonds, and new instrumentation such as the Raman spectrometer.

The book consists of 20 chapters, beginning with a comprehensive review of the development of gemology over the past 170 years, including new synthetics and new gem finds. Naturally, some of the rarer new gemstones such as musgravite are not mentioned because of the time limit one has to impose when writing such a summary. The second chapter is a short overview of the geology of gem deposits, occurrences, major gem localities, and mining techniques. Chapter 3 covers the chemical composition of gems, and Chapter 4 describes their crystallographic systems. The next three chapters describe the mineral properties relevant to gems, such as cleavage, parting, and fracture; hardness; and specific gravity and relative density (including the measurement of SG and the use of heavy liquids).

Discussed next are the optical properties of gemstones and related identification methods. Chapter 8 explains the electromagnetic spectrum and discusses color and selective absorption, coloring elements, and color centers, in addition to describing luster, sheen, and transparency. Chapter 9 covers reflection and refraction, and the refractometer and its use. It also discusses optic axes, signs, and characters, and how these are used to identify gems. Chapter 10 describes polarization and pleochroism, and explains the use of the polariscope and the dichroscope. Spectroscopy and various spectroscopic techniques, from the handheld spectroscope to various high-tech spectrometers, are covered in the next chapter.

Chapter 12 examines luminescent, electrical, and thermal properties, while the loupe, microscope, and Chelsea filter are described in the ensuing chapter. The next section explores gemstone enhancement, from ancient to the most recent practices; synthetics, from a history of early gem synthesis up to CVD synthetic diamond; key features to distinguish between synthetic and natural gems; simulants of non-organic gems; and organic gem materials and their simulants.

The design and cutting of gemstones are well summarized in Chapter 19. Great emphasis is given to the "critical angle," which is important for a stone's internal reflection; also covered are polishing methods and different diamond grading systems. The text closes with a practical guide to identifying gemstones along with a very useful flow chart,

guiding the gemologist from simple to more advanced tests.

The 10 appendices provide summaries of properties and other information for most organic, inorganic, and synthetic gem materials. These are very useful, though the bibliography could have been slightly larger. Also included are suggestions for Gem-A students, a review of gemstone weighing, and an index.

There are some minor drawbacks to this excellent textbook, such as the photos (which are mostly black and white), the omission of Madagascar as a major source of corundum, and the section on refractometers (some of which are no longer available). However, these are small details and do not detract from the large amount of important and relevant information provided, not only for the gemologist but for anyone involved with gemstones.

LORE KIEFERT

*AGTA Gemological Testing Center
New York City*

The Art of Enameling

By Linda Darty, 176 pp., illus., publ. by Lark Books [www.larkbooks.com], Asheville, NC, 2006. US\$17.95

It has been my personal experience with jewelry manufacturing instructional books that while there might be a tremendous amount of knowledge between the covers, there are inevitably blank spots, often with some critical piece of information about a project missing. This always made the concepts more difficult to

understand and apply when I tried the project myself. With this book, however, Linda Darty has created a truly complete text that encompasses all the major enameling techniques. Each of these is thoroughly explained, with photographic and technical support.

The book starts with an overview of enameling fundamentals. What is vitreous enamel? How is it manufactured? What are the material choices the artist has with this medium? The equipment list is extensive and detailed. Multiple choices are explained for each tool category, including their pros and cons. This level of detail allows beginning enamelists to more accurately and economically choose which tools to purchase, based on the type of enameling they want to pursue.

Throughout the book are “historical highlights,” in sidebars, that review when specific techniques began and who pioneered them. The book is also loaded with “hot tips,” little gems of information that are usually acquired only after years of experience and experimentation. Each one is clear and concise, with direct application to both basic enameling and more advanced techniques.

Following the fundamentals are full and clear descriptions of the enameling process, beginning with the various metal substrates and proceeding through the cleaning and preparation of materials. Explanations are given for the different methods of applying enamel to the metal, dry sifting as well as wet inlaying and liquid enamel. The firing process is broken down into its phases, illustrating the “sugar coat” texture that occurs at lower temperatures and moving through the “orange peel” and fully fused surfaces.

Colors, both transparent and opaque, are described in detail. The traits of each category are given, covering firing temperatures and soft vs. hard enamels, as well as how the colors interact with one another and different metals. These are some of the most complex and subtle aspects of

enameling, and they typically can only be learned with experience. Darty gives the reader a significant head start with her explanations and tips.

The next section deals with all the traditional enameling styles. It includes a description of each, as well as many practical examples using high-quality photographs. To demonstrate each technique, Darty walks the reader step by step through the making of an actual piece. All the steps are photographed well, and the technique is explained in detail. A thorough understanding of the difficulties and pitfalls—as well as advantages—of each technique can be learned from reading carefully through each step.

The last section of the book presents 12 different projects for readers to attempt themselves. These are explained in exacting detail, with each project broken down into easily digested steps. All the major enameling techniques are represented in this section.

Overall, I believe this is one of the best and most inspirational technical manuals for enameling ever published. Its clear and easily understood details make it an excellent reference for any metalsmith and aspiring enamelist, and even the more experienced enamelist.

MARK MAXWELL

*JA Certified Master Bench Jeweler
Gemological Institute of America
Carlsbad, California*

The Smale Collection: Beauty in Natural Crystals

By Steve Smale, with photos by Jeff Scovil and Steve Smale, 204 pp., publ. by Lithographie LLC [www.lithographie.org], East Hampton, CT, 2006. US\$50.00

The author describes this book, a gallery of some of the best mineral specimens in the Steve and Clara Smale Collection, as “neither a scientific book nor art book but a coffee

table book.” If so, one should serve “premium blend” to go with this beautifully bound and illustrated volume! Although tailored for mineral collectors, gemologists should appreciate the natural forms of the gem minerals pictured throughout.

Steve Smale is a world-renowned mathematician who, with his wife, Clara, has lived in and traveled to many of the areas that have played major roles in the development of their collection. The introduction describes the collection’s history and the places and people that influenced it. Cited are works by Desautels, Halpern, Wilson, and Bartsch and their thoughts on what defines a mineral masterpiece. The author agrees with much of what these experts say but also explains his own criteria: ideal form with variations and exceptions; ideal matrix; the crucial role of the specimen’s horizon (the point where the upper ridge of the overall specimen meets the “sky”); the impact of damage; the importance of completeness; economy (which demands that every part of the specimen play a role in its presentation); judicious trimming (done by professionals); the integrity of the specimen (as it is presented), with disclosure of any defects that are not readily apparent; and related documentation.

The specimens are arranged in order of acquisition from the collection’s beginnings in 1969. The earliest of the 99 photographs were taken by the Smales, the rest by Jeff Scovil. Nearly all of the pieces are represented by full-page color photos with a caption on the opposite page that gives the name of the mineral or principal minerals, together with the locality, dimensions, and a brief background of the piece and its acquisition. Smale prefers using popular or family names rather than scientific ones and follows this convention in his specimen titles. He also discusses his personal approach to photography, based on his observations of still life and the works of master photographers. The gallery is

followed by a short bibliography and index.

This book offers a glorious look at a world-class mineral collection and the couple who put it together. All the specimens depicted truly belong in this visually stimulating work. There is very little to fault other than a few inconsistencies in the specimen titles and the lack of explanation for why each specimen is exceptional. "Old masters" of the mineral world, such as the pyrargyrite from St. Andreasberg, Germany, are joined by modern-day classics, like the jeremejevite from Cape Cross, Namibia. I especially enjoyed the tourmalines and topazes but might give top honors to the rhodochrosite from Colorado's Sweet Home mine. While I wish I had a collection of such importance, at least I can enjoy this book for many years to come.

MICHAEL EVANS

*Gemological Institute of America
Carlsbad, California*

Horn: Its History and Its Uses

By Adele Schaverien, 281 pp., illus., publ. by the author [www.hornhistory-uses.com.au], Wahroonga, NSW, Australia, 2006. US\$60.00

Well written and very interesting, this self-published and passionate effort offers a comprehensive review of the history of horn and its craft that did not exist until now. The author, who took up hornwork in 1976 and is one of a small number of people working with horn today, spent 16 years researching her craft and its history, in addition to photographing a wide variety of horn items of both utilitarian and decorative character.

The book is divided into three sections. The first covers the regulation of horn craft and trade from medieval times to the present day. The next section focuses on materials, tools,

and techniques. The last section contains numerous illustrations and photos along with a history of horn objects detailed by type, from combs to window panes.

Before the development of plastic, horn served as a common material for lightweight objects such as fans, combs, jewelry, snuff boxes, and more. Its processing was extremely malodorous (think of burning hair), and skilled craftsmanship was required to create beautiful and useful objects. Hornworking techniques ranged from simply using the natural form of horn to make items such as drinking vessels and baby bottles, to more complicated processes that required pressing it into plates or leaves that could later be molded. Schaverien's fascinating historical account of how this was done—the book focuses primarily on British horning history—takes us back to a time of innovation, when man needed to make creative use of available organic materials.

To the gemologist, horn is a semi-transparent-to-opaque, yellow to brown to almost black material with an RI of 1.560. It has resinous-to-vitreous polish luster, uneven-to-splintery fracture, and resinous-to-dull fracture luster. When examined with magnification, it reveals an undulating, fibrous structure. In more general terms, horn can be material from the projection of an animal's head made of a sheath of hardened protein over bone, or it can be a solid outgrowth of keratin and hair (as on a rhinoceros or the bill of a bird). The most common items covered in this book are made from the horn of bovine and ovine species, including buffalo, bison, and certain types of antelope.

Horn is a material that often does not survive the test of time because it tends to decompose. Only small numbers of antique horn pieces remain in museums and private collections. This book is not only one of importance to both horners and historians,

but it will also serve as an essential reference tool for museum curators, librarians, and antique collectors.

MARY MATHEWS

*Gemological Institute of America
Carlsbad, California*

OTHER BOOKS RECEIVED

Laboratory Created Diamonds. *By Sharrie Woodring and Branko Deljanin, 39 pp., illus., publ. by European Gemological Laboratory-USA [www.eglusa.com], New York City, 2005 [no price information available].* Intended as an aid for retail jewelers and appraisers, this short booklet provides a basic review of the manufacture and identification of synthetic diamonds. Part I reviews the history and technology behind HPHT and CVD synthetics, including post-growth treatments. Part II covers the various means of identification, from basic gemological examinations to more advanced techniques such as cathodoluminescence and Raman spectroscopy.

THOMAS W. OVERTON

*Gemological Institute of America
Carlsbad, California*

Gem Raw Materials and Their Occurrence in Serbia, 2nd ed. *By Ilić Miloje, 152 pp., illus., publ. by the Yugoslavian Gemological Association, Belgrade, 2006 [in Serbo-Croatian, with English summary, no price information available].* This book reviews the gems that have been found in Serbia, including their occurrences and geologic settings. Though little if any organized mining is currently taking place, the author believes economic deposits of chalcedony, quartz, and opal, among others, may yet be developed. Several pages of color plates illustrate notable specimens of Serbian gem materials.

THOMAS W. OVERTON

GEMOLOGICAL ABSTRACTS

EDITORS

Brendan M. Laurs

Thomas W. Overton
GIA, Carlsbad

REVIEW BOARD

Christopher M. Breeding
GIA Laboratory, Carlsbad

Jo Ellen Cole
Vista, California

Sally Eaton-Magaña
GIA, Carlsbad

Eric A. Fritz
GIA Laboratory, Carlsbad

R. A. Howie
Royal Holloway, University of London

Alethea Inns
GIA Laboratory, Carlsbad

HyeJin Jang-Green
GIA Laboratory, New York

Paul Johnson
GIA Laboratory, New York

David M. Kondo
GIA Laboratory, New York

Taijin Lu
Vista, California

Wendi M. Mayerson
AGL Laboratory, New York

Kyaw Soe Moe
GIA Laboratory, New York

Keith A. Mychaluk
Calgary, Alberta, Canada

James E. Shigley
GIA Research, Carlsbad

Boris M. Shmakin
Russian Academy of Sciences, Irkutsk, Russia

Russell Shor
GIA, Carlsbad

Jennifer Stone-Sundberg
Portland, Oregon

Rolf Tatje
Duisburg, Germany

Sharon Wakefield
Northwest Gem Lab, Boise, Idaho

COLORED STONES AND ORGANIC MATERIALS

Fossils in amber: Unlocking the secrets of the past. D. Penney
[david.penney@manchester.ac.uk], *Biologist*, Vol. 53,
No. 5, 2006, pp. 247–251.

Some of the more fascinating aspects of amber are its fossil inclusions: Many small forms of life are captured with exceptional clarity. It is also important for its ability to capture interactions between organisms and for the comparisons it offers to current evolutionary processes. This article discusses some of the factors affecting the scientific community's ability to extrapolate from the amber fossil record, and looks at the particular value of the two most significant deposits (in the Baltic region and the Dominican Republic).

As with more familiar fossils preserved in carbonate rocks and sediments, the rarity of fossils in amber means that many taxonomic studies suffer from the availability of very few specimens, and this lack of adequate data worsens the older (and thus rarer) the amber samples are. The author also mentions the uncertainty involved in applying knowledge of current life to paleocommunities that may or may not have behaved similarly, as well as how scientists must try to compensate for possible bias toward the preservation of certain groups in amber. As an example, arboreal and hunting spiders are discussed in terms of their ecological niches (body size and web building in trees vs. hunting); experiments have shown with regard to size that modern tree resins trap spiders uniformly, allowing scientists in this case to form reasonable comparisons between much older fossils and more recent ecologies.

Other topics discussed range from using fossils in amber to

This section is designed to provide as complete a record as practical of the recent literature on gems and gemology. Articles are selected for abstracting solely at the discretion of the section editors and their reviewers, and space limitations may require that we include only those articles that we feel will be of greatest interest to our readership.

Requests for reprints of articles abstracted must be addressed to the author or publisher of the original material.

The reviewer of each article is identified by his or her initials at the end of each abstract. Guest reviewers are identified by their full names. Opinions expressed in an abstract belong to the reviewer and in no way reflect the position of Gems & Gemology or GIA.

© 2007 Gemological Institute of America

help study global climates (as biology can be a sensitive recorder of the environment) and the possibility of cloning extinct species using their fossil DNA (which is described as minimal).
DMK

Genesis and composition of lazurite in magnesian skarns.

S. M. Aleksandrov and V. G. Senin, *Geochemistry International*, Vol. 44, No. 10, 2006, pp. 976–988.

Gem-quality lazurite occurs in the Hindu Kush Mountains of Badakhshan, Afghanistan (Sar-e-Sang lapis lazuli deposits), and in the Pamir Mountains of Tajikistan (Lyadzhvardara). It is also found in several additional localities, such as the Lake Baikal region of eastern Russia (Slyudyanka and Malaya Bystritsa). At each of these locations, it is hosted by aluminosilicate rocks that are associated with Fe-poor, Mg-rich skarns. The skarns are formed by the metasomatic alteration of dolomites along their contact with igneous intrusive rocks. To produce lazurite, it is necessary for the alkaline hydrothermal or magmatic solutions that formed the skarns to contain sulfur (as both sulfate and sulfide) along with chlorine. However, the lazurite mineralization appears to postdate skarn formation. The magnesian skarns can also be sources of other gem minerals, including corundum and spinel. Chemical-composition data are provided for lazurite from a number of world deposits.
JES

Herkunftsbestimmung von Süßwasserzuchtperlen mit Laser Ablations ICP-MS [Provenance determination of freshwater cultured pearls using laser ablation ICP-MS]. D. E. Jacobi, U. Wehrmeister, T. Häger, and W. Hofmeister, *Gemmologie: Zeitschrift der Deutschen Gemmologischen Gesellschaft*, Vol. 55, No. 1–2, 2006, pp. 51–58 [in German with English abstract].

In Japan, freshwater pearls are cultivated mainly in Lake Biwa and Lake Kasumigaura. In the latter, a crossbreed of the mussel *Hyriopsis schlegeli* with *H. cumingii* is used, and freshwater shell beads are implanted. By contrast, Chinese cultivators generally use *H. cumingii* and *Cristaria plicata* mussels, and the cultured pearls are beadless. However, as the quality of the Chinese products continually improves, it is becoming increasingly difficult to distinguish Kasumigaura cultured pearls from Chinese products by standard visual methods.

The authors performed LA-ICP-MS analyses on 41 Kasumigaura samples and a number of Chinese freshwater cultured pearls to determine the concentrations of trace elements (Li, Be, Mg, Mn, Co, Ni, Cu, Zn, Sr, Ba, and Ag). All showed high Mn contents, which clearly distinguished them from saltwater cultured pearls. Kasumigaura samples showed lower and less variable Ba/Sr ratios than their Chinese counterparts; these reflect different trace-element compositions that are typical for the waters in which they were cultivated.
RT

Mineralogy of fossil resins of northern Eurasia. M. A. Bogdasarov, *Proceedings of the Russian Mineralogical Society*, Vol. 135, No. 6, 2006, pp. 66–78 [in Russian with English abstract].

The authors investigated the diagnostic properties and genesis of fossil resins from Cretaceous, Tertiary, and Quaternary sediments of northern Eurasia on the basis of their physical and chemical characteristics (e.g., morphology, size, mass, density, optics, mechanical and thermal properties, and chemical composition). The constitution of amorphous organic minerals with a polymeric structure allows the use of IR spectroscopy and other analytical methods. A summary of results from an investigation of the amber-bearing provinces of Baltic-Dnieper, northern Siberia, and the Russian Far East showed that the resins of Baltic-Dnieper are amber (succinite). The amber-like materials from northern Siberia and from some Far Eastern areas are mainly represented by the fragile resins retinite and gedanite, which have no value for jewelry. In contrast, the widespread fossil resins from the Sakhalin coast (Russian Far East) are rumanite and have a high potential for jewelry use.
RAH

The nanostructure of fire opal. E. Fritsch, E. Gaillou [eloise.gaillou@cnrs-immn.fr], B. Rondeau, A. Barreau, D. Albertini, and M. Ostroumov, *Journal of Non-Crystalline Solids*, Vol. 352, 2006, pp. 3957–3960.

Fire opal is typically transparent and characterized by an orange bodycolor. This color is caused by the absorption of light by needle-like iron oxide nanoparticles. Fire opal forms in rhyolitic tuffs, and gem-quality material is mined around the world. The authors studied 60 fire opals from Mexico, Brazil, Ethiopia, Kazakhstan, Tanzania, Slovakia, and the United States, and found that their structure was different from other types of opal that display play-of-color.

Narrow ranges of R.I. and S.G. values suggest that fire opal is a homogeneous material. Raman spectra showed a broad band at 325 cm⁻¹ with minor shifts. Fire opals are less amorphous than most play-of-color opals, with characteristics of opal-CT. Scanning electron microscopy and atomic force microscopy revealed that the structure of fire opal consists of random aggregations of near-spherical grains with an average diameter of 20 nm—far smaller than the 150–300 nm spheres composing the majority of play-of-color opal. The authors propose that these near-spherical grains or “nanograins” are fundamental building blocks of fire opal and possibly of many other varieties of opal as well.
KSM

Vetri naturali [Natural glasses]. M. C. Venuti, *Rivista Gemmologica Italiana*, Vol. 1, No. 1, 2006, pp. 25–37 [in Italian].

Natural glasses are formed in three situations: (1) during the cooling of certain volcanic rocks (e.g., obsidian), (2) during the impact of extraterrestrial bodies (e.g., impactite and tek-

tite), and (3) from lightning strikes (fulgurite). The author explains their formation and describes the many varieties of obsidian. Obsidian is used as an ornamental stone, and some tektites (moldavite and Libyan desert glass) can be faceted. However, synthetic glass is frequently offered as natural; examples include beer bottle glass and transparent "obsidian" from Mount St. Helens. The author states "with absolute certainty" that natural facetable obsidian does not exist and that the only known facetable natural glasses of good quality are moldavite and Libyan desert glass. RT

DIAMONDS

Diamonds from the Udachnaya pipe, Yakutia. V. Rolandi [vanda.rolandi@unimb.it], A. Brajkovic, I. Adamo, and M. Landonio, *Australian Gemmologist*, Vol. 22, No. 10, 2006, pp. 387–397.

The authors studied 10 octahedral greenish yellow to brownish orange-yellow diamond crystals (0.07–0.62 ct) from the Udachnaya mine, Sakha Republic, Russia. The main surface features included growth layers, shield-shaped laminae, negatively oriented trigons, dislocation planes, and etch features. Inclusions of Cr-spinel and Mg-ilmenite indicated that eight of the stones were peridotitic (P-type) diamonds, while two with inclusions of rutile, chromite, and garnet were eclogitic (E-type). All were identified as type IaAB diamonds. Their cathodoluminescence (CL) color reactions, surface features, and inclusions suggest that these diamonds may have formed at a temperature of ~1200°C and pressures over 5 GPa, but were later subjected to fluctuations in temperature and pressure, leading to two or more different growth stages. Raman, FTIR, and CL spectra are presented. RAH

Directional chemical variations in diamonds showing octahedral following cuboid growth. D. A. Zedgenizov, B. Harte [ben.harte@ed.ac.uk], V. S. Shatsky, A. A. Politov, G. M. Rylov, and N. V. Sobolev, *Contributions to Mineralogy and Petrology*, Vol. 151, 2006, pp. 45–57.

Most natural diamonds develop with either octahedral or cuboid morphology. However, some may show a mixed growth mechanism—which usually evolves from octahedral to cuboid—resulting in so-called coated diamonds. In this study, the authors examined 16 diamonds from Siberia that showed a reversal in this growth sequence.

The samples were polished into thin plates (50–70 µm) for study of their internal growth morphologies in detail. The cuboid cores were densely populated with micro-inclusions but did not show the well-defined fibrous structures typically present in coated diamonds. Some fibrous structures could be observed in the core during the early stages of growth. However, they were modified by high-temperature annealing during subsequent octahedral growth. With photoluminescence imagery

(excited using an ultraviolet wavelength), the cuboid zones fluoresced yellow to greenish yellow while the octahedral zones fluoresced blue to dark blue. X-ray topographs showed a dark diffraction contrast of the cuboid core created by numerous dislocations. Cathodoluminescence images showed that octahedral growth on the cuboid core began with numerous small octahedral apices that evolved to larger octahedral faces.

The micro-inclusions were identified by FTIR spectroscopy as carbonates (calcite and dolomite-ankerite), water, apatite, quartz (shifted from the normal spectral position), and silicates. The spectra showed that the cubic cores had large amounts of nitrogen B-aggregates, whereas the octahedral portion had A-aggregates. The appreciable nitrogen aggregation in the core suggests that these diamonds resided in the mantle for long periods. The quantities of nitrogen, hydrogen, vacancies, dislocations, and micro-inclusions decreased from core to rim, suggesting various modes of growth kinetics, such as a slower growth rate in the octahedral zone than the cuboid core and changes in the source fluid's composition.

Photoluminescence spectra revealed H4 and N3 centers in the cuboid cores, whereas octahedral zones showed a much higher intensity of N3 centers but no H4 defects. SIMS analysis revealed a carbon isotopic composition that was "lighter" in the core and "heavier" in the octahedral zone. The concentration of nitrogen was 846–1410 ppm in the cuboid cores to 200–600 ppm in the octahedral zones. Carbonates and water in the micro-inclusions suggested that these diamonds crystallized from fluid containing C, O, H, and N. The authors also concluded that the composition of the diamond-forming fluid fell between carbonate-rich and hydrous end-members. KSM

Natural, untreated diamonds showing the A, B and C infrared absorptions ("ABC diamonds"), and the H2 absorption. T. Hainschwang, F. Notari, E. Fritsch, and L. Massi, *Diamond and Related Materials*, Vol. 15, 2006, pp. 1555–1564.

Natural diamonds showing a combination of types IaAB and Ib (i.e., infrared absorptions related to A aggregates, B aggregates, and isolated nitrogen [C defects]) are considered extremely rare. Such diamonds are also notable for their weak-to-strong H2 absorption. The authors studied nine brown-to-yellow diamonds (0.01–0.21 ct), six of which were so-called ABC diamonds. Most of them appeared inhomogeneous; the darker core had a phantom cloud of cuboid shape created by small particles, while the lighter rim, created by octahedral growth, showed higher clarity. FTIR spectra showed additional differences between the core and the rim: The core contained high quantities of aggregated nitrogen, while the rims had lower concentrations, most as type Ib. All the ABC diamonds were inert to long- and short-wave UV excitation, but most showed luminescence in response to 425 nm light.

The H2 center is commonly observed in treated diamonds, but it is largely unknown in natural, untreated diamonds. However, it was seen in these diamonds along with a previously undocumented absorption peak at 905 nm that was tentatively attributed to hydrogen-related defects. The authors propose that the strong H2 absorption is caused by the large amount of isolated nitrogen along with A centers and the presence of vacancies. The hydrogen-related absorptions are suggestive of rapid growth in an environment that was rich in carbon, nitrogen, and hydrogen. SE-M

Some observations on diamondiferous bedrock gully trap-sites on Late Cainozoic, marine-cut platforms of the Sperrgebiet, Namibia. J. Jacob [janajacob@namdeb.com.na], J. D. Ward, B. J. Bluck, R. A. Scholz, and H. E. Frimmel, *Ore Geology Reviews*, Vol. 28, 2006, pp. 493–506.

This article reviews the bedrock morphology underlying the diamondiferous beach placer deposits of Namibia. It has been well established, since the discovery of diamonds there in 1928, that the Orange and Vaal river systems have been transporting diamonds from the southern African interior to the Atlantic coast since at least the mid-Eocene (~40–50 Ma). Longshore drift from the prevailing winds has further transported diamonds northward along the Namibian (specifically Sperrgebiet) coast for up to 120 km from the Orange River mouth to Chemeis Bay—a zone known as Mining Area No. 1 (MA1). This zone's underlying bedrock consists of alternating hard (meta-arenite) and soft (chloritic schistose) layers of Late Proterozoic meta-sediments beveled into platforms by wave action during the Quaternary Period. Differential wave erosion of the alternating layers has created “gullies”—actually, large crevices (up to 100 m long by 4 m wide and 7 m deep)—which make superb trap sites for dense clastic material (such as diamonds) that is being transported along the beach.

The authors used air photo techniques, field mapping (of exposures from mining activity), and airborne laser topographic surveys to identify three major gully types: (1) swash-parallel, (2) strike-parallel, and (3) joint gullies. Swash-parallel gullies occur only in the southernmost section of MA1 and are perpendicular to the paleo-wave fronts. Since the sediment load in the south is both high (in volume) and coarse (in grain size), the wave action overrides local geologic structures such as joints. As this coarse bedload (highest diamond counts) decreases to the north, bedrock lithology and structure become the dominant factors in gully formation.

The central section of MA1 is dominated by strike-parallel gullies, which are directly related to the dip of bedrock foliation (bedding parallel) of 80–89°W. In the north, where the sediment load is both at its lowest and finest, only joint gullies have formed along preexisting cracks in the bedrock. Further, it was found that all the

gullies are deeper and closed (i.e., creating the best diamond trap sites) on their seaward margins, while they are shallower and somewhat open on their landward end. A specific example was measured by tacheometric survey giving detailed elevations throughout the gully. The shallow incision on the landward margins of the gullies is attributed to lower wave energy (being further from the sea) of the tidal system. A model is also presented illustrating the growth of “pot holes” in the bedrock that eventually coalesce into longer and longer gullies.

KAM

GEM LOCALITIES

Amethyst-bearing lava flows in the Paraná Basin (Rio Grande do Sul, Brazil): Cooling, vesiculation and formation of geodic cavities. D. Proust [dominique.proust@hydrasa.univ-poitiers.fr] and C. Fontaine, *Geological Magazine*, Vol. 144, No. 1, 2006, pp. 53–65.

Large amethyst geodes (up to 2.5 m) are found in tholeiitic basalt lava flows near the town of Ametista do Sul in the state of Rio Grande do Sul, Brazil. This study was undertaken to better understand the degassing and cooling history of these lava flows that permitted the formation of the large amethyst geodes. Whereas some geologists have invoked the role of surface water in geode formation, the present authors conclude that the cavities resulted from the exsolution of water and other gases from the cooling lava. They attribute the elongate shape and abnormal size of some geodes to rapid cooling and the coalescing of multiple exsolving gas bubbles, respectively. JES

Ar-Ar and U-Pb ages of marble-hosted ruby deposits from central and southeast Asia. V. Garnier, H. Maluski, G. Giuliani [giuliani@crpg.cnrs-nancy.fr], D. Ohnenstetter, and D. Schwarz, *Canadian Journal of Earth Sciences*, Vol. 43, No. 4, 2006, pp. 509–532.

Ruby deposits hosted by marbles are distributed along the Himalayan mountain fold belt that formed during the Tertiary collision of the Indian plate with Asia, as well as in the Indochina crustal block extruded along shear zones during this collision. These metamorphic deposits are found in Tajikistan, Afghanistan, Pakistan, Nepal, Myanmar, and Vietnam. This study was undertaken to relate the age of their formation to the geologic events associated with the continental collision. Ruby itself is not suitable for age dating, but inclusions in ruby, and certain associated minerals, can both be dated by certain techniques.

Ar-Ar age dates of between 25 and 4.6 Ma document Oligocene-Miocene cooling ages for the ruby-bearing metamorphic belts, which in turn represent minimum ages for ruby formation. These ages are in agreement with published data on the tectonic-metamorphic history of the marbles hosting the rubies. U-Pb age dates of 54–36

Ma for zircon inclusions give a maximum Eocene age for ruby mineralization in Vietnam. The specific time of formation of each ruby deposit depended on its location within the fold belt. *JES*

Contrasts in gem corundum characteristics, eastern Australian basaltic fields: Trace elements, fluid/melt inclusions and oxygen isotopes. K. Zaw [khin.zaw@utas.edu.au], F. L. Sutherland, F. Dellapasqua, C. G. Ryan, T.-F. Yui, T. P. Memagh, and D. Duncan, *Mineralogical Magazine*, Vol. 70, No. 6, 2006, pp. 669–687.

Corundum xenocrysts from alkali basalt fields differ in their lithospheric origins (magmatic vs. metamorphic) and hence in their characteristics. Detailed comparisons are made between sapphires from Weldborough in northeastern Tasmania and those from Barrington in New South Wales. The Tasmanian sapphires had a magmatic signature (high Ga, average 200 ppm), and were dominated by Fe (avg. 3300 ppm) and variable Ti (avg. 400 ppm) as chromophores. They contained Cl, Fe, Ga, Ti, and CO₂-rich fluid inclusions, and yielded $\delta^{18}\text{O}$ values (5.1–6.2‰) in the mantle range. Geochronology on coexisting zircons suggested several sources (200–47 Ma) that were disrupted by the basaltic melts (47 ± 0.6 Ma). Corundum from Barrington included magmatic sapphires (avg. 170 ppm Ga; $\delta^{18}\text{O}$ 4.6–5.8‰) with relatively more Fe (avg. 9000 ppm) and less Ti (avg. 300 ppm). Zircon dating suggested that gem formation preceded and overlapped Cenozoic basaltic melt generation (59–4 Ma). The Barrington samples also consisted of a metamorphic sapphire-ruby suite (low Ga, avg. 30 ppm), with Cr as an important chromophore (up to 2250 ppm). Fluid inclusions were CO₂-poor, but melt inclusions suggested some alkaline melt interaction. The $\delta^{18}\text{O}$ values (5.1–6.2‰) overlapped magmatic sapphire values. The formation of the metamorphic suite may be attributed to interactions at contact zones between Permian ultramafic bodies and later alkaline fluids. *RAH*

Famous mineral localities: The Erongo Mountains, Namibia. B. Cairncross [bc@rau.ac.za] and U. Bahmann, *Mineralogical Record*, Vol. 37, No. 5, 2006, pp. 361–470.

This article provides a detailed review of the mineral wealth of the Erongo Mountains in Namibia. Originally mined for tin by German settlers in the early 1900s, this region was found to contain abundant pegmatites and their accompanying wealth of minerals. Fine crystals of aquamarine, schorl, and jeremejevite are known from various areas of the mountain complex. One of Erongo's most important finds happened in April 2000, when the first major pocket of aquamarine was discovered on the farm Bergsig 167. Various localities and their geology are discussed along with the types of minerals that come from each. Vast areas have yet to be explored because much of the land is privately owned and large northern and western

sections form part of the Erongo Mountain Nature Conservancy. Numerous maps, diagrams, and photographs of the region and its minerals are provided. *JEC*

Formation of emeralds at pegmatite-ultramafic contacts based on fluid inclusions in Kianjavato emerald, Mananjary deposits, Madagascar. Ye. Vapnik [vapnik@bgu.ac.il], I. Moroz, M. Roth, and I. Eliezri, *Mineralogical Magazine*, Vol. 70, No. 2, 2006, pp. 141–158.

Emeralds from Kianjavato on the eastern coast of Madagascar are hosted by the Ifanadiana-Angavo shear zone and formed via metasomatic processes near the contact between pegmatite and hornblendite. Fluid inclusions in emerald and quartz samples were studied by microthermometry and Raman analysis. Three main populations of inclusions were found: CO₂-rich, CH₄-rich, and H₂O-rich with a salinity of ~2 wt.% NaCl. Based on fluid-inclusion data, the emeralds crystallized at 250–450°C and 1.5 kbar.

Fluid inclusions were also studied in emeralds from Ianapera in southern Madagascar. Those emeralds are hosted by the Ampanihy shear zone and formed in the absence of pegmatites; they were found to contain mostly CO₂-related fluid inclusions.

Both shear zones resulted from collisional forces related to the formation of the early supercontinent Gondwana. At Kianjavato, the intrusion of granitic pegmatites shortly after this collisional event contributed the bulk of the fluids to the metasomatism. The regional deformation event is thought to have taken place at 530–500 Ma, and phlogopite related to the emerald-bearing veins has been dated by ⁴⁰Ar/³⁹Ar at 490 ± 8 Ma. Mantle-derived CO₂-rich fluids were channeled by the shear zones, while H₂O-rich fluids of crustal origin are related to pegmatite emplacement. The introduction of CO₂-rich fluids into graphite-bearing host rocks created a reducing environment that generated the CH₄-rich fluids. While pegmatite–host rock interactions were the main driving force behind the metasomatic formation of the Kianjavato emerald deposits, the presence of CO₂-rich fluid inclusions suggests that fluids from the shear zone also played a role. *EAF*

The variation of gemmological properties and chemical composition of gem-quality taaffeites and musgravites from Sri Lanka. K. Schmetzer [schmetzerkarl@hotmail.com], L. Kiefert, H.-J. Bernhardt, and M. Burford, *Australian Gemmologist*, Vol. 22, No. 10, 2006, pp. 485–492.

The gemmological, chemical, and spectroscopic properties of two transparent faceted taaffeites, a semitransparent taaffeite crystal, and a faceted transparent musgravite from Sri Lanka were determined. The grayish violet color of two taaffeites and the musgravite was caused by various amounts of iron, and the purplish red taaffeite contained traces of chromium in addition to moderate iron.

Variations in the RI and SG values of these specimens were correlated to their chemical composition, and in particular the sum of the concentrations of transition elements based on electron-microprobe analysis. The RI and SG values of taaffeite and musgravite overlap, so for an unequivocal determination a combination of X-ray diffraction analysis, quantitative chemical analysis, and/or Raman spectroscopy may be necessary. RAH

INSTRUMENTS AND TECHNIQUES

Gemmologia a basso costo. Costruirsi una bilancia per il peso specifico delle gemme [Gemology at low cost. How to construct a specific gravity scale for gems].

P. F. Moretti, *Rivista Gemmologica Italiana*, Vol. 1, No. 1, 2006, pp. 61–64 [in Italian].

The author describes how to set up a simple specific gravity apparatus using low-cost materials (<€50). He discusses the problems and pitfalls of its construction, the measurement procedure, and possible errors (and how to reduce them). He also explains the difference between SG and density and why this difference can be ignored. RT

JEWELRY HISTORY

Italian gemology during the Renaissance: A step toward modern mineralogy. A. Mottana [mottana@uniroma3.it], *Geological Society of America Special Paper 411*, 2006, pp. 1–21.

Significant advances in the study of gems and minerals occurred in Italy during the height of the Renaissance in the 16th century. Italy hosted the superior universities in Europe at the time (such as Ferrara and Padua) and these academic centers, together with the rediscovery of ancient knowledge from the Greeks, Romans, and Arabs, led to the publication of a number of works on minerals and gems. Around 1469, the first of what became numerous editions (over the next 150 years) of Pliny's 37-volume encyclopedia *Naturalis historia* was printed in Venice. These and other books served to transfer historical knowledge of gems from Italy to the other countries of Europe. The book *Speculum lapidum* by Leonardi (1502) serves as a marker between the speculations about gems prevalent during the Middle Ages and early scientific studies that commenced during the Renaissance. The writer Agricola, a native of Saxony who spent 1522–1526 as an apprentice in Italy, went on to publish information (both accurate and inaccurate) on minerals and gems in his *De natura fossilium* in 1546.

In the book *De la pirotechnia*, written primarily on metallurgy by Biringuccio and published in Venice in 1540, the author describes gems as stones having a special color, and divides them into transparent and translucent

categories. This was followed in 1544 by Mattioli's *I discorsi*, a book describing the (primarily medicinal) uses of minerals, gems, and other materials. A 1565 Italian translation of *Speculum lapidum* helped spread gemological knowledge among the general population, who were largely ignorant of Latin. During this same period, another book appeared in Italy that described the relationship between weight and value of 10 important gems, including diamond.

The growth of the arts in Italy during the Renaissance contributed indirectly to the development of gemology, because gems were used to decorate art objects (e.g., book covers and crucifixes) as well as for jewelry, carvings, cameos, and intaglios. The book *De subtilitate* by Cardano summarized an enormous amount of information on gems when it appeared in 1560. He ranked the key properties of gems as brightness, hardness, murkiness, and color. In order of commercial value, he listed the important stones as emerald, opal, ruby, diamond, pearl, sapphire, chrysolite (peridot), hyacinth (zircon), and smoky quartz. In a book published in 1568, the artist Cellini described the four main gems, in their order of value at the time, as ruby, emerald, diamond, and sapphire.

Published in 1587, the book *Questo è 'l libro lapidario* (compiled by Costanti) discussed how Renaissance merchants evaluated gems. For example, a good diamond should be well pointed and possess a square outline, equal faces, sharp edges, transparency, and good reflectivity. The book provided detailed tables of price vs. weight for diamond, ruby, emerald, and spinel. It also showed how gem merchants at the time were interested in learning the sources of gems and where they could be obtained at the best prices.

This period also witnessed the establishment in Italy of several museums with collections of materials from the natural world, including minerals and gems. Finally, improvements in the cutting of gemstones also took place; for example, Peruzzi is credited with introducing a four-fold symmetrical diamond cut with 58 facets, which became a precursor of the modern brilliant cut.

Near the end of the 1500s, Italy began to lose its position in culture and trade, and gemological knowledge shifted northward to Antwerp, which then became the center of diamond cutting. JES

SYNTHETICS AND SIMULANTS

Distribution of nitrogen-related defects in diamond single crystals grown under nonisothermal conditions. Y. V. Babich [babichyv@uiggm.nsc.ru] and B. N. Feigelson, *Inorganic Materials*, Vol. 42, No. 9, 2006, pp. 971–975.

Nitrogen impurity-related defects are important in both natural and synthetic diamonds. Experimental data on their distribution in internal growth sectors are presented

for yellow-brown synthetic diamonds grown from an iron-nickel solvent at 6 GPa and 1370–1550°C for 80–126 hours. At each of the selected conditions, the exact growth temperature of a crystal was varied upward and downward in a stepwise manner, with several slightly higher and lower isothermal periods lasting from 6 to 22 hours and with temperature differences of up to 110°C between periods (relative to the nominal growth temperature). The crystals were then cut into flat plates for examination.

The total nitrogen concentration in a plate ranged from 100 to 250 ppm. Nitrogen was present as C defects (≤ 150 ppm), A defects (≤ 245 ppm), and N^+ centers (≤ 25 ppm). Within a crystal, C defects prevailed at the periphery, while A defects prevailed around the seed. The A defects predominated in material grown during lower-temperature periods, while C defects predominated in synthetic diamond grown at higher temperatures. A reduction in growth temperature was also accompanied by a rise in N^+ concentration. The lower-temperature growth regions displayed yellow-green luminescence, which is a result of their higher nickel content (and increased concentration of nickel-nitrogen centers). The degree of nitrogen aggregation was influenced by nickel incorporation into the diamond structure on changes in growth temperature. The N^+ concentration increased in response to cooling steps in growth conditions, indicating that the concentration of substitutional nickel increases with carbon supersaturation and with growth rate. Thus, temperature plays a key role in determining the rate of nitrogen incorporation into the diamond structure and subsequent transformation of nitrogen-related defects.

JES

High-pressure and high-temperature annealing affects on CVD homoepitaxial diamond films. K. Ueda [kueda@will.brl.ntt.co.jp], M. Kasu, A. Tallaire, and T. Makimoto, *Diamond and Related Materials*, Vol. 15, 2006, pp. 1789–1791.

High-pressure, high-temperature (HPHT) annealing of homoepitaxial synthetic diamond films of 1 μm thickness grown via chemical vapor deposition (CVD) is reported. HPHT annealing proved advantageous for optical and electronic applications in that it improved the crystalline quality by decreasing the crystalline defects. A cubic-anvil-type high-pressure apparatus and a graphite heater were used to anneal the films at 1200°C and 6 GPa for one hour in NaCl. The samples were studied before and after annealing using cathodoluminescence (CL) spectroscopy and Hall-effect measurements. CL spectroscopy revealed improved crystalline quality and improved optical characteristics after HPHT annealing, through both a decrease in nonradiation centers and a decrease in emission bands due to interstitial carbon atoms and boron-related defects. The Hall-effect measurements showed an increase in hole mobility (the synthetic diamond films showed p-type

semiconductivity due to unintentional boron doping) with HPHT annealing, indicating a decrease in crystalline defects. The authors also observed changes in nitrogen-vacancy states as a result of HPHT annealing. JS-S

Inclusions of metal-solvent and color in B-containing monocrystals of artificial diamond. A. I. Chepurov, E. I. Zhimulev, I. K. Federov, and V. M. Sonin, *Proceedings of the Russian Mineralogical Society*, Vol. 6, No. 135, 2006, pp. 97–101 [in Russian with English abstract].

Crystals of type IIb synthetic diamond (0.1–2 ct) were grown with a cuboctohedral habit along with minor faces of {110}, {311}, and {511}. The crystals varied from blue to dark blue depending on the amount of boron; a characteristic feature was a sectorial structure expressed in a nonuniform distribution of color. Metal inclusions corresponded in composition to that of the metal solvent. The IR spectrum of a boron-bearing diamond crystal is presented together with figures showing the dependence of the a cell parameter of the metallic inclusions on the iron content of the Fe-Ni alloy. RAH

The nature of Ti-rich inclusions responsible for asterism in Verneuil-grown corundum. C. Viti [vatic@unisi.it] and M. Ferrari, *European Journal of Mineralogy*, Vol. 18, No. 6, 2006, pp. 823–834.

Verneuil-grown star corundum with variable zoning and coloration hosts three sets of acicular inclusions at 120°. The inclusions are up to 20–30 μm long and 0.1–0.4 μm wide; they are elongated parallel to the {110} faces and are polysynthetically twinned on {110}. Electron diffraction and high-resolution transmission electron microscopy (TEM) show that the inclusions are almost isostructural with the corundum matrix, even if slightly distorted to a monoclinic lattice. Chemical data obtained by TEM suggest a possible TiO_2 stoichiometry, thus indicating the presence of Ti^{4+} cations, coupled with vacancies, within the distorted corundum-like structure. Close to the ends of the TiO_2 needles, local stoichiometry is consistent with the presence of Ti^{2+} cations, possibly formed during post-growth annealing. RAH

The state of the art in the growth of diamond crystals and films. V. P. Varmin, V. A. Laptev, and V. G. Ralchenko [ralchenko@nsc.gpi.ru], *Inorganic Materials*, Vol. 42, Supp. 1, 2006, pp. S1–S18.

This article reviews the history and current status of the high-pressure synthesis of diamond single crystals and the more recent development of the low-pressure growth of polycrystalline and single-crystal synthetic diamond thin films. Synthesis methods include so-called static processes, such as the temperature-gradient technique in which diamond growth takes place on a seed in the presence of a molten metal solvent-catalyst. Lower-quality crystals up to 25 ct, and gem-quality crystals up to 5 ct, have been pro-

duced in small quantities by this method using belt, multi-piston, and multi-anvil equipment. High-pressure growth methods also include "dynamic" processes, where diamond synthesis occurs in a graphite-metal mixture subjected to the pulsed action of very high pressures generated by a shock wave, and explosive detonation of a graphite mixture, with tiny diamond crystallites being produced in both cases. Metastable low-pressure growth of diamond thin films has been perfected by using several variations of the chemical vapor deposition (CVD) technique. Here, the presence of hydrogen in the growth chamber is important to prevent the nucleation and growth of nondiamond carbon phases. Production of synthetic diamond by all of these methods has led to its increased use in numerous technological applications. *JES*

TREATMENTS

High pressure-high temperature (HPHT) natural diamond enhancement. M. A. Viktorov and M. B. Kopchikov, *Moscow University Geology Bulletin*, Vol. 61, No. 3, 2006, pp. 61–68.

The authors examined two brown diamond crystals, both before and after HPHT treatment, to document changes in their gemological properties. Annealing conditions employed temperatures of 1973–2073 K and a pressure ~6 GPa for five hours.

After treatment, the color of one crystal changed to yellow-green, and its UV fluorescence (long- and short-wave) became a more intense yellowish green. Its absorption spectrum displayed strong 415 and weak 503 nm bands, and an increase in overall absorption across the spectrum. The photoluminescence spectrum showed a pronounced 503 nm band. The color and UV fluorescence of the other crystal remained basically unchanged, although yellow phosphorescence that was present before the treatment was removed. Its absorption and PL spectra exhibited similar changes to those of the first crystal. Both samples displayed a change in cathodoluminescence colors from blue to yellowish green after treatment.

The authors discuss the changes in optical defects that occur during HPHT annealing, and conclude that a careful selection of diamonds for this type of treatment is necessary to achieve particular color changes. *JES*

Optical study of the annealing behaviour of the 3107 cm⁻¹ defect in natural diamonds. F. De Weerd [fdw@hrd.be] and A. T. Collins, *Diamond and Related Materials*, Vol. 15, 2006, pp. 593–596.

Hydrogen is a common impurity in diamond, and may be observed in the mid-infrared spectral range as the bend (1405 cm⁻¹) and stretch (3107 cm⁻¹) modes of the C-H vibration; however, hydrogen concentration and the intensity of the 3107 cm⁻¹ absorption are not proportional in diamond. The authors monitored the effect of HPHT

annealing on the 3107 cm⁻¹ defect in 14 natural type Ia diamonds. One set of diamonds was annealed at 2100°C and 7.0 GPa, and the other set at 2200°C and 7.5 GPa. In most diamonds, the 3107 cm⁻¹ absorption consistently decreased with increased annealing time, while some showed an initial increase and then a decrease thereafter. This general decrease was not surprising, as the 3107 cm⁻¹ defect is not stable at the high temperatures used in HPHT annealing and may be destroyed.

Assuming first-order kinetics and an infrared-inactive reservoir of available hydrogen in the diamond, the authors created a simple model of the 3107 cm⁻¹ defect's concentration. For the samples that showed a continual decrease in absorption, the calculations indicate that the dissociation rate is higher than the aggregation rate. In the diamonds showing an initial increase, the aggregation and dissociation rates are approximately equal. Using this model, the total hydrogen concentration in the diamond may be considered proportional to one of the calculated parameters. However, these calculated results for total hydrogen concentration did not show a correlation with nitrogen, so a relationship between nitrogen and hydrogen concentrations in diamond could not be inferred from the data. *SE-M*

Study on the wax enhancement for the unearthed jade wares by FTIR technique from ancient tombs of Shang-Zhou period in Henglingshan site of Boluo County, Guangdong Province. Z. Qiu, M. Wu, and Q. Wei, *Spectroscopy and Spectral Analysis*, Vol. 26, No. 6, 2006, pp. 1042–1045 [in Chinese with English abstract].

Jade (nephrite and jadeite) and jade-like materials (such as serpentine and fine-grained quartzite) have played an important role in Chinese culture since ancient times. Waxing has long been used by Chinese artisans to enhance the luster of polished jade. However, the early history of this treatment is unknown. In this article, the authors used FTIR techniques to study various jade and jade-like materials from the famous tombs of Henglingshan (1600–221 BC) in Guangdong Province. In addition to these 95 pieces (13 nephrite, 82 quartz and fine-grained quartzite), two modern wax-treated jadeite samples, two wax-treated quartzite "jade" pieces, and pure wax samples were analyzed for comparison.

Two or three characteristic absorption bands at 2960, 2920, and 2850 cm⁻¹ were found in the IR spectra of the ancient quartzite materials, resembling those of the pure waxes at 2956, 2918, and 2850 cm⁻¹. Absorption bands located at 2960 (very weak), 2925, and 2855 cm⁻¹ were detected in the modern jadeite pieces. These results suggest that the ancient wares were enhanced with wax, and that the wax materials were very similar to those used on modern jadeite. Thus, it appears that wax enhancement of jade and jade-like materials in China can be traced back more than 2,000 years. *TL*

MISCELLANEOUS

Angola: The new blood diamonds. R. Marques, address to the School of Oriental and African Studies, London University, Nov. 28, 2006, www.business-humanrights.org/Links/Repository/606731.

Although the civil war in Angola is long over, the government has recently enacted highly restrictive laws in the diamond-bearing provinces of Lunda Norte and Lunda Sud that deprive the local population of livelihoods outside of diamonds, reports Angolan journalist Rafael Marques. The laws prohibit all non-diamond-related economic activity, including fishing, farming, and traditional industries.

Often, with the knowledge and cooperation of mining companies, private security forces commit human rights abuses in these areas in the name of security. In addition, conflicting and confusing regulations allow many loopholes through which mining companies can exploit the independent diamond diggers. Because the activities of the independent diggers are officially prohibited, they are denied rights and protection. Yet they routinely supply the licensed buying offices with diamonds. The article concludes that the top officials of the Angolan government benefit from this situation, and thus do not want to change it. RS

A cartel's response to cheating: An empirical investigation of the De Beers diamond empire. D. J. Bergenstock [bergebst@muhllberg.edu], M. E. Deily, and L. W. Taylor, *Southern Economic Journal*, Vol. 73, No. 1, 2006, pp. 173–189.

This paper examines how De Beers reacted to massive Russian rough diamond sales during the 1990s, when it still controlled a majority of the rough diamond market. The authors found a correlation between rising Russian state budget deficits after the Soviet era and increased diamond "leaks"—sales outside the country's contract with De Beers. They believe that, in contrast to traditional cartel behavior of aggressive discounting to chasten entities that "cheat" by dealing independently, De Beers facilitated the Russians in nontraditional ways to maintain diamond price stability. These included both negotiation and accommodation [by going against its stated policy of refusing to buy leaked Russian diamonds from the open market, and actually absorbing large quantities of such goods under the guise of "Zairian" origin].

Although the strategy was successful in the short term by protecting diamond prices, it came at a high cost in the form of accumulating inventories, which contributed to the firm's decision in 2000 to end its custodial role of the diamond market and change its direction to a company selling branded diamonds. RS

Conflict diamonds and the Kimberley process: Mission accomplished or mission impossible? T. Hughes. *South African Journal of International Affairs*, Vol. 13, No. 2, 2006, pp. 115–130.

The Kimberley Process (KP), fully ratified in 2003, is a mechanism designed to stop the entry of conflict diamonds into the legitimate market by requiring all rough diamond imports to carry certificates stating that they were mined and exported in accordance with local laws. Claims that the KP has helped dramatically reduce the flow of such stones are tempered by criticism that it is not airtight, although it has been credited with preventing the re-ignition of civil wars in Angola and Sierra Leone and with keeping new wars from getting worse in the Ivory Coast and Democratic Republic of the Congo. All these countries have reported substantial increases in legitimate diamond exports since the inception of the KP.

However, the system is subject to abuse, with several countries issuing KP certificates without adequate paperwork to back claims they were legitimately mined or imported. Additionally, the KP fails to address the situation of artisanal diggers who often work in unacceptable conditions. Several programs such as the Diamond Development Initiative are a step in that direction. However, as long as artisanal mining continues unregulated, dependent on warlords and powerful middlemen, the KP will be difficult to enforce. RS

Diamonds by Linares, Gemesis may cut De Beers, Rio Tinto sales. D. Rossingh, *Bloomberg.com*, June 11, 2007, www.bloomberg.com.

This article provides an update on the commercial production of synthetic diamonds, noting that current output from all producers (largely Gemesis of Sarasota, Florida) is about 100,000 carats per year, compared to 155 million carats of natural diamonds. The report quotes market analysts stating that the output of synthetics will increase to about one million carats per year when other sources, including Boston-based Apollo Diamond Co., begin production. The analysts maintained that the average price of synthetic diamonds was \$2,500 per carat against an average of \$8,000 per carat for a natural diamond of similar weight.

The article also traces the history of Gemesis and Apollo. Apollo has produced about 1,000 stones since its beginnings in 1990 but plans to expand to hundreds of thousands of carats by 2012. Gemesis executives claim that synthetic diamonds will comprise 10% of the rough diamond market within five years.

Some analysts quoted believed synthetics would dent sales of the large diamond mining companies, while others said that synthetics would help meet predicted shortages of natural diamonds. RS